DEPARTMENT OF PHARMACY

PhD PROGRAMME IN

"PHARMACEUTICAL SCIENCE"

XXXIV CICLE

PhD Thesis

By

Rosa Sparaco

Synthesis of new molecular hybrids of antiglaucoma drugs and H_2S donors

Tutor

Prof. Ferdinando Fiorino

PhD Coordinator

Prof. Maria Valeria D'Auria

Preface

My PhD project was carried out thanks to the support of the programme "POR Campania FSE 2014/2020" in collaboration with the pharmaceutical company Genetic S.p.a. (Fisciano, Italy). I had the opportunity to achieve an Industrial PhD project, working during these years at the Department of Pharmacy of University of Naples "Federico II", Department of Chemistry of University of Durham (UK), and I also spent six months at the pharmaceutical manufacturing site of Genetic S.p.a.

The main focus of my PhD project was the design and the synthesis of new molecular entities for the treatment of glaucoma.

Glaucoma is a group of optic neuropathies consisting of retinal ganglion cells and axonal death with corresponding loss of field vision. It is one of the leading causes of irreversible blindness globally. Despite the availability of several drugs for the treatment of glaucoma, researchers are still focused on the development of new therapeutic agents that could provide a better control of the disease.

Over the last years, the scientific interest for hydrogen sulfide (H_2S) has grown due to the results obtained from studies concerning its biological roles. H_2S has been recently identified as a gaseous neurotransmitter implicated in various pathophysiological processes. It has shown a protective effect against damages related to glaucoma.

The following thesis is divided as follow: the first part has been carried out at the Department of Pharmacy of University of Naples, the second part concerns my collaboration with R&D laboratories of the pharmaceutical company Genetic S.p.a and, at the end of the thesis, I have reported as appendix the project I was involved in during my stay at the Department of Chemistry of University of Durham.

In the first section I have described the design, chemical synthesis and characterization of molecular hybrids between drugs for the treatment of glaucoma and H_2S releasing moieties. The aim of my project was to synthesize new drugs which combine the action of antiglaucoma agents and H_2S released by molecular donors to provide a synergistic heightened therapy. Hybridization

is a common strategy in drug design process aimed to obtain novel molecules potentially more effective and less toxic than the parent drugs. By the application of these new antiglaucoma entities, we expect a reduction in the administered dosage as well as adverse side effects may be minimized.

Amongst the classes of available drugs for glaucoma therapy, brinzolamide, betaxolol and brimonidine were coupled with different H_2S donors such as 4-hydroxybenzothioamide (TBZ), 5-(4-hydroxyphenyl)-3H-1,2-dithiole-3-thione (ADT-OH), S-ethyl 4-hydroxybenzodithioate (HBTA) and 4-hydroxyphenyl isothiocyanate (HPI).

The synthetized molecules were tested for their H_2S releasing properties by the research group of Prof. Vincenzo Calderone at the Department of Pharmacy of University of Pisa. The analysis were performed by amperometry to evaluate the release of H_2S in the assay buffer, but also in Human Primary Corneal Epithelial Cells (HCEs) to further study the generation of the gas from the tested compounds into the cellular environment.

In the second part I have shown the results of my six months traineeship at the R&D laboratories of Genetic S.p.a. Over the course of this experience I was involved in the development and analysis of different pharmaceutical dosage forms being studied by R&D group. I paid attention on the design of ocular formulations containing the molecular hybrids I synthetized at the University of Naples. Thanks to the expertise of Genetic scientists, we performed preliminary studies to develop antiglaucoma hybrids eye drops.

A recent approach with the purpose of increasing ocular drug bioavailability is based on the application of contact lenses as a means to release drugs. In this scenario, we performed a pilot study based on the design of molecular hybrids eluting contact lenses for glaucoma treatment.

Finally in the appendix, I have discussed about the research project I was involved in during my experience abroad at the Department of Chemistry of University of Durham (UK), in collaboration with the research group of Prof. Ian Baxendale. The first plan was to spend a year at Durham University to learn innovative synthetic techniques, such as flow chemistry, and synthetize through this approach antiglaucoma molecular hybrids. Unfortunately, due to Covid-19 pandemic, international lockdown and University closure, I could spend abroad only the last four months of my PhD. I was involved in another interesting

research project, concerning the synthesis and the characterization of novel 2-amino-3-benzoyl-thiophene derivatives as potential antileishmanial agents. During my stay at the University of Durham, I improved my synthetic skills thanks to the application of new laboratory instruments, and I deepened my knowledge about interpretation of nuclear magnetic resonance (NMR) and mass spectral data.

INDEX

Part I

Synthesis and H_2S releasing properties of molecular hybrids between drugs for glaucoma treatment and H_2S donors

Part I

Synthesis and H_2S releasing properties of molecular hybrids between drugs for glaucoma treatment and H_2S donors.

1. Glaucoma

1.1. Introduction

The glaucomas are a group of optic neuropathies characterized by progressive degeneration of retinal ganglion cells (RGCs) and damage of the optic nerve (1). Glaucoma is the leading cause of irreversible blindness and, to date, 11 million people went blind because of this disease (2). An estimated 76 million adults worldwide, ages 40 to 80, had glaucoma in 2020 and the global prevalence was 3.54%. With advancing age the likelihood of developing glaucoma is higher; therefore, due to the rapid increase in aging population, by 2040 the number of individuals with glaucoma is projected to grow up to 111.8 million (3).

1.2. Anatomy and Pathophysiology of the Eye

1.2.1. Aqueous Humor Flow

Human eye is anatomically divided into two segments known as the anterior and posterior segment. The anterior one constitutes the front third of the eye and, in its turn, is subdivided into the anterior and posterior chamber (Fig. 1).

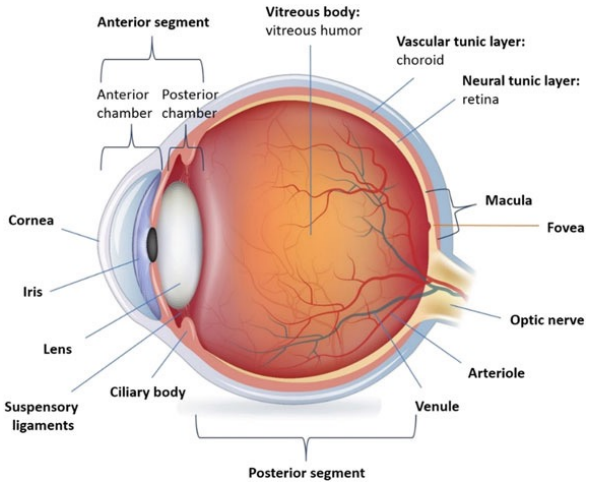

Figure 1. Schematic representation of the basic anatomy of human eye (4).

The anterior chamber is the region of space located between the cornea and the iris and is occupied by aqueous humor (AH) (4), a clear fluid that provides

nutrition, removes excretory products from metabolism, transports neurotransmitters, stabilizes the ocular structure and contributes to the regulation of the homeostasis of these ocular tissues (5).

Although the main cause of glaucoma is unknown and the pathogenesis not completely understood, intraocular pressure (IOP) is the major modifiable risk factor and is regulated by the balance of aqueous humor production and outflow, and episcleral venous pressure as well.

AH is secreted by ciliary body (CB) in the posterior chamber and subsequently passes into the anterior chamber across the pupil. Aqueous humor outflow occurs through two different pathways at the anterior chamber angle: the conventional outflow via the trabecular meshwork (TM) and Schlemm's canal (SC), and the unconventional outflow through uveal tissues (Fig. 2) (5, 6).

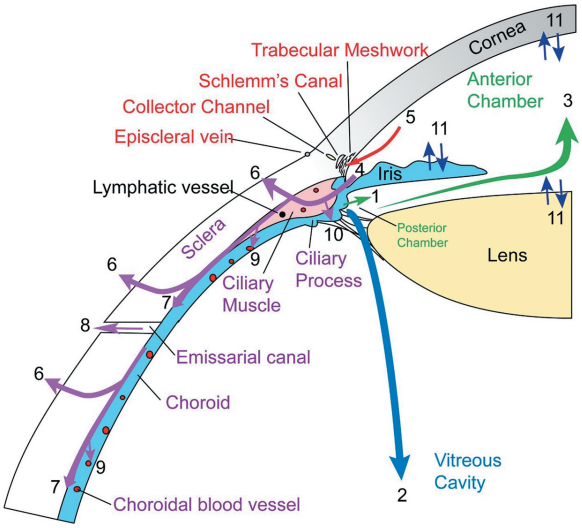

Figure 2. AH is secreted by ciliary process of the ciliary body in the posterior chamber [1] to flow, through the pupil, in the anterior chamber [3]. Some fluid drains across the vitreous cavity [2] and exits the eye. Aqueous humor outflow occurs through two different pathways at the anterior chamber angle: the conventional outflow [5] and the unconventional outflow [4]. The conventional outflow pathway of aqueous humor occurs via the trabecular meshwork, the Schlemm's canal and collector channels, then it joins the episcleral veins and the anterior ciliary veins. In the unconventional outflow pathway, fluid drains through the uveal tissues [6-9]. AH can also return back into the ciliary processes [10], where it is secreted again. There are some exchanges of aqueous humor between iris, lens, and cornea [11], but this is not considered as part of aqueous humor dynamics (7).

Under normal conditions, only the trabecular outflow pathway is relevant for the generation and maintenance of IOP, whereas the drainage via the

unconventional route is independent of the intraocular pressure (1, 4-7). In the conventional pathway, aqueous humor crosses the trabecular meshwork, the juxtacanalicular tissue (JCT) and Schlemm's canal endothelium to reach the lumen of this vessel. After exiting SC, the aqueous humor enters the aqueous veins to join, in the end, the episcleral veins (5, 8). Intraocular pressure builds up in response to the resistance provided by ocular tissues, until is high enough to allow the flow of AH across the TM into SC. The drainage of the fluid is a passive pressure-dependent transcellular mechanism (5) and active transport is not involved, as neither metabolic drugs nor temperature changes influence AH conventional outflow (7).

Aqueous humor also leaves the eye by unconventional route, passing between the bundles of the ciliary muscle. From there, it drains in many directions, including across the sclera, along the supraciliary and suprachoroidal spaces, through emissarial canals, into choroidal vessels and vortex veins, or back into the ciliary processes where is secreted again (9).

1.2.2. Intraocular Pressure

In a healthy human eye, under steady-state conditions, the production equals the outflow of aqueous humor and IOP ranges from 10 to 21 mm Hg (10). With advancing age in a normal human eye, the resistance in trabecular outflow system increases, but this is balanced by a lowered fluid production, thereby leaving intraocular pressure relatively unchanged (5, 8). Usually in patients with glaucoma, there is an increase in IOP due to a reduced outflow facility of aqueous humor (11). However, although higher IOP plays a crucial role in glaucoma development, is not always observed in these patients. As described by several population-based surveys such as the Japanese Tajimi Study, 92% of glaucoma patients involved in this report had IOP within the normal range (12).

1.2.3. Optic Nerve Head and Lamina Cribrosa in Healthy and Glaucomatous Eyes

Based on the evidences above, glaucoma is defined as an optic neuropathy associated with cupping of the optic disc and visual dysfunction that may be

caused by various pathological processes (13). The optic disc (OD) or optic nerve head (ONH), is located 15° nasally to the fovea (the center of the macula) and is composed of neural, vascular and connective tissue (Fig. 3a and 4a). It is the site where retinal ganglion cell axons coalesce, make a 90° turn, and pass through the sclera and lamina cribrosa to exit the globe as optic nerve (6, 11).

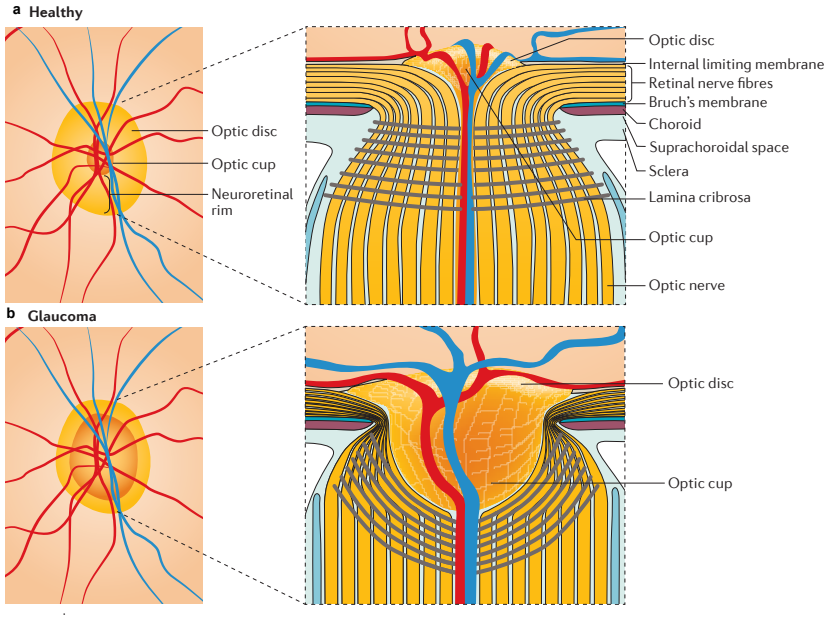

Figure 3. Optic nerve head in healthy and glaucomatous eye. a) ONH in a healthy eye. Retinal ganglion cells axons converge at the ONH and exit the eye passing through the sclera and lamina cribrosa. LC forms a barrier between the intraocular compartment of the eye which has a higher pressure and the extraocular space, where the pressure is lower. The gradient pressure across the lamina cribrosa leads to a physiological cupping of the ONH, forming the optic cup. The ONH consists also of a neuroretinal rim (NRR), occupied by retinal nerve fibre axons. b) ONH in a glaucomatous eye. Biomechanical deformation and remodeling of the ONH are associated with compression and thinning of the lamina cribrosa with following enhanced cupping of the optic cup. NRR loss is one the consequences of glaucoma neuropathies. These pathological changes involve progressive RGCs damage and death (14).

The lamina cribrosa (LC), main structural element of the optic nerve head, forms a barrier between the intraocular space and the retrobulbar space. LC is a perforated collagenous sieve-like structure, whose functions are to allow the RGCs axons and the central retinal vein to get out of the eye, the central retinal artery to enter the globe and to prevent aqueous humor in the vitreous cavity from leaving the eye. The lamina cribrosa stabilizes the IOP by forming a frontier between the intraocular compartment, which has a higher pressure, and the extraocular space, which has a lower pressure (11, 15). Because of its role,

LC is the weakest point in the wall of the pressurized eye, and elevated IOP-induced stress and strain may result in compression, deformation and thinning of the lamina cribrosa with consequent axonal transport damage (1).

The pressure gradient across the lamina cribrosa leads to a backward bowing of the optic disc to form, under physiological conditions, the optic cup (OC), a part devoid of nerve fibre. The OC is surrounded by the neuroretinal rim (NRR), the region of the OD that is occupied by the retinal nerve fibres axons.

The tissues behind the lamina cribrosa may be involved in regulating shape and extent of glaucomatous optic cup. In those regions in which the lamina cribrosa faces the central trunk of the optic nerve, backward bowing may be less marked than in the peripheral regions of the optic disc in which the lamina cribrosa may have indirect contact with the cerebrospinal fluid space (CSF). The latter, in contrast to the solid trunk of the optic nerve, is not able to resist a focally accentuated backward bowing of the LC. In glaucoma patients, the part of peripheral outer LC surface that is in direct contact with the pia mater of optic nerve, and as a result, in indirect contact with the cerebrospinal fluid, is significantly ($P < 0.001$) larger (Fig. 4b) (15), causing a deeper backward movement of LC and, subsequently, an enhanced cupping of the optic disc (Fig. 3b). The reason for the larger exposure of the posterior surface of the lamina cribrosa to the pia mater (and indirectly to the CSF) is that, because of the pathological process of glaucoma, the optic nerve volume inside the pia matter shrinks, decreasing its diameter.

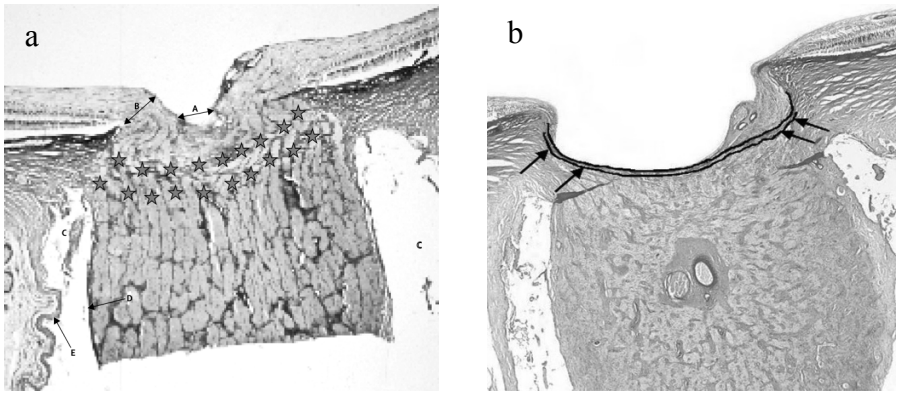

Figure 4. Histophotograph of a a) healthy and b) glaucomatous optic nerve head. In the healthy eye, the figure shows lamina cribrosa between the stars. It is located at the bottom of the optic cup (A), surrounded by the neuroretinal rim (B). The CSF space (C) is between the pia mater (D) and the dura mater of the optic nerve (E). In the glaucomatous eye, lamina cribrosa is thinner

as well the neuroretinal rim, and a deep excavation of the optic cup occurs. The arrows represent the regions of lamina cribrosa in direct contact with the pia mater and indirectly exposed to the cerebrospinal fluid space. Compared to the healthy eye, these regions of LC are significantly ($P < 0.001$) larger (11, 15).

1.2.4. Pattern of Glaucomatous Neuroretinal Rim Loss

The NRR can be partitioned into four quadrants: Inferior (I), Superior (S), Nasal (N) and Temporal (T) (Fig. 5). In a healthy eye, the inferior (I) rim is usually thicker than the superior (S), which is thicker than the nasal (N) rim and the temporal (T) is the thinnest. This is known as the ISNT rule (15).

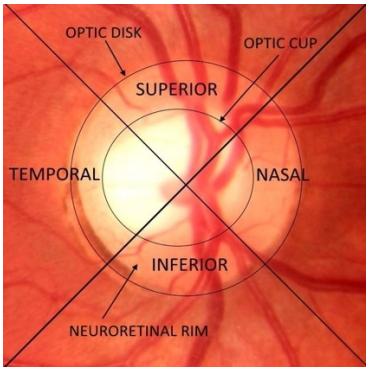

Figure 5. Neuroretinal rim (15).

In the glaucomatous eye, the neuroretinal rim is thinner and its loss occurs in a pattern with early damage preferentially in the inferior and superior disc sectors, breaking the ISNT rule and giving the characteristic vertically elongated excavation of the optic cup (16). The sequence of glaucomatous neuroretinal rim loss (inferotemporal and superotemporal - temporal horizontal - inferonasal - superonasal) suggests an increased susceptibility in these disc regions and agrees with studies (17), by which the early glaucoma defects occur mostly in the upper nasal portion of the visual field, corresponding with a loss of retinal ganglion cells adjacent to the temporal fundus raphe (15).

1.2.5. Retinal Ganglion Cells Degeneration

Retinal ganglion cells (RGCs) are specialized neurons that transmit visual information from the retina to the brain, especially to the retinorecipient areas such as the superior colliculus and lateral geniculate nucleus. RGCs have a large cell body located along the inner margin of the retina. They collect visual

stimulus by dendrites and transmit these signals from the cell body via the axons to the brain. More than 1 million RGCs axons form the optic nerve (18).

Retinal ganglion cells have a high energy consumption but can only be served by a limited blood flow because of the requirement for relative optical transparency and in addition, neurons are known to have a low glycolytic rate. Therefore, the intracellular diffusion of ATP is limited (19). The high metabolic need is reflected by a higher mitochondrial concentration. Mitochondrial respiration results in the generation of oxygen, glucose and pH gradients within a neuron. RGCs are particularly vulnerable to mitochondrial dysfunction and any disruption in the balance between oxygen availability and consumption can be dangerous for their survival (19, 20).

Progressive degeneration of retinal ganglion cells is the main event of glaucomatous optic neuropathy, however because of the slow course of the disease, patients often remain asymptomatic until glaucoma is sever and most of RGCs are lost (1, 6). Retinal ganglion cells death is a self-destructing process and once the pathway is activated, they undergo the intrinsic apoptosis program. RGCs axons in the ONH are the first compartment that are affected by IOP-induced stress in glaucoma. Not much is known about the molecular pathways involved in this process, but one of the factors responsible for axonal damage may be loss of support functions from resident glial cells, as for example loss of energy support. As a consequence, the axons become unable to sustain high energy-needed processes such as axonal transport (21). Alterations of axoplasmic transport occur early in glaucoma. Both anterograde and retrograde transport has been found to be compromised in the ONH of experimental glaucoma animal models (20-22).

A widely accepted mechanism for RGCs death is the blockade of the transport of neurotrophic factors towards the RGC soma following the axonal damage (20-22). One of the most important neurotrophic factor for RGCs survival is BDNF (brain-derived neurotrophic factor), that after being released by glial cells, it binds to TrkB receptors on axonal termini and is transported back to the cell body (20, 23). Quigley *et al*. (24) reported that the retrograde transport of BDNF occurs in rat eyes with experimental glaucoma, but is interrupted because of acute IOP elevation. Indeed they described the accumulation of bound TrkB receptors at the lamina of the rat eyes, supporting the hypothesis

that the BDNF is unable to reach the retina, contributing to the RGCs death. Over the past few years, different studies have shown that exogenous supplement of BDNF to the eyes may protect RGCs in the retina after optic nerve injury (20, 24, 25).

It is well known that excitotoxicity can cause neuronal apoptosis and is implicated in the pathophysiology of glaucoma as well. Excessive stimulation of the glutamatergic system, specifically the N-methyl-D-aspartate receptors subtypes, could contribute to death of retinal ganglion cells in glaucoma. However, data are contradictory and it is not fully understood whether an excess of glutamate has a positive or negative effect on RGCs (26, 27).

1.2.6. Oxidative Stress in Glaucoma Neuropathies

Oxidative stress can be defined as an increase over physiologic values in the intracellular concentration of reactive oxygen species (ROS) (28). These oxidants are generated during physiological processes and they have essential functions for the cells, however when the production of ROS exceeds the capacity of anti-oxidants to neutralize them, ROS are responsible for damages to macromolecules including DNA, proteins, and lipids. To date, many studies have confirmed that oxidative stress is involved in different neurodegenerative diseases like Alzheimer's disease and Parkinson's disease, but it is implicated also in ocular neuropathies like glaucoma (28).

Under normal conditions, aqueous humor contains several active oxidative agents such as hydrogen peroxide (H_2O_2) and superoxide anion (O_2^-), however, chronic oxidative stress caused by a higher concentration of ROS, can be dangerous for multiple ocular tissues via different mechanisms. In AH of POAG (primary open angle glaucoma) patients, has been detected a reduction in the level of antioxidants like glutathione (GSH), ascorbate and tyrosine as well as a significant increase in superoxide dismutase (SOD) and glutathione peroxidase activities. These data are consistent with the onset of oxidative stress in glaucomatous eye due to an elevated concentration of ROS (28).

Mitochondria have a main role in this process because they produce reactive oxygen species, but at the same time, are extremely sensitive to ROS-induced damage. Mitochondrial disfunction causes reduction of ATP synthesis and

increased production of ROS. In addition, elevated IOP is one of the reasons why ROS concentration increases. Studies have provided evidence that oxidative stress in the eyes of glaucoma patients affects blood flow to the optic nerve, limiting the oxygen supply in the retina and increasing the accumulation of ROS; alters trabecular meshwork structure impairing AH outflow; promotes retinal ganglion cells apoptosis and glial cells dysfunction (29).

1.2.7. Effects of Ligands for Serotonin 5-HT_{1A} and 5-HT_{2A} Receptors in Glaucoma Models

Serotonin (5-hydroxytryptamine, 5-HT) is an important neuromodulator in the central and peripheral nervous systems (CNS and PNS, respectively), which plays a critical role in a wide range of pathophysiological processes. Several studies have suggested that serotonin is actually involved in the pathogenesis of glaucoma. 5-HT is present in the cornea, iris and ciliary body of mammalian eyes and has been detected in the AH of different species, including humans (30). However, the role of serotonin and its receptors in glaucoma is not yet fully understood. It is known that the inhibitors of 5-HT uptake cause an increase in IOP leading to a secondary form of glaucoma called drug-induced glaucoma.

5-HT_{1A} and 5-HT_2 receptors have been detected in iris-ciliary body tissue in the rabbit. Also studies on human iris-ciliary body complex support the existence of 5-HT_1 receptors. Topically administration of 8-OH-DPAT, a 5-HT_{1A} agonist, lowers IOP in ocular normotensive rabbits. Similarly, flesinoxan, a highly potent and full 5-HT_{1A} agonist, when applied topically to the rabbit eye, reduces IOP. Moreover, it has been shown that 8-OH-DPAT and flesinoxan have also neuroprotective properties on rabbit retina, reducing the ischemia/reperfusion related damage and NMDA toxicity (31). However, the administration of 5-HT_{1A} agonists failed in ocular normotensive and ocular hypertensive eyes of Cynomolgus monkeys, showing a variable response between different species. 5-HT_2 receptor antagonists like ketanserin, lower IOP in ocular normotensive rabbit and in human eye, but these molecules also have α_1-adrenergic receptor antagonist activity and is likely that the reducing IOP effect is associated with the adrenergic antagonism (30). May *et al.* (32) tested in Cynomolgus monkey

the effect of (±)-DOI, a high-affinity partial agonist towards the 5-HT_{2A} receptor, demonstrating a reduction of IOP. This result is encouraging because human CB and TM contain mRNAs for 5-HT_{2A-C} receptors, but only 5-HT_{2A} subtype is functionally active and pharmacologically responsive (30).
Further studies to better describe the effects of serotonin and 5-HT receptors in the IOP regulation process are needed to obtain new potent and effective agents for the treatment of glaucoma.

1.3. Classification

Based on the morphology of the anterior chamber angle, glaucomas can be classified in open-angle glaucoma (OAG) and angle-closure glaucoma (ACG) (Fig. 6) (1, 4, 6, 11, 13, 18).

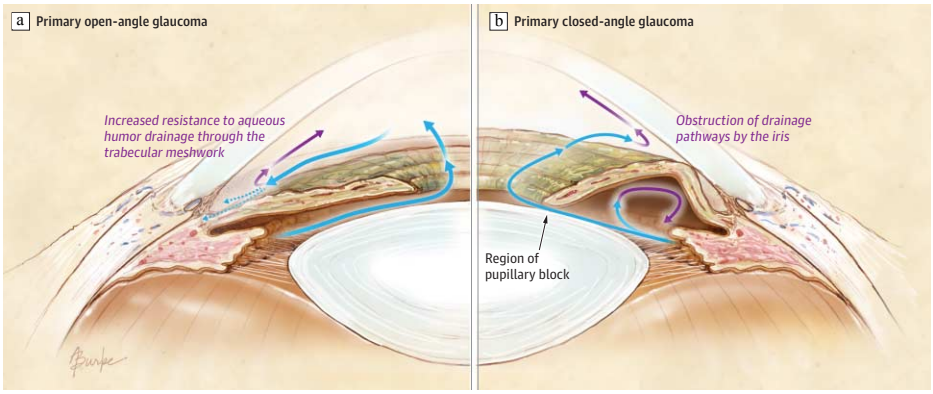

Figure 6. Open angle glaucoma and angle-closure glaucoma. a) In eyes with open-angle glaucoma, increased resistance through the trabecular meshwork causes increase in IOP, however, no obstruction is clinically visible. In angle-closure glaucoma, anatomic crowding of the iris causes blockage of aqueous humor outflow via TM. Pupillary block is the main mechanism responsible for PACG. The obstruction of AH flow through the pupil towards the anterior chamber causes higher pressure in the posterior chamber that pushes the peripheral iris forward the iridocorneal angle, against the trabecular meshwork (1).

In eyes with open-angle glaucoma there are no clinically visible perturbations in the anterior chamber angle and the aqueous humor has free access to the trabecular meshwork; in contrast, in eyes with angle-closure glaucoma the peripheral iris is anatomically in contact with the peripheral cornea and the trabecular meshwork, reducing or blocking AH drainage (4). Both open-angle and angle-closure glaucoma can be subcategorized into primary or secondary,

depending on the absence or the presence, respectively, of other disorders or conditions associated with this disease (Table 1). The main causes of primary glaucomas are still unknown, while the secondary types can occur because of neoplasia, inflammation, advanced cataract, diabetes, trauma, medications. More then 60 forms of glaucomas have been described and some of them are reported in the table below (6, 11).

Table 1: Glaucomas classification.

Open Angle Glaucoma (OAG)	Angle Closure Glaucoma (ACG)
Primary open angle glaucoma	**Primary angle closure glaucoma:**
Secondary OAG:	-Pupillary block
-Pigmentary glaucoma	-Plateau iris
-Pseudoexfoliation glaucoma	**Secondary ACG:**
-Uveitic glaucoma	-Drug induced glaucoma
-Steroid-induced glaucoma	-Neovascular glaucoma
-Traumatic glaucoma	-Lens induced glaucoma
-Glaucoma associated with increased episcleral venous pressure	

1.3.1. Primary Open Angle Glaucoma

Primary open angle glaucoma (POAG) is a chronic, slowly progressive, multifactorial, generally bilateral, but often asymmetrical, optic neuropathy. The main clinical features of POAG are open iridocorneal angle, absence of other causes of damage related to the nerve fiber bundles and cupping of the ONH with corresponding loss of visual field. POAG is the most common form of glaucomatous neuropathy and the overall global prevalence in the last 20 years on population over 40 years is 2,4% (95% CI 2,0-2,8) (33). As mentioned before, high IOP is not always detected. Patients affected by POAG can have normal levels of intraocular pressure but the optic nerve damage occurs as well. This condition has been called normal-tension glaucoma (NTG) (11, 12). POAG has an adult onset, and because patients are usually asymptomatic in the first stage, an early detection may arrest or slow the progression of the disease (6, 26, 27). If undetected and untreated, POAG may cause significant visual impairments. Population-based studies in developing countries with poor access

to eye care have confirmed that untreated POAG is a major cause of blindness (34).

There is good evidence that aging, elevated IOP, family history of primary open-angle glaucoma (35), race and other disorders like diabetes mellitus, systemic hypertension, myopia, are some of the risk factors that may influence the development of POAG (26, 27).

Genome-wide association studies have identified various loci involved in different types of glaucoma (14). The gene Myocilin (MYOC) at the GLC1A locus was the first gene to be associated with primary open-angle glaucoma. The function of corresponding protein myocilin is unknown but is produced in many tissues, including ciliary body and trabecular meshwork (36). MYOC mutations are common in patients with juvenile form of open-angle glaucoma (JOAG), but several studies have demonstrated that Myocilin mutations are found also in 3-4% of patients with adult-onset POAG (27, 37).

Treatment of POAG aims to improve the quality of life of patient, preserving the vision. IOP reduction is the only proven and accepted means to prevent or slow the progression of glaucoma. Lowering intraocular pressure has shown to be effective also for patients with normal tension glaucoma. Reduction of IOP can be achieved by topical medications, laser trabeculoplasty or surgery (6, 11, 14).

1.3.2. Primary Angle Closure Glaucoma

Patients with narrow anterior chamber angle, due to a crowded anterior segment anatomy, may develop primary angle-closure disease. PACG is diagnosed when angle closure occurs with following elevation of IOP, optic nerve damage and visual field changes. The gold standard to visualize the anatomical structure of the anterior chamber angle is gonioscopy, an exam performed by ophthalmologists (38).

Pupillary block is the most common mechanism responsible for PACG. In predisposed eyes, usually smaller and hyperopic, the contact between the lens and the iris at the pupil is closer than normal. Anatomical abnormalities such as shallow anterior chamber, anterior insertion of the iris in the ciliary body, small cornea, thick lens can cause resistance of the flow of AH from the posterior

chamber to the anterior chamber through the pupil. This pupillary block causes higher pressure in the posterior chamber that pushes the peripheral iris forward the iridocorneal angle, against the trabecular meshwork. As a result, the drainage of AH from the eye is obstructed and the intraocular pressure rises (11, 26, 38, 39). Surgical peripheral iridectomy or laser iridotomy can be useful for the treatment of angle-closure glaucoma with pupillary block. These procedures, respectively by the removal of tissue or creating an opening in the iris, allow the aqueous humor to flow from the posterior chamber to the anterior chamber of the eye, through an alternative route avoiding the pupil. As a result, the pressure differential between the two chambers decreases and the peripheral iris is not pushed anymore forward the trabecular meshwork (26).

Another mechanism responsible for PACG is plateau iris. It is necessary to distinguish plateau iris configuration and plateau iris syndrome. The main feature of these conditions is that the iris plane is flat, unlike pupillary block where the iris bows anteriorly. Plateau iris configuration consists of an eye with normal anterior chamber depth whose iris plane is flat from pupil to periphery until, near its insertion in the ciliary body, it takes a sharp turn. This twist causes a narrow angle that obstructs AH outflow. Plateau iris configuration can be detected by gonioscopy but iridectomy or iridotomy are not effective treatments for this form of angle-closure glaucoma because the flow of aqueous humor through the pupil is not involved. Some cases of PACG present both plateau iris and pupillary block, the latter representing the predominant mechanism. Unfortunately, often it is no possible to recognize one condition from the other through visual examination, until iridectomy is performed. Those rare cases, where angle closure remains unchanged following the iridectomy, are named plateau iris syndrome. It occurs usually shortly after the surgical or laser intervention, but it may also be detected after months or years (26, 38, 39).

According to the clinical presentation, ophthalmologists classify PACG in acute, intermittent or subacute, and chronic. Acute attacks of PACG consist of sudden onset of angle closure due to the iris that quickly and totally covers the trabecular meshwork, leading to a symptomatic elevation of intraocular pressure, sometimes even higher than 70 mmHg. Typical manifestations of acute PACG are eye pain and decreased vision. Subacute angle closure is characterized by recurrent and self-limiting episodes of mild ocular pain and

elevation of IOP. Unlike acute attacks, chronic PACG is gradual and asymptomatic. Progressive closure of the angle results in increased IOP over the time and optic nerve damage (26, 38, 39). Acute angle-closure glaucoma is an ophthalmic emergency which needs to be early recognized and treated by immediate medical therapy, aiming to reduce IOP (40).

The analysis conducted by George *et al.* (41) confirmed the data of many individual studies, according to which PACG causes significantly more cases of blindness (95% CI 1.99-2.87) compared to POAG. Family history (35), age and gender represent risk factors for development of PACG. Moreover, the prevalence of this form of glaucoma increases with age and is more common in females (42).

1.4. Risk Factors

In addition to elevated intraocular pressure, there are common risk factors for the development of glaucomas. Age is one of them and meta-analysis of population-based studies have demonstrated that the odds ratio for POAG is 1.73 (95% CI 1.63-1.82) for each decade increase in age beyond 40 years (11). Ethnicity plays an important role in the incidence of glaucoma. African population has the highest prevalence of glaucoma (6.11%, CI 3.83-9.13) and primary open-angle glaucoma (5.40%, CI 3.17-8.27), while the prevalence of primary angle-closure glaucoma is higher in Asian Chinese population than in Europeans and Africans because of the peculiar almond-shape eyes associated with a narrower angle (35).

Family history of glaucoma is strongly correlated with every form of this neuropathy, particularly first-degree relatives of individuals with POAG have up to an eight-fold increased risk of developing the disease compared with the general population (14).

The primary thickness of lamina cribrosa is a significant risk factor. Studies have shown that patients with severe myopia have a thinner lamina cribrosa, and this could be the reason why they have also a higher risk to be affected by glaucoma. Several clinic-based and case-control studies have suggested a relationship between glaucoma and myopia. The Blue Mountains Eye Study confirmed this relation, considering also the effects of other known glaucoma

risk factors. This association is present for eyes with low myopia and stronger for eyes with moderate-to-high myopia. Myopic eyes have also a slightly higher IOP than emmetropic or hyperopic eyes (43).

An abnormally thin LC could be one of the risk factors for primary glaucoma in patients with normal intraocular pressure. Furthermore, in these patients the cerebrospinal fluid pressure may be low, leading to an increased pressure difference between the intraocular and the retroocular space and a heightened susceptibility of optic nerve fibers.

A thin central cornea is considered as a risk factor for the incidence of glaucoma because central corneal thickness affects IOP measurements giving lower measured IOP levels. In addition, a thin cornea may be also a structural risk factor because of a hypothetical relationship with a thin lamina cribrosa (15).

Systemic hypertension, diabetes mellitus, cardiovascular disease, thyroid disorders are some of the systemic risk factors correlated with the prevalence of glaucoma. Low blood pressure might also be associated with the risk of developing this ocular neuropathy by reducing ocular perfusion pressure (the difference between systemic blood pressure and IOP) with following poor perfusion of the optic nerve. However, the evidence for the potential relationship between these systemic factors and glaucoma is weak (14).

Nutritional factors may be involved in the progression of glaucoma and the results of the study conducted by Coleman *et al*. demonstrated that a higher intake of certain fruits and vegetables full of vitamin A, C and B2, may be associated with a reduced risk of glaucoma in older woman (44).

1.5. Pharmacological Treatment

Treatment of glaucoma neuropathies aims to reduce IOP, and on the basis of causes, risk factors, severity and type of glaucoma, different medical options like topical therapy, oral therapy, surgery or laser procedure are available. First-line treatment for most form of glaucomas consists of the topical application through eye drops of IOP-lowering drugs in monotherapy or as drug combinations. Different class of medications are used to treat glaucoma and they either increase the outflow of AH from the eye (prostaglandin analogs,

cholinomimetics) or reduce its formation (α_2-adrenergic agonists, β-adrenergic antagonists, carbonic anhydrase inhibitors) (6, 11).

1.5.1. Prostaglandin analogs

Prostaglandins (PG) are endogenous fatty acids produced physiologically in our body. Prostaglandin analogs applied as eye drops on ocular surface, can reduce IOP by increasing the outflow of AH through the uveoscleral pathway. The exact mechanism of action is unknown but they stimulate PG receptors in the eye leading to relaxation of the ciliary muscles and reduction of extracellular matrix between muscle fibers, improving the drainage of the fluid from the eye. Prostaglandins available for therapies include latanoprost **1** (0.005%), bimatoprost **2** (0.03%), travoprost **3** (0.004%) and tafluprost **4** (0.0015%) (Fig. 7).

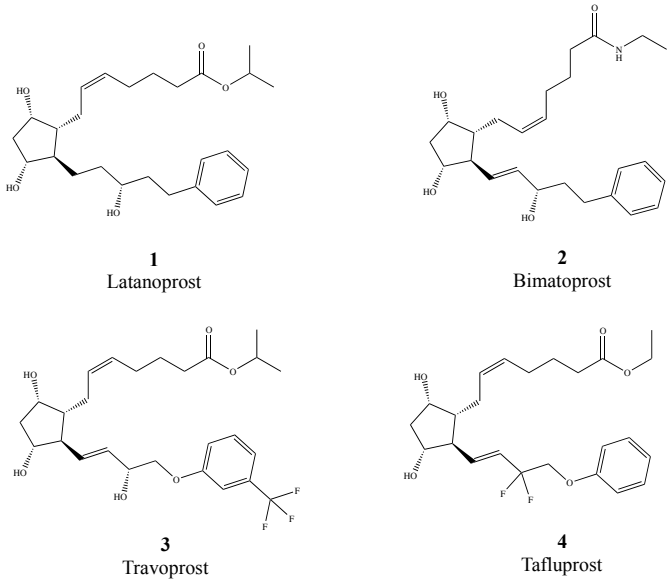

Figure 7. Chemical structures of prostaglandin analogs: Latanoprost (**1**), Bimatoprost (**2**), Travoprost (**3**), Tafluprost (**4**).

Latanoprost, travoprost and tafluprost are formulated as isopropryl ester prodrugs of their corresponding fatty acids. Bimatoprost is an amide and is often referred to as a prostamide. Once absorbed in the cornea, these agents undergo hydrolysis to free the acid prostaglandin (45). This group of drugs can reduce IOP up to 40%, they have minimal side effects since are administrated in a very low dosage and are applied once a day. For these reasons, prostaglandin analogs represent for many patients the first choice treatment. However they can cause

ocular inflammation, increased iris and periocular skin pigmentation or conjunctival hyperemia (45, 46).

1.5.2. Cholinomimetics

Pilocarpine **5** and carbachol **6** are cholinomimetics or miotics used to treat glaucoma (Fig. 8). They bind muscarinic receptors in the ciliary body and through muscle contraction, increase aqueous humor outflow from the eye via the TM pathway. Although IOP reduction following their topical administration can reach up to 40%, the cholinomimetics use is limited because of their known side effects profile and the frequent administration (1-2 drops up to 6 times/day) (46, 47). Main ocular side effects include pupillary miosis, refractive myopia, cataract formation, accommodative spasm while systemic side effects consist of vomiting, nausea, diarrhea, tachycardia, bronchospasm and sweating (48).

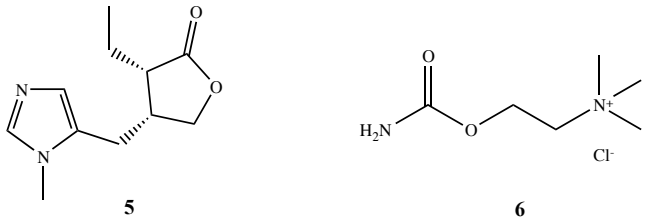

5
Pilocarpine

6
Carbachol

Figure 8. Cholinomimetics for the treatment of glaucoma.

1.5.3. α_2-Adrenergic agonists

α_2-Adrenergic agonists act as vasoconstrictor at the level of ciliary body and reduce aqueous humor production (Fig. 9). Apraclonidine **7**, a less lipophilic derivative of clonidine **8**, is a α_1, α_2-selective agonist, approved by FDA for the prevention of IOP spikes after laser iridotomy procedures (48). It is indicated for short-term adjunctive treatment in patients on maximally tolerated medical therapy with uncontrolled IOP in order to delay surgery. Long-term treatments are limited because of high rates of tachyphylaxis (47).

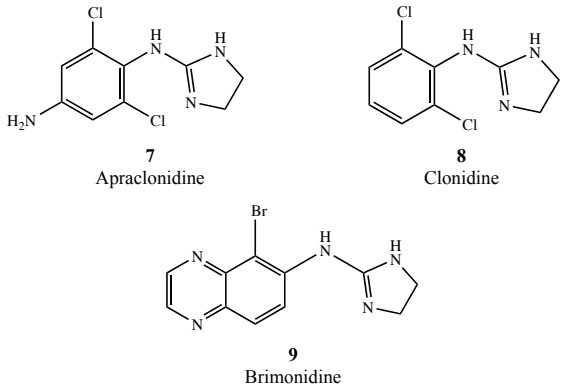

Figure 9. Chemical structures of Apraclonidine (**7**), Clonidine (**8**) and Brimonidine (**9**).

Brimonidine **9** is a α_2-selective agonist and is the most prescribed medication among the drugs belonging to this class. Brimonidine is able to reduce AH production and also to increase the outflow via uveoscleral pathway. Studies have proven that this drug also shows neuroprotective effects on RGCs after optic nerve crush injury. The mean IOP reduction reached by brimonidine eye drops instillation (2h after instillation) is 26% (47). The IOP-lowering effect is comparable to those of β-blockers like timolol or betaxolol. Brimonidine is more lipophilic than apraclonidine, is used at lower concentration (0.2%) and it has less local side effects including blepharoconjunctivitis. Systemic side effects include dry mouth, dry nose, fatigue and headache (47). Compared to clonidine and apraclonidine, brimonidine does not affect ocular blood flow or visual field quality. It is contraindicated in infants, children, and in patients receiving monoamino oxidase inhibitors (48).

1.5.4. β-Adrenergic Antagonists

β-Adrenergic antagonists or β-blockers reduce IOP by decreasing AH production after the inhibition of β-receptors in the ciliary body. These drugs have been the most used medications all over the world to treat glaucoma. They are divided in two categories: non-selective β-blockers and selective (or cardioselective) β-blockers (Fig.10) (47).

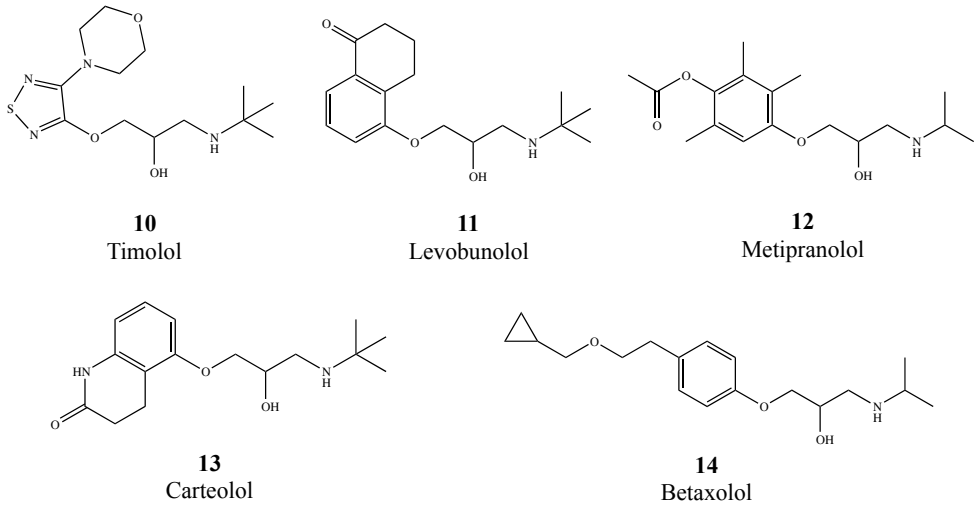

10
Timolol

11
Levobunolol

12
Metipranolol

13
Carteolol

14
Betaxolol

Figure 10. Chemical structures of β-blockers.

Timolol **10**, levobunolol **11**, metipranolol **12** and carteolol **13** belong to non-selective β-blockers and inhibit both β_1 and β_2 receptors. These drugs are applied topically but, however, can be absorbed and may have several systemic side effects involving cardiovascular and bronchopulmonary functionality, like bradycardia, arrhythmia, bronchospasm or worsening of asthma (48).

Timolol was released for use in ophthalmology in 1978 (49). It is available in 0.1, 0.25 and 0.5% eye drops solution, to apply twice a day, or as gel formulation to apply once a day (47). After 7 hours from instillation, timolol 0.5% can lower IOP by up to 50%. It has been proved that this drug is more effective during daytime, with a nocturnal efficacy reduced to half that achieved during the day. Anyway, timolol is effective as latanoprost during the daytime (50). Several fixed dose combinations between timolol and other antiglaucoma drugs (timolol 0.5%/dorzolamide 2%, timolol 0.5%/latanoprost 0.005%, timolol 0.5%/brinzolamide 0.2%) are currently used in therapy, providing a greater reduction in IOP and a better safety profiles than concomitant administration of the two constituents.

Levobunolol shows similar efficacy and safety of timolol. Eye drops solution (0.5 or 1%) applied twice a day, reduce IOP by a mean of 27%. Levobunolol inhibits AH production and also leads to ciliary artery dilatation because of the blockade of Ca^{2+} channels (47).

Metipranolol from 0.1 to 0.6% decreases IOP in the same measure of timolol 0.25 or 0.5% and levobunolol 0.5%, with a mean reduction by 20-29% (47).

Long term use of metipranolol has been associated with episodes of granulomatous anterior uveitis even if the etiology of intraocular inflammation caused by this drug remains unclear. Metipranolol has also shown antioxidant proprieties (48).

Carteolol is a non selective β-adrenergic antagonist but, at the same time, is a partial β-adrenergic agonist. Due to this peculiar activity, less local and systemic side effects like respiratory and cardiovascular effects, may occur. However no significant differences have been reported between topical administration of carteolol 1% and timolol 0.5% about ocular hypotensive action and safety profile (47).

Betaxolol **14** is a selective β_1-adrenergic antagonist used for the pharmacological treatment of glaucoma. Applied as 0.25 or 0.5% eye drops, reduces IOP in a range from 13 to 30%. Although mean IOP reduction following betaxolol application is lower than that following timolol administration, betaxolol shows less systemic side effects. In addition, this drug improves ocular blood flow and visual function, suggesting a neuroprotective role. Reduced pulmonary side effects associated with the higher affinity of betaxolol for cardiac β_1 receptors, make this agent useful for glaucoma patients with pre-existing pulmonary disease (47-49).

1.5.5. Carbonic anhydrase inhibitors

Carbonic anhydrase (CA) inhibitors are used in therapy as diuretics, antiglaucoma drugs, antiepileptics (Fig. 11). They inhibit carbonic anhydrase, an enzyme responsible for hydration of CO_2 to bicarbonate and protons. In the management of glaucoma they reduce AH production in the ciliary body and, as a result, IOP is decreased. The CA isoforms involved in glaucoma are CA II, IV and XII. The first generation of systemic CA inhibitors (acetazolamide **15**, methazolamide **16** and ethoxzolamide **17**) are highly effective in inhibiting CA isoforms present in the ciliary body, with following IOP reduction by 25-30%, however they have several side effects due to the blockade of CA isoforms all over the body (51).

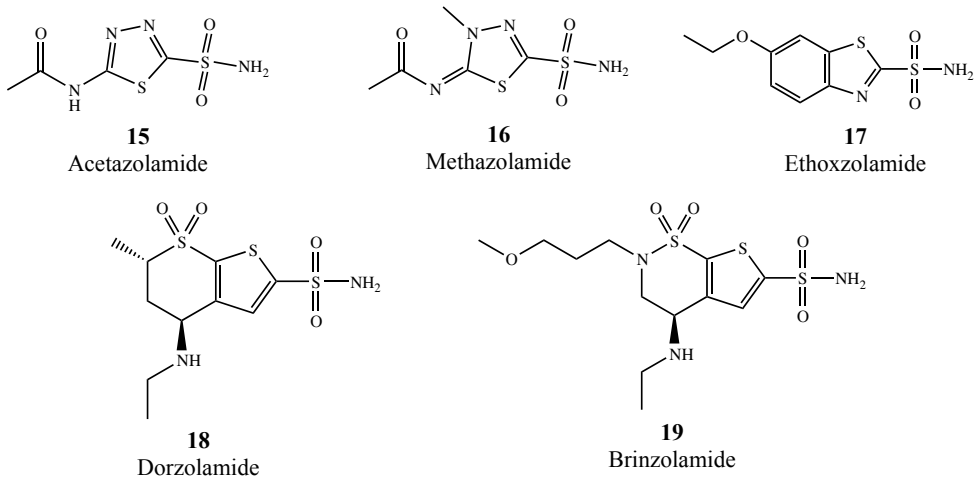

Figure 11. Carbonic anhydrase inhibitors.

The second generation of CA inhibitors (dorzolamide **18** and brinzolamide **19**) are currently used to treat glaucoma, since they are available as topical eye drops and act selectively on the CA isoforms of ciliary epithelium (46). Dorzolamide is applied as 2% solution and brinzolamide as 1% suspension, both twice a day (51). These agents may reduce IOP by up to 20% and show a synergistic effect when they are applied as combinations with other antiglaucoma drugs. Moreover also ocular blood flow is improved. Main ocular side effects following topical CA inhibitors administration include stinging, burning and itching (48).

1.5.6. New targets for antiglaucoma drugs

Despite the established success of the mentioned therapies, some patients are still unable to control or lower IOP toward a target level that ensures a slower rate of the disease progression. Lately, new targets have been approached and novel therapeutic agents could be available soon.

Rho kinase inhibitors (Fig. 12), as ripasudil **20** and netarsudil **21**, are inhibitors of ROCK1 and ROCK2, Rho-associated proteins kinases that act as effectors of Rho proteins family (RhoA, RhoB, RhoC). In the eye, ROCKs proteins are expressed in TM, SC, ciliary muscle and optic nerve head and their inhibition leads to reduction of AH outflow resistance (48). Rho inhibitors acting on cytoskeleton and extracellular matrix, modify TM and Schlemm's canal, improving conventional outflow pathway of the fluid (51, 52).

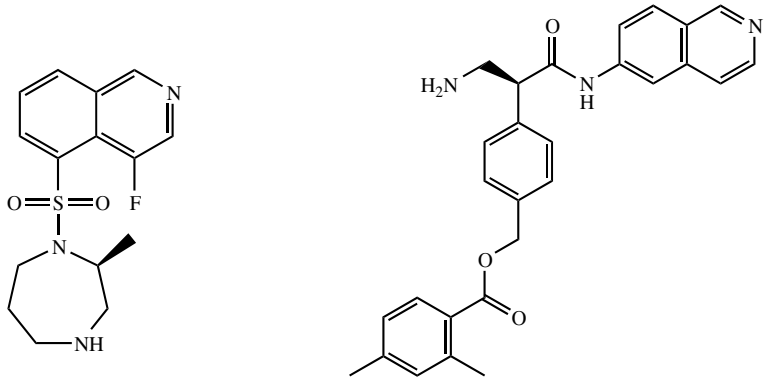

20
Ripasudil

21
Netarsudil

Figure 12. Chemical structures of Rho-kinase inhibitors.

Nitric oxide (NO) is an endogenous gas-transmitter and in the last years different studies have proven that it plays a role in IOP control and glaucoma pathology, showing that exogenous administration through NO-releasing compounds decreases IOP. Latanoprostene bunod (LBN) **22** is a molecular hybrid between latanoprost and butanediol mononitrate, a nitric oxide donating molecule (Fig. 13). Once applied, is hydrolyzed by corneal esterase into its active agents latanoprost acid and butanediol mononitrate, that is in turn metabolized to free NO. The combination of two active compounds enhances IOP reduction since latanoprost improves uveoscleral pathway and NO increases trabecular outflow (48). LBN has been approved in United States in 2017 (52).

Adenosine, an endogenous nucleoside, and its receptors (A1, A2a, A2b and A3) can regulate IOP. Studies have found that A1 activation in the ciliary body reduces AH formation, while A1 activation in TM and SC improves the fluid outflow. In contrast non- A1 receptors stimulation increases IOP (52). Trabodenoson **23** is an adenosine analogue and a potent A1 receptor agonist (Fig. 13). In normotensive Cynomolgous monkeys and in rabbits, administrated respectively at doses of 10-1000 μg and 5-150 μg, this compound brings to IOP reduction by 20-25% (48).

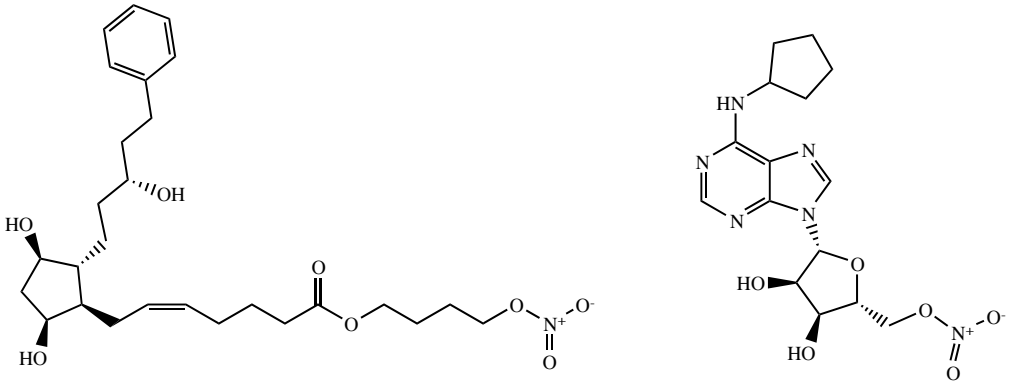

22
Latanoprostene bunod

23
Trabodenoson

Figure 13. Chemical structures of Latanoprostene bunod (**22**) and Trabodenoson (**23**).

2. H_2S

2.1. Introduction

H_2S is a colorless, flammable and pungent gas. Although was traditionally considered as a toxic compound, recently H_2S has been recognized as third endogenous gas-transmitter, besides nitric oxide (NO) and carbon monoxide (CO) (53). Several studies have shown that it plays a role in different physio-pathological processes (Fig.14), for example acts as cardioprotective agent (54), modulates inflammation (55), reduces oxidative stress (56), induces bronchial relaxation (57), provides a cytoprotective effect (58).

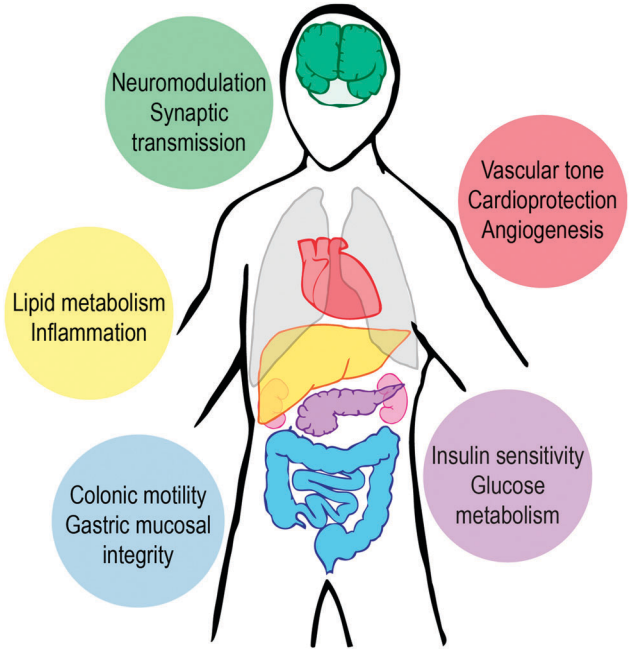

Figure 14. Some of the physiological activities of H_2S in human body. H_2S is involved as signaling molecule in the brain, cardiovascular system, endocrine system, and gastrointestinal system (59).

2.2. Properties of Hydrogen Sulfide

H_2S is a hydrogenated sulfur compound with the sulfur oxidation state that is -2. This molecule is similar to water but H_2S has a 92.1° bond angle (Fig. 15) and the electronegativity of sulfur is comparable to that of hydrogen (respectively 2.44 and 2.20), therefore the dipolar moment is lower (0.97 D) than for water (1.85 D).

Figure 15. Molecular structure of water (H_2O) and hydrogen sulfide (H_2S).

As a result, H_2S is unable to form hydrogen bonds and is a gaseous molecule at atmospheric pressure and ambient temperature, with a boiling point of 60°C (60).

H_2S is water soluble (101.3 mM/atm at 25°C) and in aqueous solution is a weak acid with pKa_1 value of 6.98 at 25°C (6.76 at 37°C) and pKa_2 of 19 (Fig.16).

$$H_2S \overset{ka_1}{\rightleftharpoons} H^+ + HS^- \overset{ka_2}{\rightleftharpoons} 2H^+ + S^{2-}$$

Figure 16. Dissociation of H_2S.

At physiological pH and 37°C, the hydrosulfide anion HS^- is the predominant sulfide species while the sulfide anion S^{2-} is present at extremely low concentration. Both species H_2S and HS^- are responsible for the biological activities of H_2S and, in addition, HS^- is a nucleophile, which quickly reacts with endogenous electrophile and metal center in biological molecules.

H_2S is a lipophilic compound and easily crosses lipid bilayer membranes of cells (61).

2.3. Production and Catabolic Pathways

In mammals, H_2S is produced through both enzymatic and non enzymatic pathways, but the enzymatic route is the main endogenous source of this gas. Enzymes involved in H_2S production are CBS (cystathionine β-synthase), CSE (cystathionine γ-liase), MST (3-mercaptopyruvate sulfurtransferase) and CAT (cysteine aminotransferase) (Fig. 17) (62).

2.3.1. CBS

Cystathionine β-synthase catalyzes the β-replacement of L-serine with L-homocysteine (Hcy) to form L-cystathionine and water. This reaction

constitutes one step of the reverse transulfuration pathway that transforms methionine in cysteine via cystathionine.

When cysteine replaces serine as substrate in the β-replacement reaction, H_2S is released. In addition, CBS is involved in the substitution of cysteine by water to give serine and H_2S, and in the condensation of two molecules of cysteine to release lanthionine and H_2S. However, the reaction between cysteine and homocysteine is the kinetically favorite to produce H_2S (63).

Maclean and Kraus (64) found that in the reaction with homocysteine, L-serine is a better substrate than cysteine, and serine is more abundant than cysteine inside the cells. These data could explain the reason why serine inhibits the formation of H_2S from cysteine and 2-mercaptoethanol by 50% even in the presence of a sixfold higher concentration of cysteine.

CBS is a pyridoxal-phosphate (PLP, vitamin B6) dependent enzyme. Is a homotetramer consisting of 63-kDa subunits and every monomer is formed by 551 amino acid residues. The NH_2 terminal presents the binding sites for PLP and for heme, the latter acting as redox-dependent gas sensor. The COOH terminal domain, instead, is responsible for S-adenosyl-L-methionine (AdoMet or SAM) binding and following activation of the enzyme (65).

CBS was first found in the brain and is preferentially expressed in astrocytes. However, further studies have demonstrated that CBS is present also in the vascular endothelial cells (65).

2.3.2. CSE

Cysthathionine γ-liase catalyzes the next step of the reverse transulfuration pathway, which is the hydrolysis of C-γ-S bond of cystathionine to give L-cysteine, α-ketobutyrate and ammonia. The same reaction, starting from homocysteine alone, produces H_2S. CSE is also involved in the α, β-elimination of L-cysteine to form H_2S, NH_3 and pyruvate. This enzyme catalyzes the reactions route that gives L-cystine, through the formation of thiocysteine, pyruvate and NH_3, producing subsequently cysteine, S-alkenyl-mercaptocysteine (CysSR) and H_2S (65).

However, CSE has a strict specificity for L-cysteine as main substrate for H_2S production and it has been demonstrated that exogenous administration of L-

cysteine increases CSE expression and sulfide generation, with consequential protective effects in ischemic heart (66).

CSE is present in cardiovascular and respiratory system and is responsible for H_2S production also in the liver, kidney, uterus, placenta and pancreatic islets while CSE levels in brain are very low.

This enzyme is a tetramer and every subunit has a molecular weight of 54 kDa. It is located in the cytoplasm and is a PLP-dependent enzyme (65).

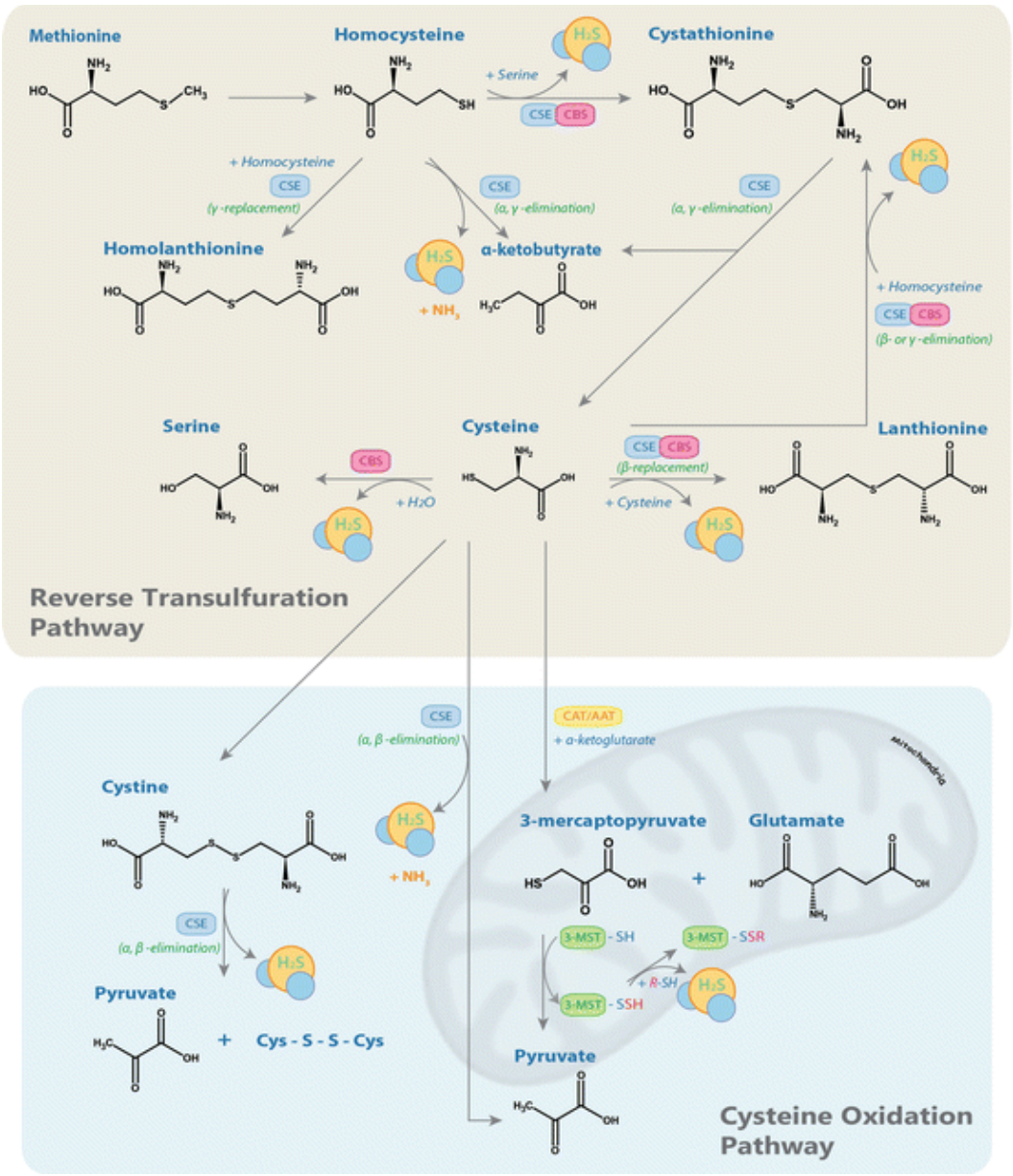

Figure 17. Enzymatic pathways involved in H_2S production. Endogenous generation of H_2S is based mainly on reverse transulfuration pathway and oxidation of cysteine. Some of these reactions occur in the mitochondria. CBS= cystathionine β-synthase; CSE= cystathionine γ-liase; 3-MST= 3-mercaptopyruvate sulfurtransferase; CAT= cysteine aminotransferase (62).

2.3.3. MST and CAT

β-mercaptopyruvate sulfurtransferase (MST) and cysteine aminotransferase (CAT) work together in the same pathway to produce sulfane sulfur. CAT catalyzes the transamination reaction between cysteine and α-ketoglutarate to form 3-mercaptopyruvate (3-MP), that is the substrate of MST. The latter is involved in the transfer of the sulfur from 3-MP to the cysteine located in its active site to give persulfide and pyruvate. Subsequently, from MST-bound persulfide, in the presence of a reductant like thioredoxin, DTT and DHLA, H_2S is released (65).

MST and CAT are localized in the cytosol and mitochondria. MST is an enzyme zinc-dependent; CAT uses PLP as cofactor. Aspartate is a potent inhibitor of CAT and while the cellular concentration of cysteine in many tissues is low (~ 30-100 μM), the aspartate concentration is high (for example ~ 730 μM and 4 mM in mouse liver and brain). However, the mitochondrial cysteine concentration in rat is higher (~ 0.7-1 mM) and the contribution to H_2S production from MST/CAT pathway is increased in tissues where the concentration of cysteine is higher or the expression of CBS and/or CSE is lower (63).

MST is expressed in kidney, liver, aorta, brain, vascular endothelial tissues and smooth muscles while CAT is present in the vascular endothelium (63).

2.3.4. Non-enzymatic Production of H_2S

Endogenous production of H_2S through non-enzymatic pathways are a minor source of this gas (65) and the involved processes are still not well characterized. The non-enzymatic reduction of elemental sulfur via reducing equivalents obtained from glucose oxidation, is one of the reactions involved in H_2S production (53). Increased oxidative stress and hyperglycemia promote the sulfide release from this path.

Starting from cysteine, H_2S is also released by non-enzymatic route in the plasma and red blood cells. This process involves iron and vitamin B6 at physiological temperature, pH and oxygen conditions (67).

Some vegetables like garlic, are natural sources of H_2S. Among garlic-derived compounds, allicin decomposes in water to free diallyl sulfide (DAS), diallyl disulfide (DADS), diallyl trisulfide (DATS) and ajoene, that induce H_2S production in a thiol-dependent manner (54).

2.3.5. Catabolism of Hydrogen Sulfide

H_2S is mainly metabolized by oxidation in mitochondria, where is first oxidized to thiosulfate and then to sulfite and sulfate, to be excreted in the end through urine, feces and flatus. In the rat liver, H_2S is metabolized especially as sulfate, in the kidney as a mixture of thiosulfate and sulfate, and in the lung, thiosulfate is the main product of sulfide metabolism.

In mitochondria, sulfide oxidation can be catalyzed by sulfide quinone oxidoreductase (SQR) or by persulfide dioxygenase (ETHE1) (Fig.18). SQR catalyzes oxidation of H_2S, passing through a persulfide intermediate. This enzyme uses coenzyme Q as electron acceptor. ETHE1 is involved in the second step of the mitochondrial sulfide oxidation pathway, that is the oxidation of persulfide, generated by SQR, to sulfite (63).

In the mitochondrial matrix, H_2S can also be oxidized via non-enzymatic pathway to thiosulfate, that subsequently is converted to sulfite and/or sulfate by sulfide-detoxifying enzymes. In particular, thiosulfate cyanide sulfurtransferase (TST) is responsible for the oxidation of thiosulfate to sulfite, that is later converted to sulfate and excreted from the body (65).

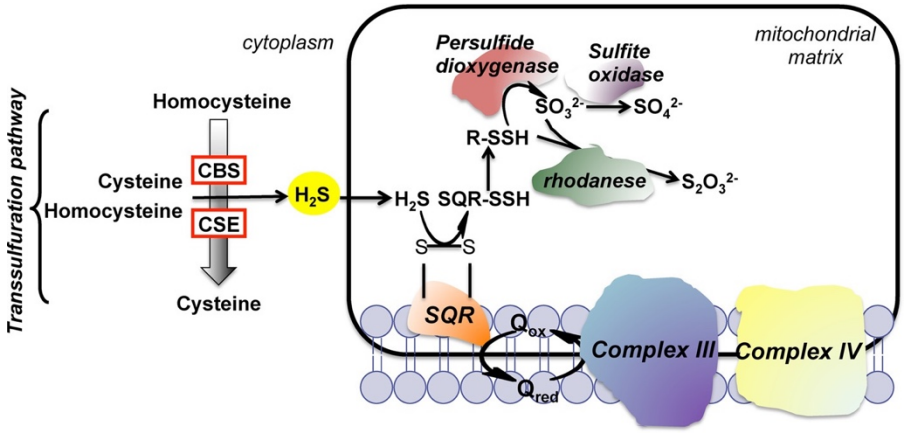

Figure 18. Enzymatic pathways involved in H_2S catabolism. H_2S is oxidized in the mitochondria by SQR to generate persulfide (SQR-SSH). In the next step, the persulfide is oxidized by ETHE1 to form sulfite that can either be catabolized by rhodanese or by sulfite

oxidase. Electrons released in the reaction catalized by SQR are captured by ubiquinone and transferred to the electron transport chain at the level of complex III (63).

H_2S can undergo methylation reaction in the cytosol to give methanethiol (CH_3SH), that is further methylated to dimethylsulfide (CH_3SCH_3), a relatively non toxic compound. These reactions are both catalyzed by thiol S-methyl-transferase (TSMT). *In vitro* measurements on rats colonic and cecal mucosa demonstrated that the rate of methylation reaction of H_2S is very slow and is only about 1/10000 the rate of H_2S oxidation, therefore, this gas is preferentially metabolized via oxidation (68).
Moreover, H_2S can be scavenged by methemoglobin to form sulfhemoglobin, or by metallo- or disulfide-containing molecules such as oxidized glutathione (GSSG) (53, 65).

2.4. H_2S Donors

Despite the interesting effects of H_2S in human body, as a gaseous compound, it cannot be considered an ideal drug. For this reason, scientists worked on the development of molecules able to release endogenous H_2S (named H_2S donors), that could be used as biological instruments and potential drugs (54).
Inorganic salts like sodium hydrosulfide (NaHS), sodium sulfide (Na_2S) and calcium sulfide (CaS) represent the early H_2S donors and they have been long employed in biological studies to investigate the therapeutic effects of hydrogen sulfide (54, 69).
As reported above, some vegetables like garlic and onions but also broccoli and watercress, are rich in organosulfur compounds as polysulfide (allicin **24**, diallyl sulfide **25**, diallyl disulfide **26**, diallyl trisulfide **27**) (Fig. 19) and isothiocyanates (allyl isothiocyanate **28**, erucin **29**, benzyl isothiocyanate **30**, 4-hydroxybenzyl isothiocyanate **31**) (Fig. 20), molecules able to release H_2S in the presence of thiols like cysteine or GSH (69).

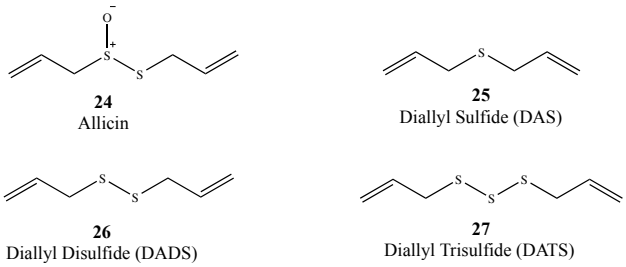

Figure 19. Chemical structures of some organosulfur compounds of garlics.

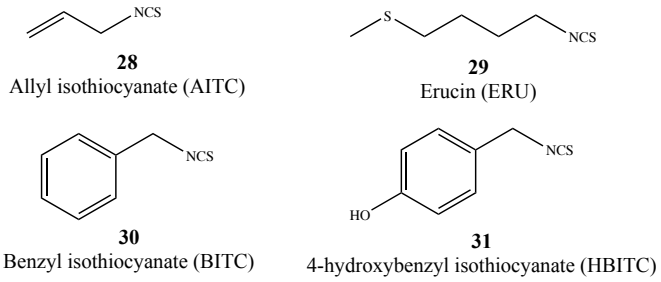

Figure 20. Chemical structures of natural isothiocyanates.

The most promising H_2S releasing compounds are the synthetic donors, characterized by an enhanced safety profile and a better pharmacokinetic that mimic the time course of the physiologic H_2S release. Some of the synthetic H_2S donors will be presented below.

Lawesson's reagent (2,4-bis(4-methoxyphenyl)-1,3,2,4-dithiadiphosphetane-2,4-disulfide) **32** is a sulfurization reagent commonly used in organic synthesis. In aqueous solution H_2S release from this donor is fast and not controllable, therefore starting from Lawesson's reagent GYY4137 (morpholin-4-ium-4-methoxyphenyl-(morpholino)-phosphinodithioate) **33** has been developed (Fig. 21). This compound represents one of the first slow-releasing H_2S donors and has been widely used by researchers to study the endogenous role of H_2S. It slowly releases hydrogen sulfide via hydrolysis (54, 69).

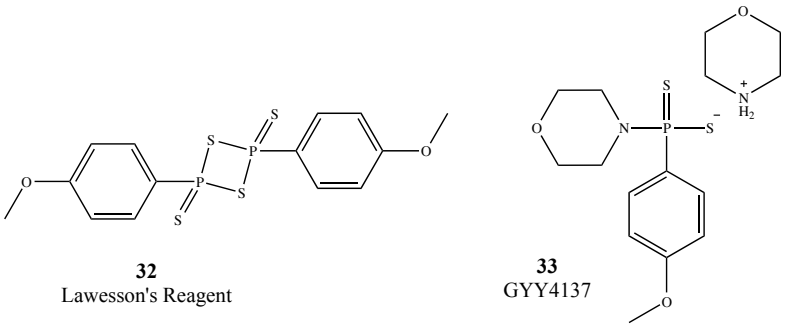

Figure 21. Chemical structures of Lawesson's reagent and GYY4137.

Other known hydrolysis-triggered H_2S donating compounds are 1,2-dithiole-3-thiones (DTTs). Noteworthy donors belonging to this class are anethole dithiolethione (ADT) **34** and its O-demethylated derivative ADT-OH (5-(p-hydroxyphenyl)-3H-1,2-dithiole-3-thione) **35** (Fig. 22).

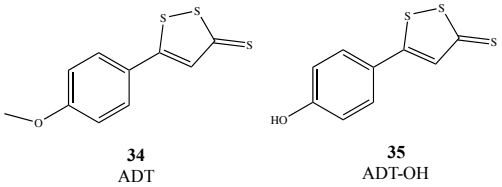

Figure 22. Most used DTTs as H_2S donors.

Arylthioamides **36** and isothiocyanates **37** are thiol activated H_2S donors and the nature of the aryl or R group may influence the sulfide releasing rates (Fig. 23) (69-71).

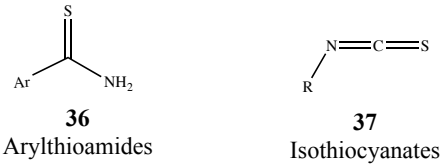

Figure 23. Chemical structures of thiol triggered H_2S donors.

2.5. Generation of H_2S in Ocular Tissues

The scientific literature concerning the biological effects of endogenous hydrogen sulfide is continuously growing. In human, H_2S concentration in tissues varies in a board range (10-300 μM), according to age, tissue and measuring methods.

The discovery of the enzymes that mediate H_2S production in ocular tissues suggested a potential physiological role for this gas-transmitter also in the eye (Fig. 24) (72).

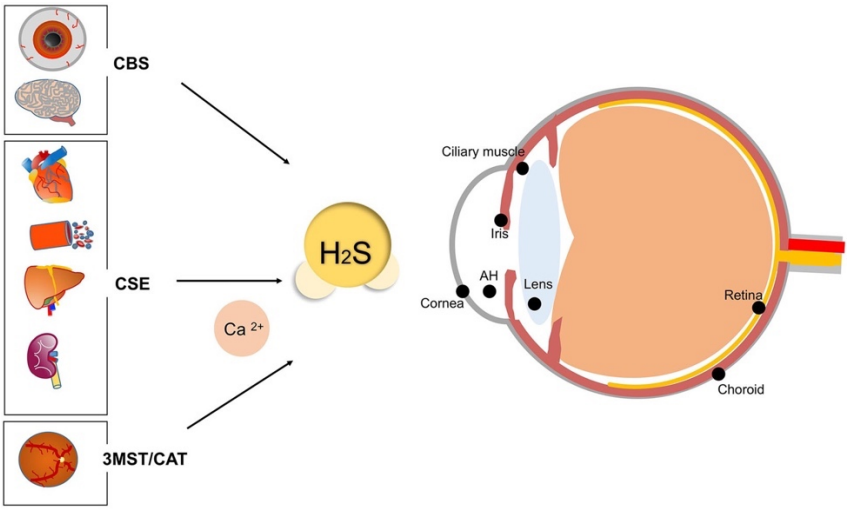

Figure 24. CBS, CSE, 3MST/CAT are responsible for endogenous H_2S synthesis in ocular tissues. CSE and CAT activities are regulated by intracellular concentration of Ca^{2+}. These H_2S-producing enzymes have been found in conjunctiva, corneal epithelial layer, iris, ciliary body, retina, optic nerve. The highest concentration of endogenous transmitter is present in cornea and retina, while the vitreous aqueous is devoid of H_2S (72).

CBS is found in all ocular tissues including conjunctiva, corneal epithelial layer, iris, ciliary body, retina, optic nerve. It has a lower expression in whole lens while is absent in vitreous humor. Conjunctiva and cornea, due to the anatomical position, are exposed to a higher oxidative stress, therefore an increased presence of CBS in these tissues could provide the adequate amount of cysteine necessary to synthesize GSH and neutralize ROS. The same happens in the epithelial layer of cornea, where a higher concentration of oxygen reactive species stimulates the activity of CBS. CSE and 3-MST/CAT pathways are active in the retina, where the highest amount of endogenous H_2S is detected (17 ± 2.1 nmoles/mg protein). The inhibitors of CSE propargylglycine (PAG, 1 mM) and CBS aminooxyacetic acid (AOA, 1 mM), reduce the production of H_2S in bovine retina by 56.8 and 42%. On the other hand, the activator of CBS, SAM (100 μM), H_2S donors like NaHS (1 μM) and Na_2S (100 μM) stimulate the endogenous release of the sulfide, while L-cysteine (10-300 μM) induces a concentration-dependent increase of H_2S production in bovine retina (73).

Different ocular diseases related to retinal degeneration like glaucoma, AMD (age-related macular degeneration), DR (diabetic retinopathy) are characterized by reduction of endogenous H_2S levels, expression of CBS, CSE and 3-MST (74). Deficiency of H_2S or its substrates are also related to myopia, cataract, optic atrophy and retinal detachment (72). Huang and coworkers found that in chronic ocular hypertension (COH) rat model, the retinal protein expression of H_2S synthetizing enzymes (mainly CSE) is decreased and, as a result, the retinal endogenous H_2S level is reduced as well (75). In contrast, Liu *et al.* demonstrated that after seven weeks of elevated IOP in rats retina, 3-MST is 3-fold upregulated compared with controls (76). Furthermore, the retinal expression of CBS tends to increase in aging eyes, probably because of age related oxidative stress or pathological conditions such as retinal degeneration (77).

2.6. H_2S and Glaucoma

Based on the evidence above, the protective role of H_2S in physiological functions of the eye and its implication in ocular diseases have been studied for a long time, to better understand the pathogenic processes and to find new therapeutic tools.

Studies in cellular or animal models of Alzheimer's disease or Parkinson's disease, have already demonstrated the neuroprotective effect of H_2S through anti-inflammatory, anti-apoptotic and antioxidant activities (56, 72, 74, 76).

As assumed consequence of the deficiency of enzymes involved in sulfide production, H_2S plasma levels in POAG patients have been found to be markedly lower than OHT (ocular hypertension) and NTG patients. Besides, in glaucoma patient's plasma levels of homocysteine and cysteine are elevated and studies have proven that increased plasma Hcy levels induce change in the microvasculature of the optic nerve head, impair ocular blood flow, active RGCs apoptosis and increase reactive oxygen species (74, 78).

H_2S protects RGCs from oxidative damage increasing the concentration of glutathione (Fig. 25) (56). GSH is one of the most common antioxidants in the human body, able to neutralize free radicals through the sulfhydryl group of the cysteine in its active site. It has been shown that knockout of a gene for an

enzyme involved in the synthesis of GSH, leads to spontaneous apoptosis of RGCs and damage to the optic nerve in mice without elevated IOP (56). H_2S can stimulate the production of GSH by enhancing the activity of γ-glutamylcysteine synthetase (γ-GCS), one of the enzymes involved in its synthesis (72, 79).

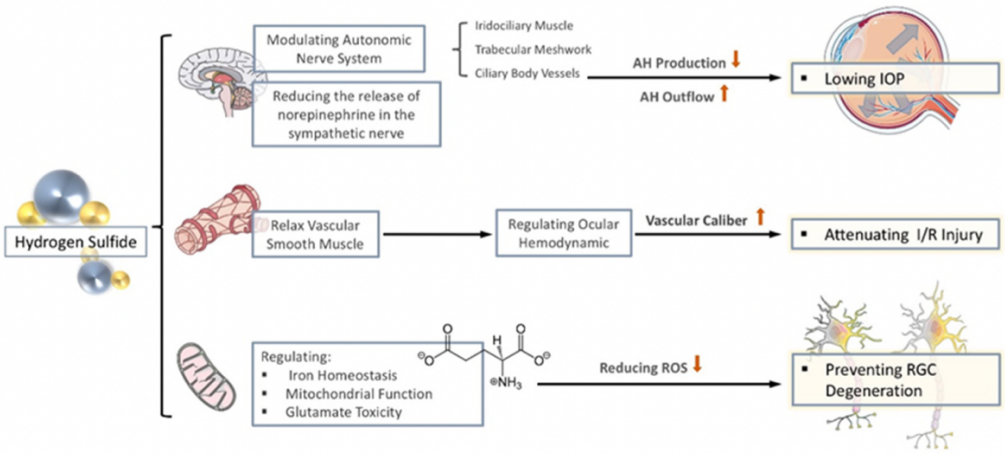

Figure 25. Effect of H_2S in glaucoma. The protective role of hydrogen sulfide in glaucoma neuropathies is expressed by several effects: H_2S can lower IOP through the modulation of AH production and outflow. By relaxing vascular smooth muscle, increases ocular blood flow and reduces the ischemia-reperfusion related damage. H_2S also acts as a neuroprotective agent, preventing RGCs degeneration and death (56).

Cystine is the main source of cysteine, necessary to produce GSH. Oxidative stress causes elevated concentrations of glutamate, responsible for excitotoxicity and neuronal damage. Glutamate competes with cystine to enter in the cell therefore in the presence of high extracellular concentration of glutamate, the synthesis of GSH is decreased. H_2S may prevent this competition by increasing the cysteine/cystine transporters on the cell membrane, reducing glutamate excitotoxicity induced damage (79).

In vitro and *in vivo* studies showed that GYY4137 exerts neuroprotective effects on RGCs. The addition of the slow-releasing H_2S donor (100 nM) *in vitro*, can reduce in a concentration-dependent manner, RGCs damage related to oxidative stress and elevated hydrostatic pressure. Moreover, after the intravitreal injection of GYY4137 (100 nM) in Spargue-Dawley rats, RGCs survival is improved in a retinal ischemia-reperfusion injury (IRI) model and optic nerve crush model. Therefore, GYY4137 may be effective to protect retinal ganglion cells under glaucomatous condition (76).

Inhaled H_2S (80 ppm), administrated 1.5 h after IRI of retinal ganglion cells, reduces significantly ($P < 0.001$) cell death and inhibits the expression of NOX4, a member of the NADPH oxygenase family, involved in the production of reactive oxygen species (80).

The treatment with NaHS (5.6 mg/kg) in experimental glaucoma model has shown to restore H_2S level and enhance RGCs survival in COH rats without impact on IOP (75).

Iron homeostasis is involved in the neurodegenerative changes associated with glaucoma. In the cells, iron is mainly located in the protoporphyrin ring of heme and alteration of heme release may cause oxidative stress and cellular apoptosis. H_2S can regulate heme release through the modulation of heme oxygenase and biliverdin reductase A activity (56).

As reported in the previous chapter, mitochondria have a main role in the regulation of RGCs functionality and survival. The effect of hydrogen sulfide on mitochondrial energy production depends on its concentration. At low concentration, through the catabolic mitochondrial pathway, H_2S releases electrons that are captured by electron transport chain, stimulating the production of ATP (Fig. 18). On the other hand, at high concentration, H_2S inhibits cytochrome c oxidase, with following reduction in the synthesis of ATP but also in the production of ROS. Furthermore, by decreasing ATP concentration, H_2S opens K_{ATP} channels and is likely that activations of ion channels combat glutamate neurotoxicity (81).

The process of ganglion cell apoptosis is mediated by several proteins and signaling pathways and involves the activation and/or upregulation of pro-apoptotic molecules and the suppression of anti-apoptosis proteins. Erisgin *et al*. (82) found that NaHS (100 nmol/L) in OHT rats, by decreasing the expression of pro-apoptotic proteins such as Bax, caspase-3 and p53 in the retina, prevents RGCs apoptosis. However, it has a limited effect on the cornea. Scheid and coworkers (80) confirmed the inhibitory effect of inhaled H_2S (80 ppm) on Bax expression in IRI animal model, but they also proved that H_2S upregulates the anti-apoptotic Bcl-2 protein in the retina. In addition, H_2S inhalation provides an anti-inflammatory activity, decreasing inflammatory cytokines expression (IL-1β and TNF-α) and the phosphorylation of NF-κB.

H_2S-vasorelaxant effect has been widely demonstrated in several type of blood vessels (53, 54, 65) from different species and appears to be mediated by the activation of K_{ATP} channels (81). The vasorelaxation of small blood vessels occurs faster because the effect of H_2S is higher at below physiological O_2 levels (65). The ocular vasculature is formed by small blood vessels with low partial pressure of oxygen, therefore H_2S may exert a better vasodilatory effect improving also ocular blood flow (56). Liu *et al*. shown that the intravitreal administration of GYY4137 (1 nM) increases retinal arterial diameter by 10.26% and venous diameter by 8.95% in glaucoma animal model (76).

H_2S plays a role also in ocular structures implicated in AH production and outflow as well as IOP control. This gas-transmitter increases the concentration of cyclic adenosine monophosphate (cAMP) in porcine ocular anterior segments with following improvement in AH outflow. An *ex vivo* study has demonstrated that H_2S, by inhibition of phosphodiesterases (PDEs), leads to accumulation of cAMP and cyclic guanosine monophosphate (cGMP) in the eye reducing the TM cells volume and promoting AH outflow (72).

H_2S, both endogenous and released by NaHS (1 μM) and Na_2S (1-100 μM), can induce a negative regulatory effect on sympathetic neurotransmission in porcine iris-ciliary body. As a result, the atrial outflow of AH is increased and IOP is reduced (83).

3. Aim of the Research

Currently available pharmacological therapies for glaucoma rely on the administration of eye drops. Due to the eyelids, tear-flow and anatomycal barriers of the eye, only 1% or even less of the administered dose is absorbed, for this reason the medications have to be instilled several times a day and the patients must be treated with two or more drugs. Therefore, one of the contributing factors to the low success of therapies, in same cases, is the poor patient's adherence. In addition, ophthalmic drugs are often associated with local side effects (conjunctivite, red eyes) but also systemic side effects following their absorption in the systemic circulation (48).

The request of new therapeutic instruments characterized by a better drug delivery system and the need to well understand the pathological processes to find other approaches to treating this disease, are the main focus of the glaucoma research (4).

The encouraging data obtained from H_2S studies in ocular disorder models and the application of H_2S donors as new potential therapeutic treatments drew the interest of scientists worldwide.

In the last decades, H_2S releasing molecules have been coupled with several pharmaceutical active compounds to synthetize novel molecular hybrids with the purpose of associating the functionality of the parent drugs and endogenous H_2S. By this approach, new chemical entities have been developed with good results as antiflammatory or cardioprotective agents (54, 69).

An interesting example of an antiglaucoma drug conjugated to a H_2S donor is ACS67 **38** (Fig. 26), molecular hybrid of latanoprost acid and ADT-OH (84).

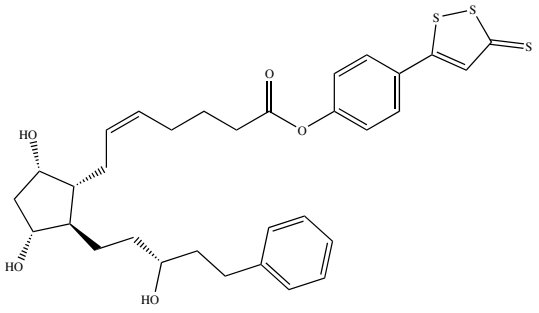

38
ACS67

Figure 26. Chemical structure of molecular hybrid between Latanoprost acid and ADT-OH.

Studies confirmed the potentiality of this drug that combine the IOP-lowering effect of latanoprost and the neuroprotective activity of H_2S, released via hydrolysis *in vivo* or *in vitro* by ADT-OH. ACS67 (0.005%) applied topically in glaucomatous pigmented rabbit, allows a 30.8% reduction in IOP compared to the effect of latanoprost. Even after repeated administrations in a five-day time course, ACS67 leads to a 27% IOP reduction versus latanoprost. These data confirm the contribution of the H_2S-donor moiety to the reduction of IOP in glaucoma animal model (84). Osborne *et al.* (85) found that ACS67 (5-20 μM) and ADT-OH (10-50 μM) protect RGC-5 cells in culture from the insult caused by H_2O_2; reduce the production of ROS; increase the synthesis of GSH. In addition, latanoprost hybrid counteractes the ischemia-reperfusion related insult to rats retina. The study performed by Salvi and coworkers (86) proved that ACS67 (10 μM) reduces by 37.6% ($P < 0.001$) the release of sympathetic neurotransmitters on bovine iris-ciliary body, showing a higher potency than latanoprost.

On the basis of the data reported above, and considering the expertise of my research group in the field of H_2S donors and their applications to synthetize novel chemical entities (87-90), the main topic of my PhD project was the design, synthesis and characterization of new molecular hybrids between drugs for the treatment of glaucoma and H_2S donating moieties. The aim was to synthesize a compound which combines the action of antiglaucomatous drugs and H_2S released by donors, through different chemical and enzymatic mechanisms. The idea was to enhance the efficacy of the IOP-lowering medications with the promising effect of H_2S, to provide a synergistic heightened therapy. The molecular hybrids must be stable enough to be administered but once absorbed in the eye, they undergo *in vivo* metabolic reactions that trigger the disintegration of the hydrids, allowing the antiglaucoma drug and the H_2S donor to interact with their biological target. By the application of these new entities, we expect a reduction in the administered dosage as well as adverse side effects of previously studied drugs may be minimized.

For the synthesis of the new molecular hybrids, amongst the different classes of antiglaucomatous drugs, brinzolamide, betaxolol and brimonidine were selected as native compounds for their higher reactivity and affordable cost.

These parent agents have been coupled with H_2S donors already described by my research group as effective H_2S releasing molecules, such as 4-hydroxybenzothioamide (TBZ) (91), 5-(4-hydroxyphenyl)-3H-1,2-dithiole-3-thione (ADT-OH) (84, 88), S-ethyl 4-hydroxybenzodithioate (HBTA) (89), 4-hydroxyphenyl isothiocyanate (HPI) (70). In addition, an acetic or succinic spacer has been introduced as a linker between the two parts to facilitate the formation of the hybrid.

Table 2: Chemical structures of new molecular hybrids between antiglaucoma drugs and H_2S donors.

1a
Brinzolamide-TBZ
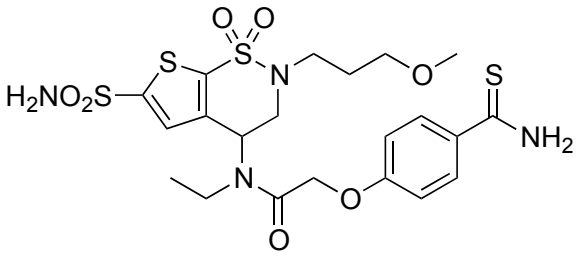
1b
Brinzolamide-ADTOH
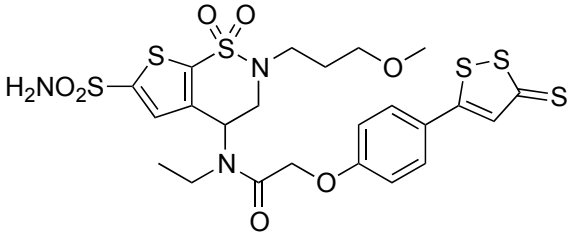
1c
Brinzolamide-HBTA
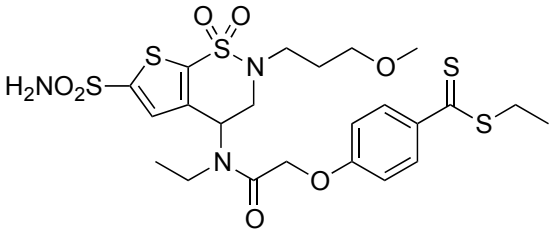
1d
Brinzolamide-HPI
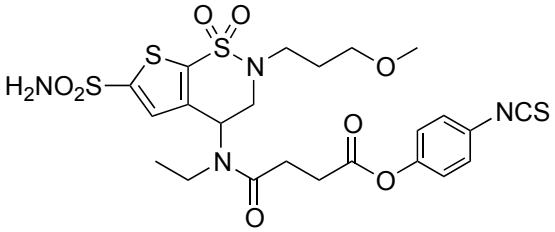

2a
Betaxolol-TBZ
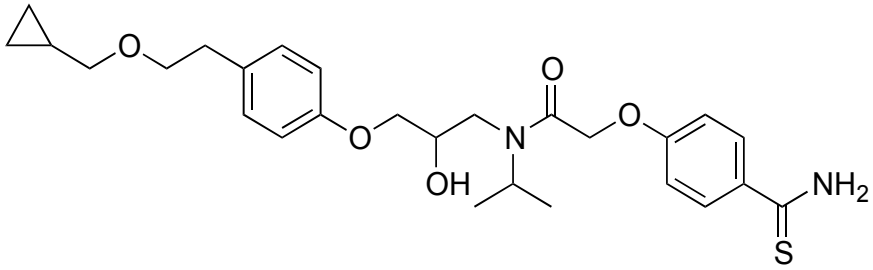
2b
Betaxolol-ADTOH
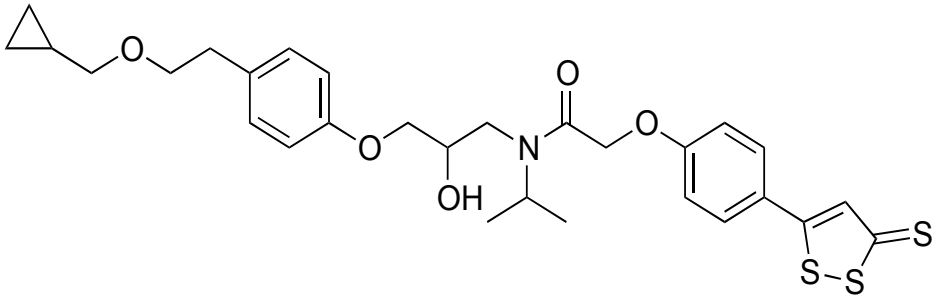
2c
Betaxolol-HBTA
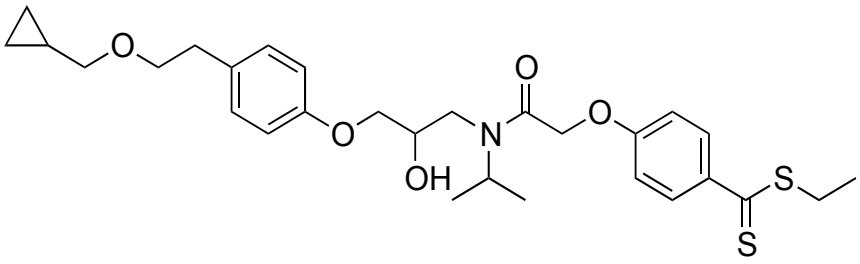
2d
Betaxolol-HPI
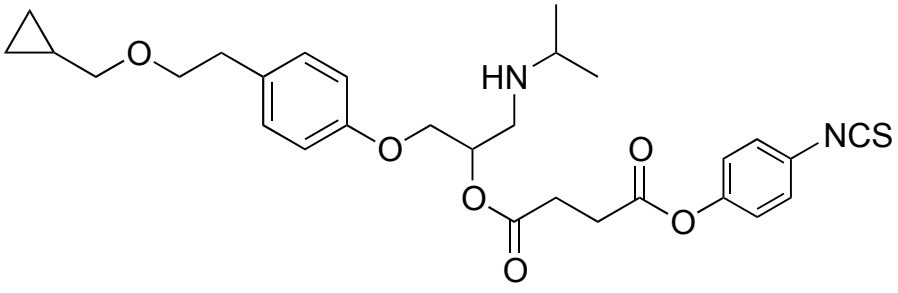

3a
Brimonidine-TBZ
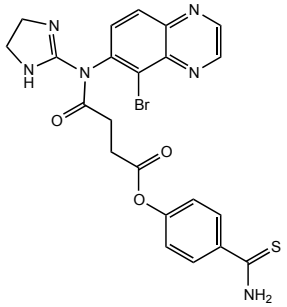
3b
Brimonidine-ADTOH
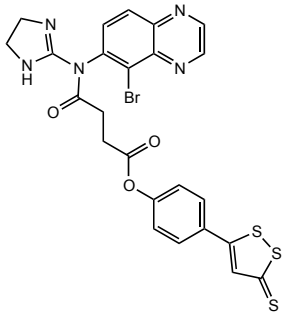
3c
Brimonidine-HBTA
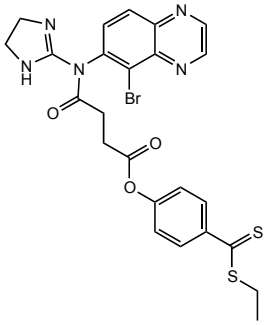
3d
Brimonidine-HPI
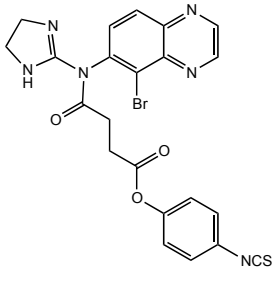

4. Chemistry

Chemical structures of compounds **1a-1d**, **2a-2d**, **3a-3d** are represented in Table 2. The synthetic routes for the synthesis of molecular hybrids of brinzolamide (**1a-1d**), betaxolol (**2a-2d**) and brimonidine (**3a-3d**) are summarized respectively in Scheme 1, Scheme 2 and Scheme 3.

The general procedure for the synthesis of compounds **1a-1c** and **2a-2c** is as follow: brinzolamide **1** or betaxolol **2** solubilized in DMF, were condensed with the H_2S donors previously conjugated to an acetic spacer (compounds **4b-6b**), by TBTU coupling in the presence of HOBt and N,N-diisopropylethylamine.

The synthesis of compound **1d** started from the conversion of brinzolamide in its acid derivative by treatment with succinic anhydride in acetonitrile. The following coupling reaction of the brinzolamide intermediate, solubilized in DMF, with 4-hydroxyphenyl isothiocyanate (HPI **7**) was performed using TBTU, HOBt and N,N-diisopropylethylamine as coupling agents.

Betaxolol **2** was treated with an excess of succinic anhydride and a catalytic amount of DMAP in anhydrous CH_2Cl_2 to give the corresponding hemi-succinated ester that was coupled with HPI in the presence of EDAC·HCl and DMAP, obtaining the compound **2d.**

Via one-pot reaction, brimonidine **3** solubilized in anhydrous DMF, was first converted into its acid derivative by treatment with succinic anhydride and DMAP, and then the obtained intermediate was coupled with the H_2S donors (**4-7**) by means of EDAC·HCl and DMAP, giving the corresponding compounds **3a-3d**.

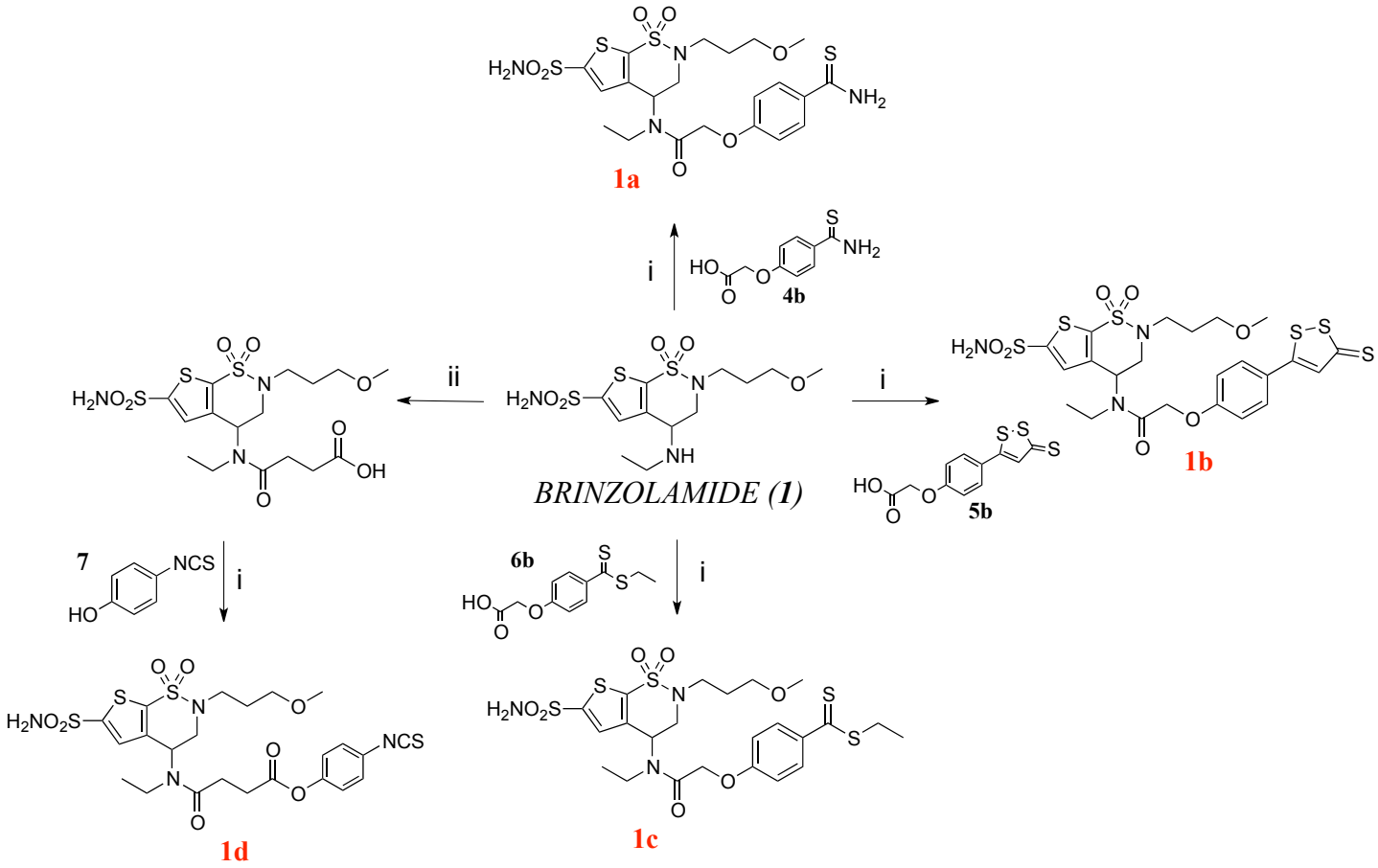

Scheme 1: Synthesis of molecular hybrids of Brinzolamide (**1a-1d**).

Reagents and conditions i) TBTU (1.2 eq.), HOBT (1.2 eq.), DIPEA (2 eq.), DMF, rt, 12h. ii) succinic anhydride (1.1 eq.), ACN, reflux, 12h.

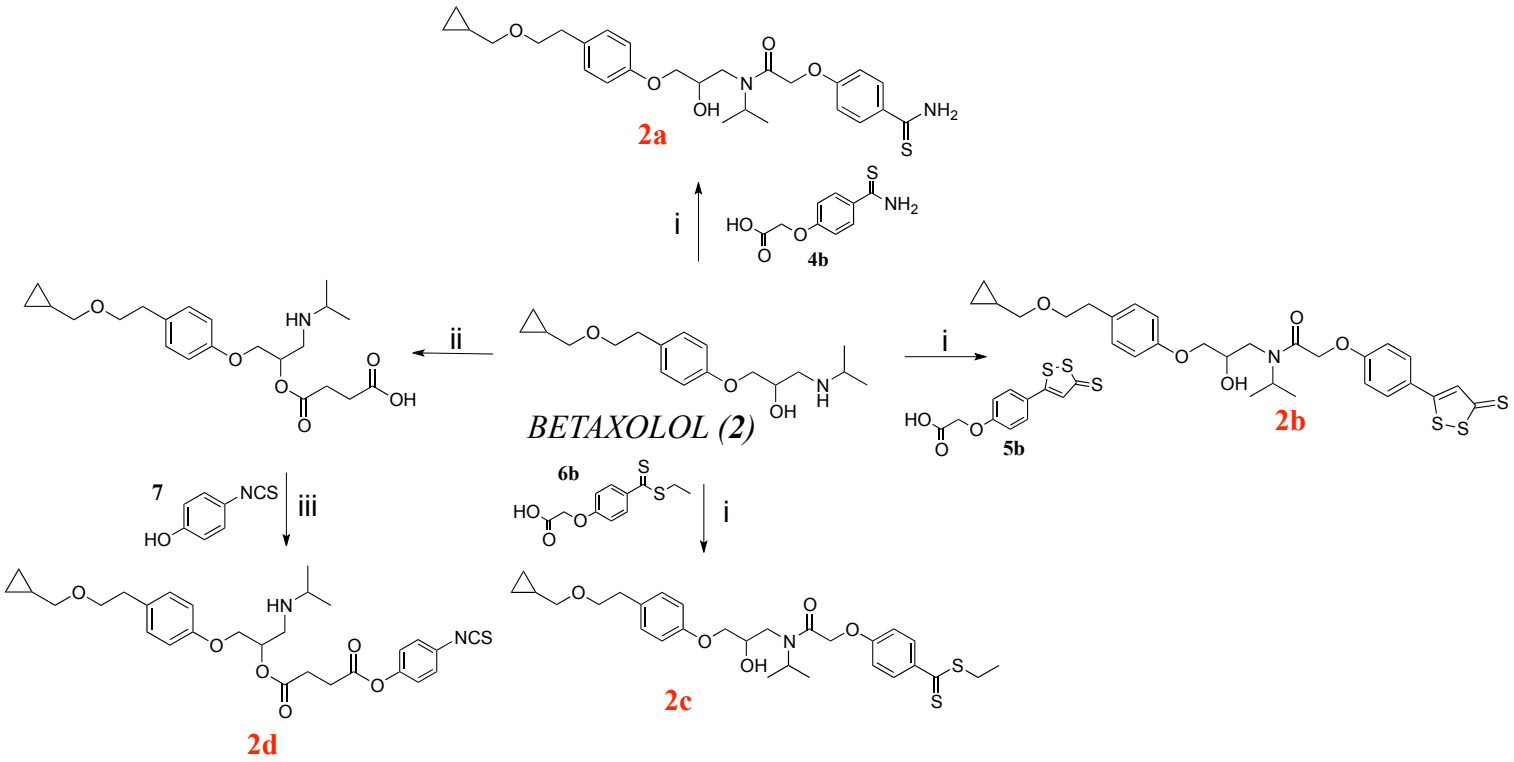

Scheme 2: Synthesis of molecular hybrids of Betaxolol (**2a-2d).**

Reagents and conditions i) TBTU (1.2 eq.), HOBT (1.2 eq.), DIPEA (2 eq.), DMF, rt, 12h. ii) succinic anhydride (1.5 eq.), DMAP (0.1 eq.), anhydr. DCM, rt, 6h. iii) EDAC·HCl (1.5 eq.), DMAP (1.5 eq.), anhydr. THF, rt, 12h

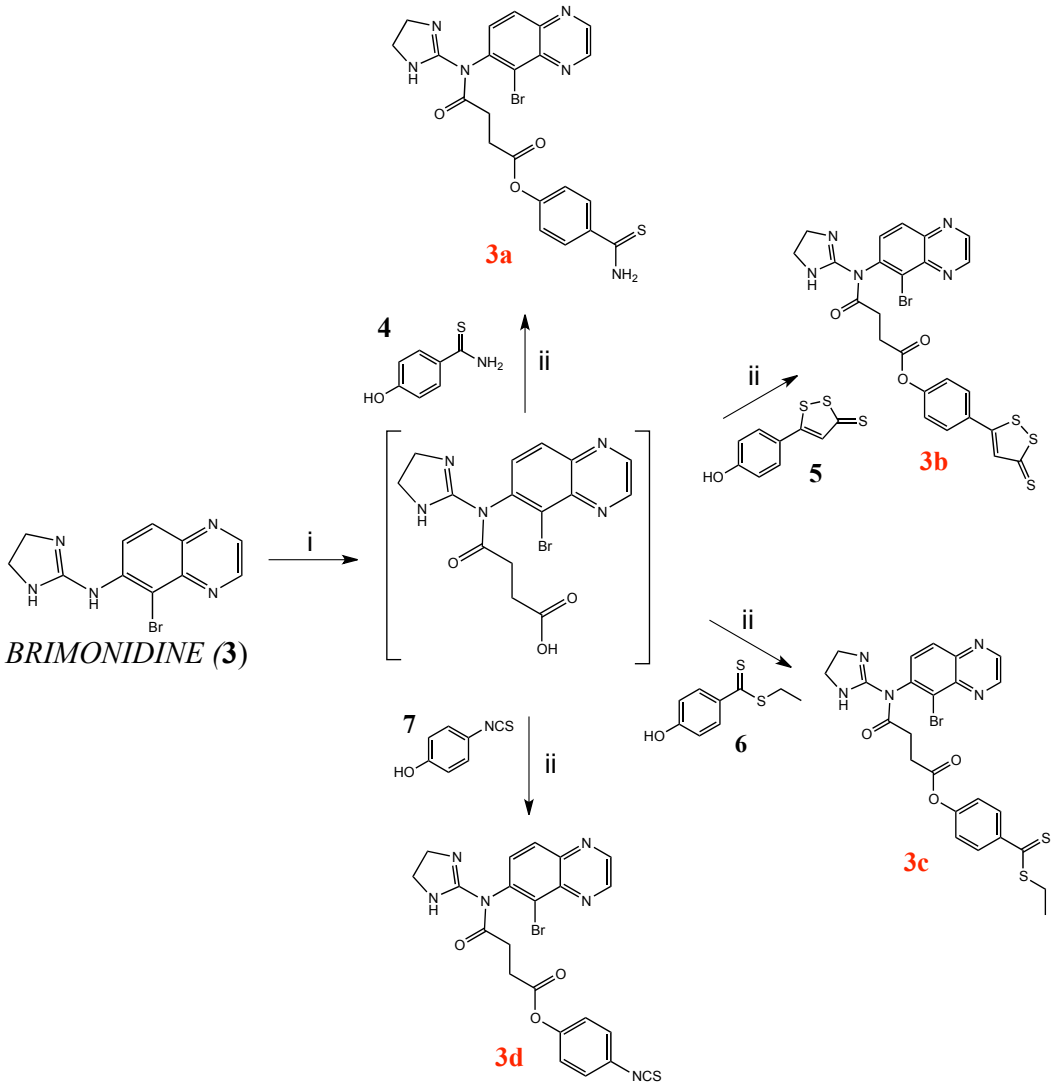

Scheme 3: Synthesis of molecular hybrids of Brimonidine (**3a-3d**).

Reagents and conditions i) succinic anhydride (1.1 eq.), DMAP (0.1 eq.), anhydr. DMF, rt, 12h. ii) EDAC·HCl (1.5 eq.), DMAP (1.5 eq.), anhydr. DMF, rt, 12h.

The H_2S-releasing moieties **4** and **7** (4-hydroxybenzothioamide TBZ and 4-hydroxyphenyl isothiocyanate HPI, respectively) are commercially available. ADT-OH (5-(4-hydroxyphenyl)-3H-1,2-dithiole-3-thione) **5** was synthetized by reacting trans-anethole and sulfur in DMF (Scheme 4) according to a process reported in literature (92). The H_2S donor HBTA (S-ethyl 4-hydroxybenzodithioate) **6** was obtained following the synthetic procedure described by my research group (Scheme 5) (89).

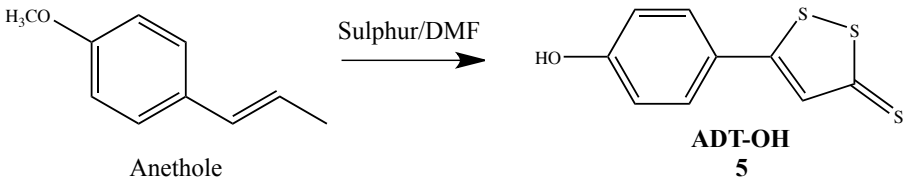

Scheme 4. Synthesis of ADT-OH.

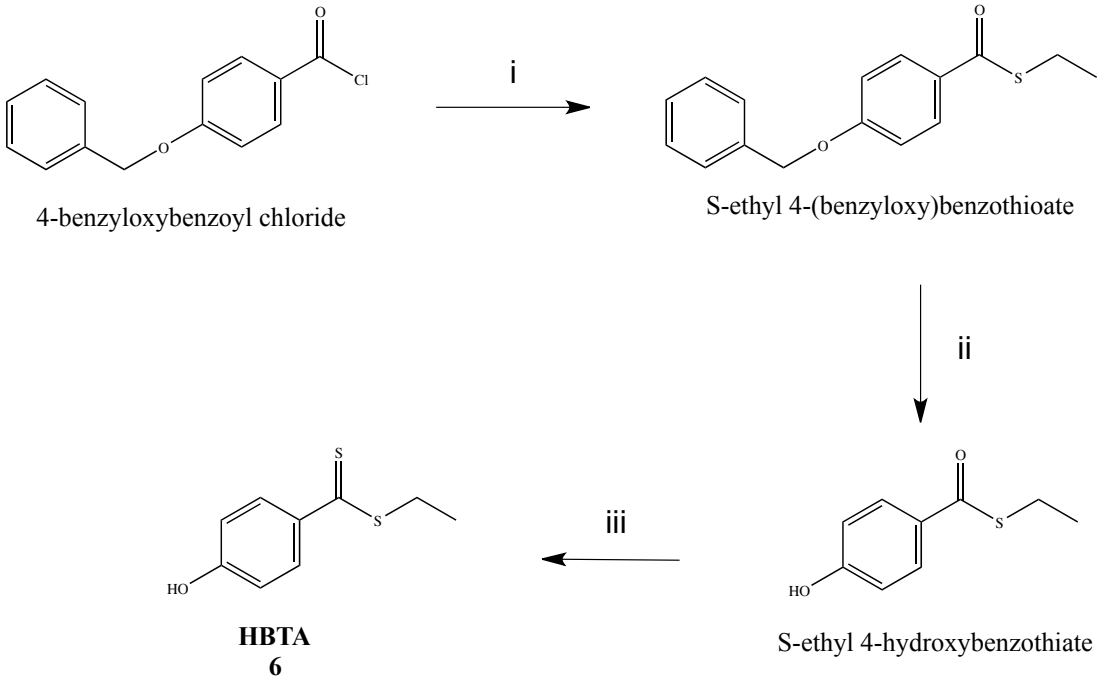

Scheme 5. Synthesis of HBTA.

Reagents and conditions: i) CH_3CH_2SH (1.5 eq.), triethylamine, anhydrous CH_2Cl_2, MW (300W, 50°C), 8 min; ii) 1,2,3,4,5-pentamethylbenzene (10 eq.), BCl_3 (8 eq.), anhydrous CH_2Cl_2, -78 °C; 30 min; iii) Lawesson's reagent (0.6 eq.), toluene, MW (500W, 110°C), 1h.

Scheme 6 reports the synthetic route for introducing an acetic spacer on the H_2S donors **4-6**. TBZ, ADT-OH and HBTA were reacted with tert-butyl bromoacetate in the presence of NaH in DMF to give intermediates **4a-6a**, that were successfully deprotected by treatment with a 10% (v/v) TFA solution in CH_2Cl_2.

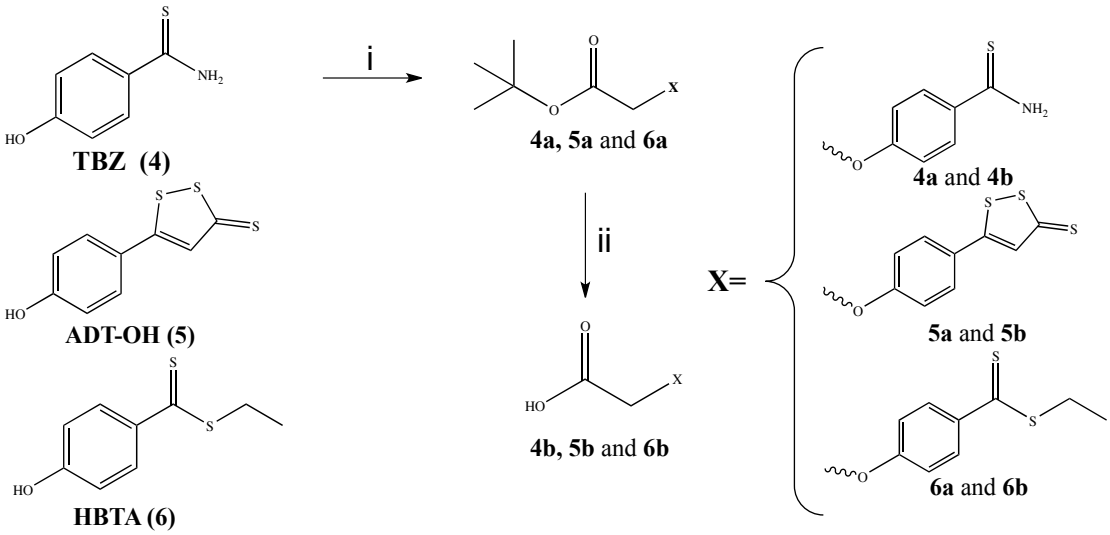

Scheme 6: Synthesis of H_2S-donors derivatives.

Reagents and conditions: i) tert-butyl bromoacetate (1.2 eq.), NaH (1 eq.), DMF, rt, 12h. ii) 10% (v/v) TFA in anhydr. DCM, rt.

5. Results and Discussion

The new synthetized molecular hybrids were sent for the analysis of their biological activity to the research group headed by Prof. Vincenzo Calderone at the Department of Pharmacy of the University of Pisa, to characterize the H_2S release from the new chemical entities and thus to perform a qualitative/quantitative description of the process.

5.1. Amperometric evaluation of H_2S release

The H_2S-generating properties of the compounds **1a-1d**, **2a-2d**, **3a-3d** were evaluated by amperometry, allowing a "real time" detection of the released H_2S with high sensitivity and selectivity (70). The assay was performed in an aqueous phosphate buffer, in the absence (– L-Cys) or in the presence (+ L-Cys) of L-Cysteine 4 mM. The thiol group of the L-Cysteine mimic the endogenous free thiols in the cells. In Table 3 are reported the C_{max} values, representing the highest concentration of H_2S (μM) recorded during the experiments and released by the H_2S donating moieties and molecular hybrids (100 μM) in the experimental conditions.

Table 3. Values of C_{max} (μM) relative to H_2S-generation following the incubation in the assay buffer of the free H_2S donors (**4-7**) and antiglaucoma hybrids (**1a-1d**, **2a-2d**, **3a-3d**) at concentration of 100 μM, in the presence and in the absence of L-Cysteine 4 mM; n.d.= not detected (H_2S release < 0.4 μM). Data are reported as means ± SEM.

Compd. (100 μM)	H_2S release (μM)		Compd. (100 μM)	H_2S release (μM)		Compd. (100 μM)	H_2S release (μM)	
	+ L-Cys	- L-Cys		+ L-Cys	- L-Cys		+ L-Cys	- L-Cys
BRINZOLAMIDE 1	-	-	**1a**	0,4 ± 0,2	n.d.	**2d**	0,5 ± 0,1	n.d.
BETAXOLOL 2	-	-	**1b**	0,9 ± 0,3	0,4 ± 0,1	**3a**	1,2 ± 0,5	n.d.
BRIMONIDINE 3	-	-	**1c**	3,5 ± 0,3	n.d.	**3b**	0,9 ± 0,4	n.d.
TBZ 4	1,6 ± 0,3	n.d.	**1d**	2,1 ± 0,4	0,4 ± 0,1	**3c**	1,7 ± 0,5	n.d.
ADT-OH 5	1,8 ± 0,5	1,1 ± 0,3	**2a**	0,5 ± 0,2	n.d.	**3d**	6,2 ± 0,5	0,8 ± 0,1
HBTA 6	3,5 ± 0,5	n.d.	**2b**	n.d.	n.d.			
HPI 7	15 ± 0,2	3.4± 0,7	**2c**	0,5 ± 0,1	n.d.			

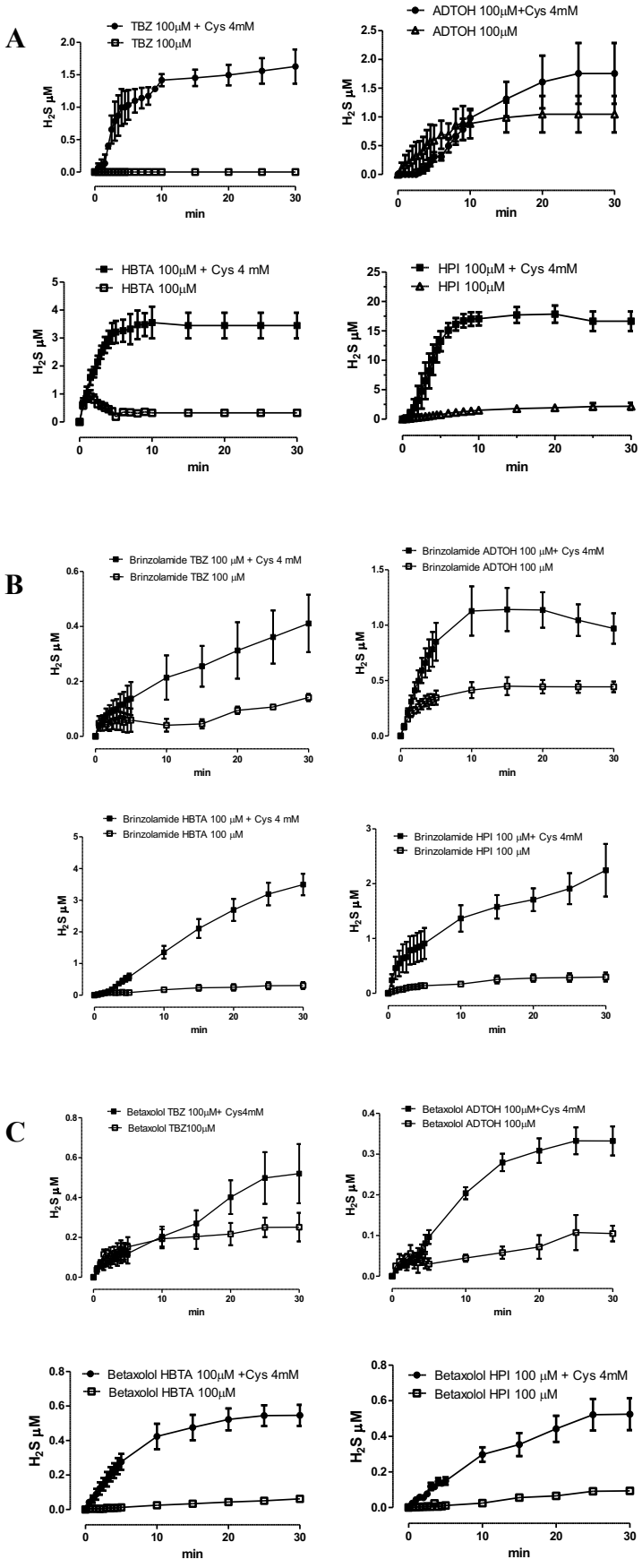
A
TBZ 100μM + Cys 4mM
TBZ 100μM
ADTOH 100μM+Cys 4mM
ADTOH 100μM
HBTA 100μM + Cys 4 mM
HBTA 100μM
HPI 100μM + Cys 4mM
HPI 100μM
B
Brinzolamide TBZ 100 μM + Cys 4 mM
Brinzolamide TBZ 100 μM
Brinzolamide ADTOH 100 μM+ Cys 4mM
Brinzolamide ADTOH 100 μM
Brinzolamide HBTA 100 μM + Cys 4 mM
Brinzolamide HBTA 100 μM
Brinzolamide HPI 100 μM+ Cys 4mM
Brinzolamide HPI 100 μM
C
Betaxolol TBZ 100μM+ Cys4mM
Betaxolol TBZ100μM
Betaxolol ADTOH 100μM+Cys 4mM
Betaxolol ADTOH 100μM
Betaxolol HBTA 100μM +Cys 4mM
Betaxolol HBTA 100μM
Betaxolol HPI 100 μM + Cys 4mM
Betaxolol HPI 100 μM
H2S μM
min

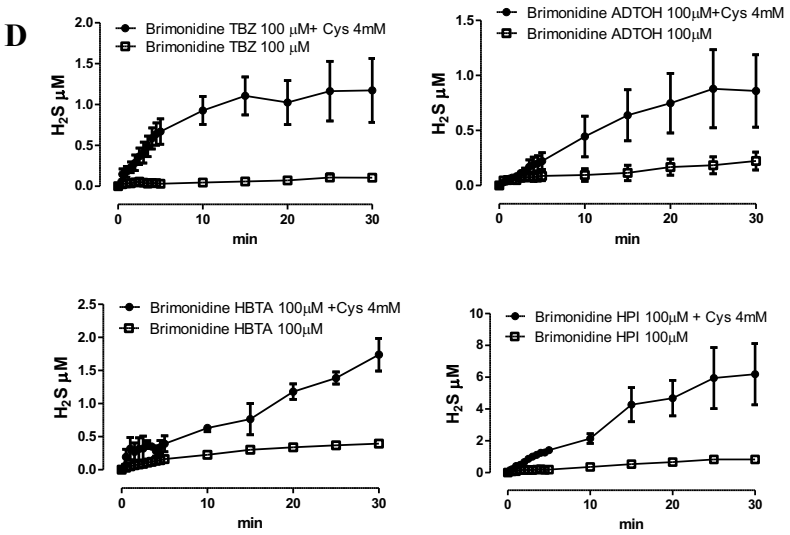

Figure 27. Curves describe the increase of H_2S concentration, with respect to time, recorded by amperometry after the incubation of free H_2S donors **4**-**7** (A), brinzolamide derivatives **1a**-**1d** (B), betaxolol derivatives **2a**-**2d** (C) and brimonidine derivatives **3a**-**3d** (D) in the assay buffer, in the absence or in the presence of L-cysteine 4 mM. The vertical bars indicate the SEM.

As illustrated in the Figure 27, the amperometric assay demonstrated that in the absence of L-Cysteine, all the compounds had a completely negligible release of H_2S (< 0,4 μM), except ADT-OH **5** and HPI **7**. These data proved that the presence of a thiol group activates and/or enhances the H_2S generation from the tested compounds. Therefore, they act as "smart H_2S donors" since these agents can donate the gaseous transmitter only in biological environment, *i.e.*, in the presence of organic thiols (70, 88, 93).

All brinzolamide hybrids (compound **1a**-**1d**) showed a L-Cysteine dependent generation of H_2S. Nevertheless, the hybrid brinzolamide-TBZ (**1a**) had the lowest release (C_{max} = 0,4 ± 0,2 μM) while the compound **1c** (brinzolamide-HBTA) showed a slow and considerable production of H_2S, and within the series of the brinzolamide hybrids, demonstrated the highest C_{max} (3,5 ± 0,3 μM). Amperometric data obtained from the hybrid drug **1c** confirmed the promising results collected by my research group (89), suggesting HBTA as an innovative and effective thiol-triggered H_2S donor.

The molecular hybrids synthetized starting from betaxolol (**2a**-**2d**), had a weak H_2S release, enhanced by the presence of L-Cysteine. The curves H_2S-release vs time in the absence or in the presence of L-Cys for compound **2a** (betaxolol-TBZ), were almost overlapping. The poor releasing properties of betaxolol

hybrids may be due to the chemical structure of betaxolol that makes the H_2S donating moieties more susceptible to hydrolysis before H_2S formation.
Compounds **3a-3d** required the presence of L-Cys to get a detectable generation of H_2S. The hybrid brimonidine-HPI **3d** showed the best releasing profile, with progressive and time-related slow gas donation. The compound **3d** produced a significant H_2S generation with a C_{max} value of 6,2 ± 0,5 μM. Also in this case, data from amperometric assay corroborated the studies performed by the research group of Prof. Calderone that indicate isothiocyanates as promising H_2S donors (70, 94). Furthermore, as illustrated by Lin *et al.*, the endogenous H_2S release from isothiocyanates occurs in the presence of thiols (mainly GSH or L-Cys). In particular, the authors showed that isothiocyanates react rapidly with the cysteine to form an adduct, which then undergoes intramolecular cyclization reaction to release in the end H_2S (71). In addition, the electronic effect of the substituents linked to the isothiocyanate may influence the H_2S formation rate.

5.2. Intracellular H_2S release in HCEs

The H_2S releasing properties of the novel molecular hybrids were tested also in Human Primary Corneal Epithelial Cells (HCEs), to better understand the H_2S formation into the cellular environment without adding any exogenous thiol.
The detection of intracellular H_2S was performed by spectrofluorometric measurements using the dye 3′-methoxy-3-oxo-3H-spiro-(isobenzofuran-1,9′-xanthen)-6′-yl-(pyridin-2-yldisulfanyl) benzoate (Washington State Probe-1,WSP-1). WSP-1 can react specifically and irreversibly with H_2S generated by the tested compounds, releasing a fluorophore detectable with a spectrofluorometer. The increase in the fluorescence compared to the blank is expressed as fluorescence index (FI) (93). The FI values of the H_2S donors and the hybrids were compared to the FI value of diallyl disulfide (DADS), considered as reference sulfide donor and responsible for a significant H_2S production ($P < 0.001$). The addition of the vehicle (1% DMSO) caused a poor increase of fluorescence, probably related to the endogenous production of H_2S.
The experiments were performed in HCEs because the cornea is the major route for topical ocular drugs absorption and the corneal epithelium is the most

anterior layer of the cornea as well as the main barrier for drug absorption from the tear fluid to the anterior chamber of the eye (95, 96).

In the Figure 28 are represented the H_2S formation values of the donating moieties (100 μM) **4**-**7**. The compounds TBZ **4** and ADT-OH **5** incubated in HCEs led to a weak and not significant H_2S-release, almost comparable to that of the vehicle, showing their inability to enter the cell and produce H_2S. On the other hand, HBTA **6** and HPI **7** promoted an elevated and significant ($P < 0.001$) increase of WSP-1 fluorescence. S-Ethyl 4-hydroxybenzodithioate (HBTA) demonstrated a massive H_2S production, higher than the reference compound DADS.

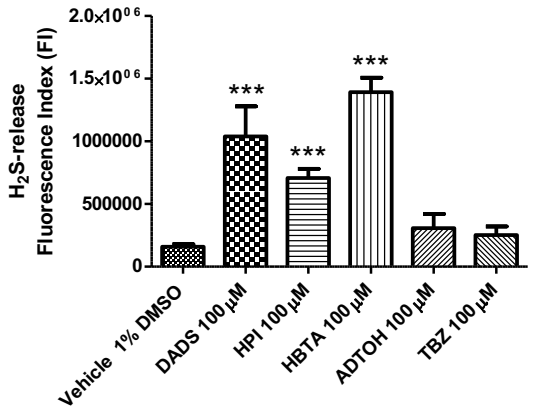

Figure 28. Cumulative H_2S release (expressed as area under the curve of the WSP-1 fluorescence in the recording time) after the incubation of the vehicle, the tested compounds (**4**-**7**) and diallyl disulfide (DADS) (100 μM). Data were expressed as mean ± standard error. Three different experiments were carried out, each in triplicate. ANOVA and Student t test were applied as statistical analyses; when required, the Bonferroni post hoc test was used to calculate the significance level (* $P < 0.05$; ** $P < 0.01$; *** $P < 0.001$).

The intracellular H_2S releasing profiles of compounds **1a**-**1d** (100 μM), reported in Figure 29, show that all brinzolamide hybrids evocated a significant H_2S release. Compound **1a** (brinzolamide-TBZ) had an enhanced H_2S production compared to the free TBZ moiety. The addition of the hybrid brinzolamide-ADTOH (**1b**) in HCEs caused a higher increase in FI value than 1,3-dithiole-2-thione. The incubation of compounds **1c** and **1d** (brinzolamide-HBTA and brinzolamide-HPI, respectively) promoted a significant H_2S release ($P < 0.001$).

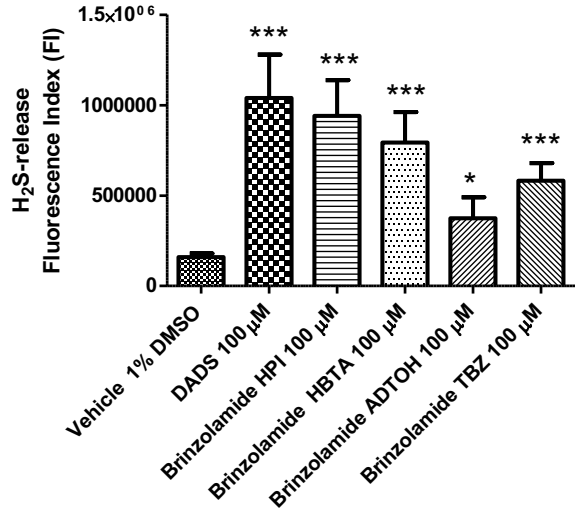

Figure 29. Cumulative H_2S release (expressed as area under the curve of the WSP-1 fluorescence in the recording time) after the incubation of vehicle, the tested compounds (**1a-1d**) and diallyl disulfide (DADS) (100 µM). Data were expressed as mean ± standard error. Three different experiments were carried out, each in triplicate. ANOVA and Student t test were applied as statistical analyses; when required, the Bonferroni post hoc test was used to calculate the significance level (* $P < 0.05$; ** $P < 0.01$; *** $P < 0.001$).

Compounds **2a** betaxolol-TBZ and **2b** betaxolol-ADTOH did not cause any significant increase in fluorescence (Fig. 30). The addition of molecular hybrids betaxolol-HBTA (**2c**) and betaxolol-HPI (**2d**) to WSP-1 preloaded HCEs evoked a mild but significant increase in the intracellular H_2S levels ($P < 0.001$).

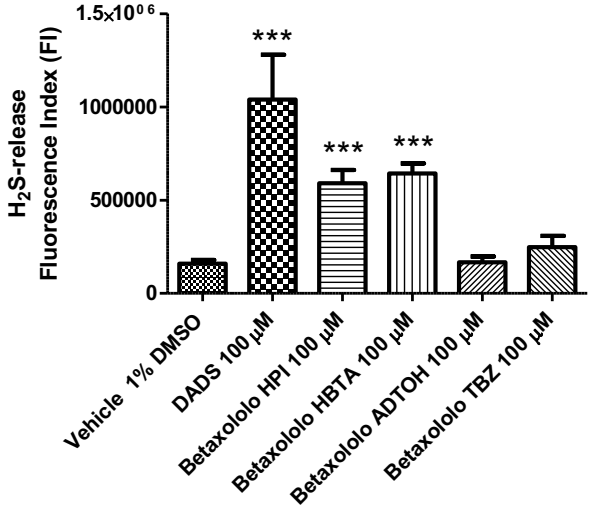

Figure 30. Cumulative H_2S release (expressed as area under the curve of the WSP-1 fluorescence in the recording time) after the incubation of vehicle, the tested compounds (**2a-2d**) and diallyl disulfide (DADS) (100 µM). Data were expressed as mean ± standard error. Three different experiments were carried out, each in triplicate. ANOVA and Student t test were

applied as statistical analyses; when required, the Bonferroni post hoc test was used to calculate the significance level (* $P < 0.05$; ** $P < 0.01$; *** $P < 0.001$).

In Figure 31 are graphically represented the results of the fluorometric assay of brimonidine hybrids. All the compounds led to a significant release of hydrogen sulfide ($P < 0.001$), except for ADT-OH conjugated hybrid (**3b**). Among the compounds **3a-3d**, the molecular hybrid **3d** (brimonidine-HPI) showed the highest increase in fluorescence.

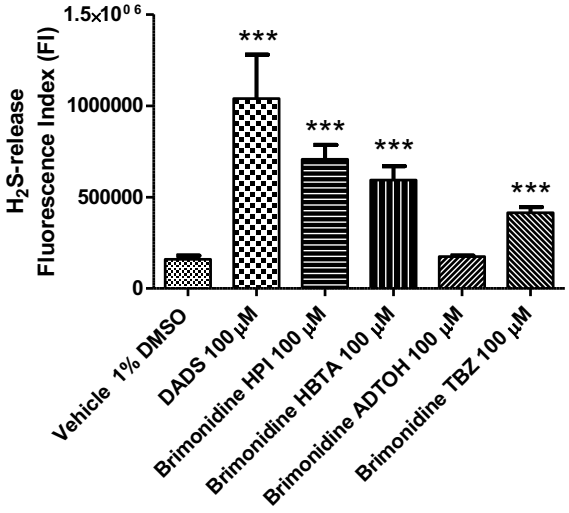

Figure 31. Cumulative H_2S release (expressed as area under the curve of the WSP-1 fluorescence in the recording time) after the incubation of vehicle, the tested compounds (**3a-3d**) and diallyl disulfide (DADS) (100 µM). Data were expressed as mean ± standard error. Three different experiments were carried out, each in triplicate. ANOVA and Student t test were applied as statistical analyses; when required, the Bonferroni post hoc test was used to calculate the significance level (* $P < 0.05$; ** $P < 0.01$; *** $P < 0.001$).

Analyzing the data from the amperometric and the fluorometric assays, the molecular hybrids synthetized by coupling HBTA **6** and HPI **7** with antiglaucoma drugs (**1-3**), released a higher amount of H_2S in aqueous buffer as well as in the cells, compared to the molecular hybrids of TBZ **4** and ADT-OH **5**. Furthermore, evaluating the influence of the antiglaucoma drugs in H_2S release, betaxolol hybrids demonstrated a weak generation of H_2S. This behavior may be related to the chemical instability of the compounds in the experimental conditions or to the reduced steric accessibility of the H_2S donor moieties by the thiol, due to the chemical structure of betaxolol.

Therefore, compounds **1c**, **1d** and **3d** showed the best releasing profiles, leading to an enhanced H_2S production. Besides the amount of the gas-transmitter produced, also the H_2S releasing kinetic influence the biological activity. The amperometic assay demonstrated that these hybrids had a progressive and long lasting release of H_2S in the presence of L-Cysteine, acting as smart H_2S donors. These features are considered as indispensable for the potential clinical application of H_2S donors, since they avoid the side effects related to a fast release (typical of the sulfide and hydrosulfide salts) and also mimic the endogenous H_2S production.

6. Experimental Section

6.1. Materials and Methods

Brinzolamide and brimonidine were purchased from Abcr (Germany); betaxolol was purchased from Carbosynth (UK). All reagents, solvents and other chemicals were commercial products obtained from Merck (Germany). Melting points, determined using a Buchi Melting Point B-540 instrument (Switzerland), are uncorrected and represent values obtained on recrystallized or chromatographically purified material. ^{1}H and ^{13}C NMR spectra were recorded on a Bruker Advanced 400 MHz spectrometer (USA). Spectra of brinzolamide and brimonidine derivatives were recorded in DMSO-d_6. Spectra of betaxolol hybrids were recorded in CD_3OD and $CDCl_3$ (compound **2d**). Chemical shifts are reported in ppm. The following abbreviations are used to describe peak patterns when appropriate: s (singlet), d (doublet), t (triplet), m (multiplet), q (quartet), qt (quintet), dd (doublet of doublet), td (triplet of doublets), bs (broad singlet). Mass spectra of the final products were recorded on a LTQ-XL mass spectrometer equipped with an HESI ion source (Thermo Fisher Scientific, USA). All reactions were followed by thin-layer chromatography, carried out on Merck silica gel 60 F_{254} plates with a fluorescent indicator, and the plates were visualized with UV light (254 nm). Preparative chromatographic purifications were performed using a silica gel column (Kieselgel 60). Solutions were concentrated with a Buchi R-114 rotary evaporator at low pressure.

6.2. Synthesis of Compounds 1a-1d

6.2.1. 2-(4-carbamothioylphenoxy)-N-ethyl-N-(2-(3-methoxypropyl)-1,1-dioxido-6-sulfamoyl-3,4-dihydro-2H-thieno[3,2-e][1,2]thiazin-4-yl)acetamide

Brinzolamide-TBZ, compound 1a.

Commercially available brinzolamide **1** (1.00 g; 2.61 mmol) was solubilized in DMF (30 mL) and condensed with the derivative **4b** (0.551 g; 2.61 mmol), via TBTU (1.00 g; 3.13 mmol) and HOBt (0.423 g; 3.13 mmol) coupling in the

presence of N,N-diisopropylethylamine (0.910 mL; 5.22 mmol). The mixture was stirred at room temperature for 12 hours. The solvent was evaporated and the residue was then purified by silica gel open chromatography using dichloromethane/methanol as eluent (9:1 v/v). The compounds **1a** was then isolated as a yellowish oil. Yield 0.628 g; 41.7 %.

^{1}H NMR (400 MHz, DMSO-d_6) δ: 9.59 (bs, 2H), 9.28 (bs, 2H), 7.88 (d, J = 8.5 Hz, 2H), 7.65 (s, 1H), 6.80 (d, J = 12.5 Hz, 2H), 4.40 (s, 2H), 4.12 - 4.10 (m, 1H), 3.87 - 3.85 (m, 2H), 3.39 - 3.35 (m, 3H), 3.23 (s, 3H), 3.17 - 3.15 (m, 1H), 2.83 - 2.77 (m, 2H), 1.83 - 1.80 (m, 2H), 1.08 (t, J = 7.0 Hz, 3H); ^{13}C NMR (101 MHz, DMSO-d_6) δ: 199.13, 173.05, 161.67, 151.95, 131.60, 129.62, 128.51, 127.69, 124.95, 119.56, 113.99, 110.13, 69.31, 69.10, 58.40, 54.23, 49.01, 45.84, 29.02. ESI-MS *m/z* $[M+H]^+$ calculated for $C_{21}H_{28}N_4O_7S_4$ 576.73, found = 577.2.

6.2.2. N-ethyl-N-(2-(3-methoxypropyl)-1,1-dioxido-6-sulfamoyl-3,4-dihydro-2H-thieno[3,2-e][1,2]thiazin-4-yl)-2-(4-(3-thioxo-3H-1,2-dithiol-5-yl)phenoxy)acetamide

Brinzolamide-ADTOH, compound 1b.

Following the synthetic procedure described above for **1a**, compound **1b** was synthetized starting from brinzolamide **1** (1.00 g; 2.61 mmol) and the derivative **5b** (0.742 g; 2.61 mmol). Orange solid. Yield 0.889 g; 52.4 %. Mp 154.1 - 155.6° C.

^{1}H NMR (400 MHz, DMSO-d_6) δ: 8.2 (bs, 2H), 7.82 (d, J = 8.5 Hz, 2H), 7.73 (s, 1H), 6.93 (d, J = 12.5 Hz, 2H), 5.76 (s, 1H), 4.47 (s, 2H), 3.94 - 3.93 (1H, m), 3.63 - 3.60 (m, 2H), 3.39 - 3.35 (m, 3H), 3.23 (s, 3H), 3.18 - 3.14 (m, 1H), 2.89 - 2.87 (m, 2H), 1.84 - 1.80 (m, 2H), 1.13 (t, J = 7.4 Hz, 3H); ^{13}C NMR (101 MHz, DMSO-d_6) δ: 215.13, 174.47, 172.87, 162.56, 134.48, 129.21, 128.50, 127.80, 124.98, 123.84, 119.60, 116.05, 110.08, 69.30, 69.13, 58.41, 54.05, 48.78, 45.85, 29.01, 17.20. ESI-MS *m/z* $[M+H]^+$ calculated for $C_{23}H_{27}N_3O_7S_6$ 649.87, found = 650.1.

6.2.3. ethyl 4-(2-(ethyl(2-(3-methoxypropyl)-1,1-dioxido-6-sulfamoyl-3,4-dihydro-2H-thieno[3,2-e][1,2]thiazin-4-yl)amino)-2-oxoethoxy)benzodithioate

Brinzolamide-HBTA, compound 1c.

Following the synthetic procedure described above for **1a**, compound **1c** was synthetized starting from brinzolamide **1** (1.00 g; 2.61 mmol) and the derivative **6b** (0.670 g; 2.61 mmol). Pink solid. Yield 1.280 g; 78.9 %. Mp 174.0 - 175.6°C. ^{1}H NMR (400 MHz, DMSO-d_6) δ: 8.19 (bs, 2H), 7.95 (d, J = 8.8 Hz, 2H), 7.59 (s, 1H), 6.85 (d, J = 12.5 Hz, 2H), 4.43 (s, 2H), 3.83 - 3.80 (m, 1H), 3.62 - 3.58 (m, 2H), 3.40 - 3.34 (m, 5H), 3.21 (s, 3H), 3.15 - 3.13 (m, 1H), 2.70 - 2.65 (m, 2H), 1.80 - 1.78 (m, 2H), 1.31 (t, J = 6.1 Hz, 3H), 1.05 (t, J = 7.0 Hz, 3H); ^{13}C NMR (101 MHz, DMSO-d_6) δ: 225.99, 172.69, 163.44, 155.90, 137.46, 128.79, 128.48, 114.81, 110.25, 69.29, 69.15, 58.38, 54.05, 45.82, 43.25, 31.01, 29.02, 18.54, 17.18, 12.84. ESI-MS *m/z* $[M+H]^+$ calculated for $C_{23}H_{31}N_3O_7S_5$ 621.83, found = 622.1.

6.2.4. 4-isothiocyanatophenyl 4-(ethyl(2-(3-methoxypropyl)-1,1-dioxido-6-sulfamoyl-3,4-dihydro-2H-thieno[3,2-e][1,2]thiazin-4-yl)amino)-4-oxobutanoate

Brinzolamide-HPI, compound 1d.

The synthesis of compound **1d** occurs in two steps. The first reaction was performed in acetonitrile (20 mL) as solvent, with azeotropic elimination of water from the system (97). Succinic anhydride (0.287 g; 2.87 mmol) was added to a solution of brinzolamide **1** (1.00 g; 2.61 mmol) and the mixture was stirred overnight at reflux. The solvent was evaporated under reduced pressure and the crude residue was then purified by silica gel open chromatography (dichloromethane/methanol 9:1 v/v) to obtain the acid derivative of brinzolamide as colorless oil. Yield 0.891 g; 70.6 %. ESI-MS *m/z* $[M+H]^+$ calculated for $C_{16}H_{25}N_3O_8S_3$ 483.58, found = 484.4.

In the second step, the synthetized intermediate (1.00 g; 2.07 mmol) was solubilized in DMF (30 mL) and condensed with 4-hydroxyphenyl isothiocyanate (HPI) **7** (0.313 g; 2.07 mmol), by TBTU coupling (0.796 g; 2.48 mmol), in presence of HOBt (0.335 g; 2.48 mmol) and N,N-diisopropylethylamine (0.721 mL; 4.14 mmol). The mixture was stirred at room temperature for 12 hours. The solvent was evaporated and the crude material was purified by silica gel open chromatography using ethyl acetate/diethyl ether

as eluent (9,5:0,5 v/v). Then the compound **1d** was isolated by crystallization from n-hexane as a white solid. Yield 0.572 g; 44.8 %. Mp 95.5 – 96.4° C.
^{1}H NMR (400 MHz, DMSO-d_6) δ: 8.00 (bs, 2H), 7.46 (d, J = 8.5 Hz, 2H), 7.25 (s, 1H), 7.17 (d, J = 12.5 Hz, 2H), 4.00 - 3.97 (m, 1H), 3.61 - 3.58 (m, 2H), 3.47 - 3.42 (m, 1H), 3.37 (t, J = 6.1 Hz, 2H), 3.22 (s, 3H), 3.21 - 3.18 (m, 1H), 2.83 - 2.77 (m, 6H), 1.85 - 1.81 (m, 2H), 0.99 (t, J = 7.1 Hz, 3H); ^{13}C NMR (101 MHz, DMSO-d_6) δ: 171.65, 150.00, 149.12, 142.83, 139.95, 134.15, 129.85, 127.84, 127.70, 127.63, 123.70, 69.25, 58.40, 45.74, 31.42, 29.60, 29.14, 28.60, 22.53, 14.80, 14.43. ESI-MS *m/z* $[M+H]^+$ calculated for $C_{23}H_{28}N_4O_8S_4$ 616.75, found = 617.1.

6.3. Synthesis of Compounds 2a-2d.

6.3.1. 2-(4-carbamothioylphenoxy)-N-(3-(4-(2- (cyclopropylmethoxy ethyl) phenoxy)-2-hydroxypropyl)-N- isopropylacetamide

Betaxolol-TBZ, compound 2a.

Compound **2a** was obtained according to the procedure reported above for **1a**, starting from betaxolol **2** (1.00 g; 3.25 mmol) and the intermediate **4b** (0.686 g; 3.25 mmol). Yellow solid. Yield 0.511 g; 31.4 %. Mp 73.1 – 74.5° C.
The analysis of ^{1}H, ^{13}C and bidimensional NMR spectra showed that betaxolol hybrids **2a** - **2c** are a mixture of *cis*/*trans* isomers (Fig. 32). As reported in details in the literature, unsymmetrically N,N-disubstituted amides are characterized by a hindered rotation around the C(O)-N bond but the energy difference between the two conformations is small and the molecules are a combination of *cis/trans* isomers (98-101). The rate of conversion between conformational isomers of betaxolol hybrids is sufficiently slow to allow a chemical sift difference of signals arising from *cis* and *trans* isomers.

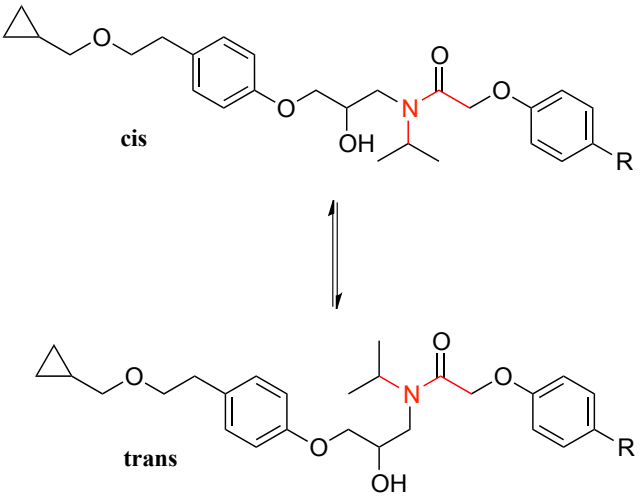

Figure 32. Conformations of Betaxolol hybrids

^{1}H NMR (400 MHz, CD_3OD) δ: 7.95 (d, *J* = 4.5 Hz, 2H), 7.92 (d, *J* = 4.6 Hz, 2H), 7.17 (d, *J* = 4.3 Hz , 2H), 7.15 (d, *J* = 6.4 Hz, 2H), 6.99 (d, *J* = 4.4 Hz, 2H), 6.97 (d, *J* = 4.5 Hz, 2H), 6.89 (d, *J* = 8.5 Hz, 2H), 6.83 (d, *J* = 8.6 Hz, 2H), 5.19 (d, *J* = 15 Hz, 1H), 4.98 (s, 2H), 4.90 (d, *J* = 14.9 Hz, 1H), 4.36 - 4.32 (m, 1H), 4.25 - 4.17 (m, 2H), 4.04 - 4.02 (m, 1H), 3.99 - 3.97 (m, 1H), 3.92 - 3.94 (m, 1H), 3.87 - 3.85 (m, 1H), 3.66 - 3.64 (m, 2H), 3.61 (d, *J* = 5.2 Hz, 1H), 3.59 (d, *J* = 5.2 Hz, 1H) 3.55 - 3.54 (m, 1H), 3.39 (d, *J* = 7.0 Hz, 1H), 3.37 (d, *J* = 6.9 Hz, 1H), 3.31 (d, *J* = 3.6 Hz, 2H), 3.30 (d, *J* = 6.9 Hz, 2H), 2.80 (td, *J* = 7.1 Hz, 2.0 Hz, 2H) 1.34 (t, *J* = 6.1 Hz, 3H), 1.32 (d, *J* = 6.8 Hz, 3H), 1.28 (d, *J* = 6.6 Hz, 3H), 1.03 -1.00 (m, 1H), 0.49 - 0.51 (m, 2H), 0.19 - 0.17 (m, 2H); ^{13}C NMR (101 MHz, CD_3OD) δ: 202.53, 202.40, 171.08, 170.79, 162.86, 158.71, 158.56, 133.97, 133.56, 132.97, 132.64, 131.00, 130.92, 130.59, 130.43, 115.51, 115.45, 115.07, 115.02, 76.60, 72.84, 72.80, 71.44, 71.27, 70.18, 70.12, 67.85, 67.71, 50.48, 49.84, 48.14, 45.78, 36.31, 21.67, 21.28, 20.68, 20.16, 11.40, 3.41. ESI-MS *m/z* $[M+H]^+$ calculated for $C_{27}H_{36}N_2O_5S$ 500.65, found = 501.4.

6.3.2. N-(3-(4-(2-(cyclopropylmethoxy)ethyl)phenoxy)-2-hydroxypropyl)-N-isopropyl-2-(4-(3-thioxo-3H-1,2-dithiol-5-yl)phenoxy)acetamide

Betaxolol-ADTOH, compound 2b.

Compound **2b** was obtained according to the procedure reported above for **1a**, starting from betaxolol **2** (1.00 g; 3.25 mmol) and the intermediate **5b** (0.924 g; 3.25 mmol). Orange oil. Yield 0.699 g; 37.5 %.

^{1}H NMR (400 MHz, CD_3OD) δ: 7.73 (d, *J* = 4.5 Hz, 2H), 7.48 (d, *J* = 20.4 Hz, 2H), 7.15 (d, *J* = 8.5 Hz, 2H), 7.11 - 7.08 (m, 4H), 7.07 (d, *J* = 4.5 Hz, 2H), 6.88 (d, *J* = 4.5 Hz, 2H), 6.78 (d, *J* = 4.6 Hz, 2H), 5.50 (s, 1H), 5.26 (d, *J* = 15.1 Hz, 1H), 5.02 (s, 2H), 4.95 (d, *J* = 15 Hz, 1H), 4.36 - 4.29 (m, 1H), 4.26 - 4.15 (1H, m), 4.04 - 3.95 (1H, m), 3.88 - 3.78 (1H, m), 3.63 (t, *J* = 7.1 Hz, 2H), 3.55 (d, *J* = 5.8 Hz, 1H), 3.50 (q, *J* = 7.0 Hz, 2H), 3.38 (d, *J* = 6.8 Hz, 1H), 3.29 (d, *J* = 2.1 Hz, 2H) 3.27 (d, *J* = 2.1 Hz, 2H), 2.81 - 2.78 (m, 2H) 1.35 - 1.28 (m, 3H), 1.19 (t, *J* = 7.0 Hz, 3H), 1.04 - 1.01 (1H, m), 0.53 - 0.49 (m, 2H), 0.21 - 0.17 (m, 2H); ^{13}C NMR (101 MHz, CD_3OD) δ: 217.21, 174.88, 174.58, 170.83, 170.53, 163.41, 162.93, 158.70, 158.56, 135.81, 135.67, 132.99, 132.65, 130.99, 130.88, 129.85, 129.66, 126.21, 126.14, 125.80, 116.94, 116.88, 115.52, 115.39, 76.59, 72.81, 71.60, 71.25, 70.15, 70.03, 67.86, 67.75, 66.91, 50.50, 49.84, 48.06, 45.63, 38.88, 36.61, 30.89, 30.75, 21.69, 21.27, 20.68, 20.17, 15.43, 11.40, 3.43. ESI-MS *m/z* $[M+H]^+$ calculated for $C_{29}H_{35}NO_5S_3$ 573.79, found = 574.31

6.3.3. ethyl 4-(2-((3-(4-(2-(cyclopropylmethoxy)ethyl)phenoxy)-2-hydroxypropyl)(isopropyl)amino)-2-oxoethoxy)benzodithioate

Betaxolol-HBTA, compound 2c.

Compound **2c** was obtained according to the procedure reported above for **1a**, starting from betaxolol **2** (1.00 g; 3.25 mmol) and the intermediate **6b** (0.833 g; 3.25 mmol). Pink oil. Yield 0.816 g; 46.0 %.

^{1}H NMR (400 MHz, CD_3OD) δ: 8.07 (d, *J* = 4.8 Hz, 2H), 8.04 (d, *J* = 4.8 Hz, 2H), 7.17 (d, *J* = 6.5 Hz, 2H), 7.12 (d, *J* = 6.6 Hz, 2H), 6.98 (d, *J* = 4.8 Hz, 2H), 6.96 (d, *J* = 4.8 Hz, 2H), 6.89 (d, *J* = 4.5 Hz, 2H), 6.82 (d, *J* = 4.4 Hz, 2H), 5.22 (d, *J* = 14.9 Hz, 1H), 4.99 (s, 2H), 4.92 (d, *J* = 14.9 Hz, 1H), 4.38 - 4.31 (m, 1H), 4.24 - 4.18 (m, 3H), 4.05 - 3.95 (m, 2H), 3.94 - 3.91 (m, 1H), 3.86 - 3.81 (m, 1H), 3.61 (t, *J* = 7.1 Hz, 2H), 3.58 (d, *J* = 5.3 Hz, 1H), 3.54 - 3.52 (m, 1H), 3.42 - 3.36 (m, 4H), 3.30 (d, *J* = 3.1 Hz, 2H), 3.28 (d, *J* = 3.0 Hz, 2H), 2.82 - 2.78 (m, 2H), 1.39 (td, *J* = 7.4, 2.0 Hz, 3H), 1.30 - 1.35 (m, 6H), 1.28 (d, *J* = 6.6 Hz, 3H), 1.06 - 0.99 (m, 1H), 0.53 - 0.49 (m, 2H), 0.21 - 0.17 (m, 2H); ^{13}C NMR (101 MHz, CD_3OD) δ: 202.92, 202.59, 170.88, 170.60, 163.94, 163.53, 158.69, 158.53, 140.03, 139.74, 132.94, 132.55, 130.99, 130.90, 129.82, 129.56, 115.50, 115.43, 115.32, 76.58, 72.85, 72.80, 71.43, 71.21, 70.14, 70.07,

67.81, 67.73, 50.47, 49.81, 48.08, 45.72, 36.31, 31.93, 31.85, 21.67, 21.27, 20.69, 20.18, 12.87, 11.40, 3.42. ESI-MS *m/z* $[M+H]^+$ calculated for $C_{29}H_{39}NO_5S_2$ 545.75, found = 546.32

6.3.4. 1-(4-(2-(cyclopropylmethoxy)ethyl)phenoxy)-3-(isopropylamino)propan-2-yl (4-isothiocyanatophenyl) succinate

Betaxolol-HPI, compound 2d.

Betaxolol **2** (1.00 g; 3.25 mmol), solubilized in anhydrous methylene chloride (30 mL), was treated with a catalytic amount of DMAP (0.040 g; 0.32 mmol). The solution was cooled to 0°C, and succinic anhydride (0.488 g; 4.87 mmol) was added with the mixture being stirred at room temperature for 6h. The solvent was concentrated in vacuo and the resulting hemi-succinated ester was isolated by silica gel open chromatography (dichloromethane/methanol 9:1 v/v) as an oil. Yield 0.539 g; 40.7 %. ESI-MS *m/z* $[M+H]^+$ calculated for $C_{22}H_{33}NO_6$ 407.50, found = 408.6.

The intermediate (1.00 g; 2.45 mmol) was linked to HPI **7** (0.370 g; 2.45 mmol) using EDAC·HCl (0.703 g; 3.67 mmol) and DMAP (0.448 g; 3.67 mmol) as coupling agents in anhydrous THF (20 mL), for 12h at room temperature. The solvent was removed to obtain the crude product. The residue was loaded on a silica gel open column and eluted with methylene chloride/ethyl acetate (9.5:0.5 v/v). The combined and evaporated fractions gave compound **2d** as a colorless oil. Yield 0.395 g; 29.8 %.

^{1}H NMR (400 MHz, $CDCl_3$) δ: 7.22 (d, *J* = 4.5 Hz, 2H), 7.13 (d, *J* = 8.6 Hz, 2H), 7.09 (d, *J* = 4.5 Hz, 2H), 6.83 (d, *J* = 4.7 Hz, 2H), 4.18 - 4.11 (m, 1H), 4.04 - 3.93 (m, 2H) 3.83 - 3.78 (m, 1H), 3.61 (t, *J* = 7.4 Hz, 2H), 3.46 (dd, *J* = 14.7, 1.8 Hz, 2H), 3.28 (d, *J* = 6.9 Hz, 2H), 2.95 - 2.80 (m, 6H), 2.00 (bs, 1H) 1.29 (d, *J* = 6.7 Hz, 3H), 1.23 (d, *J* = 6.5 Hz, 3H), 1.07 - 1.03 (m, 1H), 0.55 - 0.50 (m, 2H), 0.21 - 0.17 (m, 2H); ^{13}C NMR (101 MHz, $CDCl_3$) δ: 173.76, 171.53, 157.01, 149.49, 136.02, 131.67, 130.04, 128.93, 126.86, 123.04, 114.40, 75.78, 72.32, 71.93, 69.70, 49.18, 46.36, 35.60, 29.61, 28.54, 21.23, 20.83, 10.76, 3.12. ESI-MS *m/z* $[M+H]^+$ calculated for $C_{29}H_{36}N_2O_6S$ 540.67, found = 541.3.

6.4. Synthesis of Compounds 3a-3d

6.4.1. 4-carbamothioylphenyl 4-((5-bromoquinoxalin-6-yl)(4,5-dihydro-1H-imidazol-2-yl)amino)-4-oxobutanoate

Brimonidine-TBZ, compound 3a.

To a solution of brimonidine **3** (1.00 g; 3.42 mmol) in anhydrous DMF (5 mL) under a nitrogen atmosphere, was added dropwise succinic anhydride (0.376 g; 3.76 mmol) and DMAP (0.041 g; 0.34 mmol) solubilized in DMF (10 mL) at room temperature and the mixture was stirred overnight. Subsequently TBZ (4-hydroxybenzothioamide) **4** (0.524 g; 3.42 mmol), EDAC·HCl (0.983 g; 5.13 mmol) and DMAP (0.627 g; 5.13 mmol) were added. The reaction mixture was stirred at room temperature for 12h. The solvent was removed in vacuo and the residue was purified by column chromatography on silica gel (ethyl acetate/ dichloromethane 8:2 v/v). The yellow solid **3a** was obtained by re-crystallization with diethyl ether. Yield 0.610 g; 33.8 %. Mp 121.8 – 123.4° C. ^{1}H NMR (400 MHz, DMSO-d_6) δ: 9.88 (bs, 1H), 9.52 (bs, 1H), 8.95 (s, 1H), 8.83 (s, 1H), 7.99 (d, J = 8.5 Hz, 1H), 7.94 (d, J = 8.2 Hz, 2H), 7.59 (d, J = 8.9 Hz, 1H), 7.15 (d, J = 8.5 Hz, 2H), 7.11 (bs, 1H), 3.94 - 3.93 (m, 2H), 3.54 - 3.52 (m, 2H), 3.37 - 3.35 (m, 2H), 2.94 - 2.92 (m, 2H); ^{13}C NMR (101 MHz, DMSO-d_6) δ: 199.52, 171.79, 171.69, 153.24, 150.89, 149.89, 146.04, 143.89, 141.83, 140.47,137.42, 129.36, 129.23, 128.46, 121.60, 115.38, 44.07, 38.93, 32.50, 29.24. ESI-MS *m/z* $[M+H]^+$ calculated for $C_{22}H_{19}BrN_6O_3S$ 526.04, found = 527.2.

6.4.2. 4-(3-thioxo-3H-1,2-dithiol-5-yl)phenyl 4-((5-bromoquinoxalin-6-yl)(4,5-dihydro-1H-imidazol-2-yl)amino)-4-oxobutanoate

Brimonidine-ADTOH, compound 3b.

Compound **3b** was synthetized following the synthetic route applied for the synthesis of **3a**. Brimonidine **3** (1.00 g; 3.42 mmol) was coupled with ADT-OH (5-(4-hydroxyphenyl)-3H-1,2-dithiole-3-thione) **5** (0.774 g; 3.42 mmol). Orange solid. Yield 0.700 g; 34.1 %. Mp 128.1 – 129.5° C.

^{1}H NMR (400 MHz, DMSO-d_6) δ: 8.94 (s, 1H), 8.83 (s, 1H), 7.99 (d, J = 6.0 Hz, 1H), 7.83 (d, J = 10 Hz, 2H), 7.59 (d, J = 8.6 Hz, 1H), 7.29 (d, J = 8.1 Hz, 2H), 7.12 (bs, 1H), 5.70 (s, 1H), 3.94 - 3.91 (m, 2H), 3.54 - 3.52 (m, 2H), 3.38

- 3.35 (m, 2H), 2.95 - 2.93 (m, 2H); ^{13}C NMR (101 MHz, DMSO-d_6) δ: 215.96, 173.24, 171.79, 171.62, 154.07, 150.89, 149.90, 146.05, 143.91, 141.83, 140.48, 136.23, 129.31, 129.17, 128.46, 123.51, 123.47, 115.39, 44.08, 38.94, 32.54, 29.30. ESI-MS *m/z* $[M+H]^+$ calculated for $C_{24}H_{18}BrN_5O_3S_3$ 598.98, found = 600.1.

6.4.3. 4-((ethylthio)carbonothioyl)phenyl 4-((5-bromoquinoxalin-6-yl)(4,5-dihydro-1H-imidazol-2-yl)amino)-4-oxobutanoate

Brimonidine-HBTA, compound 3c.

Compound **3c** was synthetized following the synthetic route applied for the synthesis of **3a**. Brimonidine **3** (1.00 g; 3.42 mmol) was coupled with HBTA (S-ethyl 4-hydroxybenzodithioate) **6** (0.678 g; 3.42 mmol). Pink solid. Yield 0.869 g; 44.4 %. Mp 160.5 – 162.1° C.

^{1}H NMR (400 MHz, DMSO-d_6) δ: 8.94 (s, 1H), 8.83 (s, 1H), 8.02 (d, J = 8.5 Hz, 2H), 7.99 (d, J = 8.9 Hz, 1H), 7.60 (d, J = 8.6 Hz, 1H), 7.25 (d, J = 7.6 Hz, 2H), 7.11 (bs, 1H), 3.93 (t, J = 7.7 Hz, 2H), 3.55 (t, J = 6.0 Hz, 2H), 3.41 - 3.35 (m, 4H), 2.96 - 2.90 (m, 2H), 1.35 (t, J = 7.3 Hz, 3H); ^{13}C NMR (101 MHz, DMSO-d_6) δ: 225.4, 171.32, 171.06, 154.18, 150.41, 149.42, 145.56, 143.42, 141.83, 141.36, 140.00, 128.83, 127.98, 127.89, 122.00, 114.90, 43.59, 38.45, 32.02, 31.14, 28.31, 12.13. ESI-MS *m/z* $[M+H]^+$ calculated for $C_{24}H_{22}BrN_5O_3S_2$ 571.03, found = 572.2

6.4.4. 4-isothiocyanatophenyl 4-((5-bromoquinoxalin-6-yl)(4,5-dihydro-1H-imidazol-2-yl)amino)-4-oxobutanoate

Brimonidine-HPI, compound 3d.

Compound **3d** was synthetized following the synthetic route applied for the synthesis of **3a**. Brimonidine **3** (1.00 g; 3.42 mmol) was coupled with HPI (4-hydroxyphenyl isothiocyanate) **7** (0.517 g; 3.42 mmol). Pale yellow solid. Yield 1.146 g; 63.8 %. Mp 159.0 – 160.5°C.

^{1}H NMR (400 MHz, DMSO-d_6) δ: 8.94 (s, 1H), 8.83 (s, 1H), 7.98 (d, J = 8.9 Hz, 1H), 7.58 (d, J = 8.9 Hz, 1H), 7.49 (d, J = 8.7 Hz, 2H), 7.19 (d, J = 8.7 Hz, 2H), 7.09 (bs, 1H), 3.92 (t, J = 7.8 Hz, 2H), 3.52 (t, J = 6.3Hz, 2H), 3.36 (t, J = 7.8, 2H), 2.90 (t, J = 6.2 Hz, 2H); ^{13}C NMR (101 MHz, DMSO-d_6) δ: 171.26, 150.41, 149.42, 145.57, 143.42, 141.36, 140.00, 133.66, 128.83, 127.98,

127.39, 127.21, 123.28, 121.60, 116.33, 114.91, 43.59, 38.45, 32.05, 28.74. ESI-MS *m/z* $[M+H]^+$ calculated $C_{22}H_{17}BrN_6O_3S$ 524.03, found = 525.1.

6.5. Synthesis of Compounds 4a-6a

6.5.1. Tert-butyl 2-(4-carbamothioylphenoxy)acetate (4a)

In a neck flask sodium hydride (60% dispersion in mineral oil, 0.261 g; 6.53 mmol) was suspended in DMF (10 mL) and the suspension was stirred and cooled to 0°C. A solution of TBZ (4-hydroxybenzothioamide) **4** (1.00 g; 6.53 mmol) in DMF (2 mL) was added dropwise. After 10 minutes a solution of tert-butyl bromoacetate (1.16 mL; 7.84 mmol) in DMF (2 mL) was added dropwise. The mixture was stirred at room temperature for 12h. The solution was concentrated in vacuo and the crude residue was purified by silica gel open chromatography (dichloromethane as eluent) to give intermediate **4a** as a yellowish solid. Yield 1.427 g; 81.7 %. ESI-MS *m/z* $[M+H]^+$ calculated $C_{13}H_{17}NO_3S$ 267.34, found = 268.6.

6.5.2. Tert-butyl 2-(4-(3-thioxo-3H-1,2-dithiol-5-yl)phenoxy)acetate (5a)

Compound **5a** was synthetized from ADT-OH (5-(4-hydroxyphenyl)-3H-1,2-dithiole-3-thione) **5** (1.00 g; 4.42 mmol) and tert-butyl bromoacetate (0.783 mL; 5.30 mmol) in the presence of NaH (0.177 g; 4.42 mmol), following the procedure adopted for the synthesis of **4a**. Brown solid. Yield 0.957 g; 63.6 %. ESI-MS *m/z* $[M+H]^+$ calculated $C_{15}H_{16}O_3S_3$ 340.48, found = 342.0.

6.5.3. Tert-butyl 2-(4-((ethylthio)carbonothioyl)phenoxy)acetate (6a)

Compound **6a** was synthetized from HBTA (S-ethyl 4-hydroxybenzodithioate) (1.00 g; 5.04 mmol) and tert-butyl bromoacetate (0.893 mL; 6.05 mmol) in the presence of NaH (0.202 g; 5.04 mmol), following the procedure adopted for the synthesis of **4a**. Pink solid. Yield 0.821 g; 52.1 %. ESI-MS *m/z* $[M+H]^+$ calculated $C_{15}H_{20}O_3S_2$ 312.45, found = 313.8.

6.6. General Procedure for the Synthesis of Compounds 4b-6b

Intermediates **4a**-**6a** were dissolved in a 10% (v/v) TFA solution in anhydrous dichloromethane (10 mL) and stirred at room temperature until the compound was completely deprotected. Solvent was then removed by reduced pressure

distillation and the compounds **4b**-**6b** were obtained by re-crystallization with diethyl ether.

6.6.1. 2-(4-carbamothioylphenoxy)acetic acid **(4b)**

Synthetized from intermediate **4a**. Yellowish solid. Yield 91.1 %. ESI-MS *m/z* $[M+H]^+$ calculated $C_9H_9NO_3S$ 211.24, found = 212.1.

6.6.2. 2-(4-(3-thioxo-3H-1,2-dithiol-5-yl)phenoxy)acetic acid **(5b)**

Synthetized from intermediate **5a**. Orange solid. Yield 95.4 %. ESI-MS *m/z* $[M+H]^+$ calculated $C_{11}H_8O_3S_3$ 284,37, found = 285.2.

6.6.3. 2-(4-((ethylthio)carbonothioyl)phenoxy)acetic acid **(6b)**

Synthetized from intermediate **6a**. Pink solid. Yield 93.2 %. ESI-MS *m/z* $[M+H]^+$ calculated $C_{11}H_{12}O_3S_2$, found 256.34 = 257.9.

6.7. *In vitro* Evaluation

6.7.1. Amperometric determination of H_2S release

The H_2S-releasing properties of compounds **1a**-**1d**, **2a**-**2d**, **3a**-**3d** were evaluated by amperometry, through an Apollo-4000 Free Radical Analyzer (World Precision Instrument- WPI) detector and H_2S-selective minielectrodes (ISO-H_2S-2, WPI) endowed with gas-permeable membranes (87). The experiments were carried out at room temperature. Following the instructions of the manufacturer, a "PBS buffer 10x" was prepared ($NaH_2PO_4 \cdot H_2O$ 1.28 g, $Na_2HPO_4 \cdot 12H_2O$ 5.97 g, NaCl 43.88 g in 500 mL of H_2O) and stocked at 4°C. Immediately before the experiments, the "PBS buffer 10x" was diluted in distilled water (1:10), to obtain the assay buffer (AB); pH was adjusted to 7.4. The H_2S-selective minielectrode was equilibrated in 2 mL of the AB, until the recovery of a stable baseline. Then, 20 µL of a dimethyl sulfoxide (DMSO) solution of the tested compounds were added (final concentration 100 µM; final concentration of DMSO in the AB 1%). The generation of H_2S was observed for 30 min. When required by the experimental protocol, L-Cysteine 4 mM was added, before the H_2S releasing molecule. The relationship between the amperometric currents (recorded in pA) and the corresponding concentrations of H_2S was determined by calibration curves with increasing concentrations of

NaHS (1 μM, 3 μM, 7 μM) at pH 4.0. The curves relative to the progressive increase of H_2S vs time, following the incubation of the tested compounds, were analyzed by a fitting curve using the software GraphPad Prism 6.0. The parameter of C_{max} (the highest concentration of H_2S obtained during the recording time) and TCM_{50} (time required to reach a concentration = ½ C_{max}) were calculated and expressed as mean ± standard error from five different experiments. ANOVA and Student t-test were selected as statistical analysis, $P < 0.05$ was considered representative of significant statistical differences.

6.7.2. Cell culture

Human Primary Corneal Epithelial Cells (HCEs) were grown in Corneal Epithelial Cell Basal Media supplemented with Corneal Epithelial Cell Growth Kit components and 1% of 100 units/ml penicillin and 100 mg/ml streptomycin (Sigma Aldrich) in a tissue culture flask at 37 °C in a humidified atmosphere and 5% CO_2. HCEs were cultured up to about 90% confluence and 24 h before the experiment, the cells were seeded onto a 96-well black plate, clear bottom pre-coated with gelatin 1% (from porcine skin, Sigma Aldrich), at density of 72 × 10^3 per well. Cells were split 1:2 twice a week and used until passage 18.

6.7.3. Evaluation of H_2S release on HCEs

After 24 h to allow cell attachment, the medium was replaced and cells were incubated for 30 min in the buffer standard (HEPES 20 mM, NaCl 120 mM, KCl 2 mM, $CaCl_2 \cdot 2H_2O$ 2 mM, $MgCl_2 \cdot 6H_2O$ 1 mM, Glucose 5 mM, pH 7.4, at room temperature) containing the fluorescent dye WSP-1 (Washington State Probe-1, 1,3'-methoxy-3-oxo-3H-spiro[isobenzofuran-1,9'-xanthen]-6'yl 2-(pyridin-2-yldisulfanyl) benzoate, Cayman Chemical) at the concentration of 100 μM (59, 93). Then the supernatant was removed and replaced with a solution of the tested compounds or diallyl disulfide (DADS) as a known H_2S-donor in buffer standard (91). When WSP-1 reacts with H_2S, it releases a fluorophore detectable with a spectrofluorometer at excitation and emission wavelengths of 465-515 nm (87, 90, 93). The increasing of fluorescence

(expressed as fluorescence index = FI) was monitored after 30 min, using a spectrofluorometer (EnSpire, Perkin Elmer).

6.7.4. Statistical Analysis

Experimental data were analyzed by a computer fitting procedure (software: GraphPad Prism 6.0) and expressed as mean ± standard error; three different experiments were performed, each carried out in three replicates. ANOVA and Student t test were selected as statistical analyses; when required, the Bonferroni post hoc test was used. $P < 0.05$ was considered as representative of significant statistical differences.

7. Conclusion

Glaucoma is a collection of optic neuropathies described as degeneration of optic nerve head and loss of retinal ganglion cells. In 2020, it has been ranked as the second leading cause of blindness (102) and the number of glaucoma patients is expected to rise in the next 20 years (3).

The biological basis of glaucoma is still not completely clear but elevated intraocular pressure (IOP) has been defined as the major risk factor for glaucoma development and progression (10, 12, 20).

For most forms of glaucoma, included normotensive glaucoma, pharmacological treatment is currently based on the IOP control through topical medications. However, the last topical agent for glaucoma therapy approved by Food and Drug Administration (FDA), dates to more than twenty years ago (48). Therefore, with the increasing prevalence of glaucoma worldwide, the exigency of new therapies is emerging.

In the last decades, several studies have proven the pathophysiological and pharmacological role of H_2S and the interest of scientific research towards this new gas-transmitter is constantly growing. Recent data showing H_2S involvement in ocular diseases (72), especially in optic neuropathies like glaucoma (75, 76), have paved the way for the potential application of H_2S donors in glaucoma treatment.

During my PhD, I worked on the synthesis and characterization of new molecular hybrids between currently available drugs for glaucoma therapy and H_2S releasing compounds, to improve the efficacy of antiglaucoma medications and reduce side effects.

I synthetized hybrid derivatives of brinzolamide (carbonic anhydrase inhibitor; compounds **1a**-**1d**), betaxolol (β-blocker; compounds **2a**-**2d**) and brimonidine (α_2-adrenergic agonist; compounds **3a**-**3d**).

The new molecular entities (100 μM) were tested for their H_2S releasing properties via amperometric and fluorometric assays.

The amperometric studies were carried out in a phosphate buffer solution to evaluate the H_2S release in aqueous environment. Furthermore, L-Cysteine 4 mM was added to simulate the free thiols naturally found in the cells. All the synthetized hybrids showed a completely negligible H_2S production in the

absence of L-Cys, proving that the thiol group act as a trigger for the release of the sulfide. Betaxolol hybrids (compounds **2a-2d**) demonstrated poor H_2S releasing properties both in the absence or in the presence of L-Cys.

The release of H_2S was studied also in Human Primary Corneal Epithelial Cells (HCEs) for describing the process in a biological substrate, without adding exogenous thiols. The experiments were performed through a fluorescent dye, WSP-1.

Also fluorometric assay confirmed a weak H_2S donation from betaxolol hybrids. Chemical structure of betaxolol could be responsible for the limited H_2S releasing properties of its derivatives (**2a-2d**).

Amperometric and fluorometric data showed that molecular hybrids of TBZ (**1a-3a**) and ADT-OH (**1b-3b**) had a low release of H_2S compared to HBTA and HPI derivatives (**1c-3c** and **1d-3d**, respectively). Noteworthy, compounds **1c** (brinzolamide-HBTA), **1d** (brinzolamide-HPI) and **3c** (brimonidine-HPI) demonstrated to be the best H_2S releasing hybrids with a massive production of H_2S both in the aqueous solution (in the presence of L-Cys) and in the intracellular environment.

These preliminary results confirm the hybridization as a promising strategy in the drug design process. By the synthesis of a new molecular entity, through the combination of two or more, identical or different drugs, with or without a linker, the aim is to enhance the efficacy of the parent agents, reducing their toxicity (103). Moreover, based on the clinic data, the idea of combining powerful H_2S donors like HBTA or HPI with more efficacious IOP-lowering drugs like prostaglandin analogs, could be an interesting strategy to obtain new tools for the treatment of glaucoma.

Further studies *in vitro* are planned to be performed to analyze the effects of the synthetized molecular hybrids on the survival of RGC-5 (retinal ganglion cells 5) cell line in culture, exposed to toxic agents like ROS. For the evaluation of *in vivo* activity, the native antiglaucoma drugs and the hybrid derivatives will be administered in glaucoma animal models to describe the contribution of the sulfureted moieties to IOP reduction.

Part II

Design and development of ocular delivery systems for antiglaucoma hybrids

1. Introduction

My PhD project was carried out in collaboration with the pharmaceutical company Genetic S.p.a (Fisciano, Italy). During the six months I spent in Genetic R&D laboratories, I approached the development and analysis of different pharmaceutical dosage forms, according to the good laboratory practice (GLP) principles.

I was involved in the entire development process of a new medication, starting from the design of the formulation, setting and validation of analytical methods, preparation of laboratory batches, testing of raw material and finished product, and execution of stability studies. I collaborated on research projects actually ongoing and I had the chance to improve my practical skills through the use of innovative technical instruments.

Genetic S.p.a has a long experience in the research, development and manufacturing of innovative therapeutic tools, especially ocular dosage forms. Over the course of my experience in the pharmaceutical manufacturing site, under the supervision of my company tutor, I worked on the design and formulation of new ocular preparations containing the molecular hybrids I synthetized at the Department of Pharmacy of University of Naples.

2. Preliminary Study for Antiglaucoma Hybrids Eye Drops

To date, eye drops represent the first choice means for the treatment of glaucoma patients. This ophthalmic dosage form can be an aqueous or oily solution, suspension or emulsion (104).

Topical instillation of eye drops on the front of the eye is a simple route of administration for treating conditions affecting the anterior structure of the eye such as cornea, conjunctiva, sclera, trabecular meshwork. Through this delivery path the systemic absorption of drugs is reduced, therefore fewer side effects may occur. In addition, this approach is easy, economic, noninvasive and not painful for patients (105).

Pharmaceutical solutions are the most common dosage forms for ocular administration due to the simplicity of the development and production process. Ophthalmic preparations are sterile; the pH value should be around 7.4 and

osmolarity around 310 mOsm/kg (106). Single and multidose products are available. Viscosity-modifying agents, preservatives, antioxidants, surfactants are some of the excipients used in these formulations. Because of the sterility requirement, for multidose product is essential the choice of antimicrobial preservative. Benzalkonium chloride is commonly used in ocular preparations and it helps to reduce bacterial and fungal growth in multidose recipients. However, a heated debate is in progress within the scientific community due to a potential association between the use of benzalkonium chloride as a preservative in ophthalmic preparations and ocular toxicity (107).

In general, ophthalmic solutions are prepared by dissolution of active pharmaceutical ingredient (API) and excipients in water for injection (WFI). A key step is the sterilization process: it can be carried out at the end, on the manufactured and packaged product through moist heat procedure or by exposure to gamma radiations. However, several drugs are heat-labile, therefore is necessary to operate in aseptic conditions and once the solution is manufactured, it undergoes to a sterile filtration or autoclaving prior to the filling phase (108).

The ideal formulation of an ocular dosage form is still object of study for scientists and pharmaceutical companies worldwide, mainly because of the poor bioavailability of topically applied drugs (105, 109). Anatomical structure of the eye is complex and is characterized by mechanical, cellular and enzymatic barriers. They play a critical role protecting the eye from infections and insults but at the same time, are an obstacle for drug delivery. The outermost layer of the eye is the tear film, secreted by lacrimal glands, it protects and hydrates the inner structures. Considering that the capacity of conjunctival sac is low and is approximately 30 μL, the tear film (volume around 7 μL) further dilutes drug concentration applied on ocular surface (110). Also lacrimal turnover affects molecules bioavailability. Tear fluid influences physico-chemical properties of ocular dosage forms. Indeed, to avoid irritation, damage and increase of tear production, the pH value of topical formulations should be approximately 7.4, representing pH of tear film. In the same way, physiological osmolality of tears is around 290-310 mOsm/kg, therefore the osmolality value of preparations should not be lower than 100 mOsm/kg and higher than 640 mOsm/kg (106, 109, 110).

As reported in Part I, corneal absorption is the major limit for bioavailability of both hydrophobic and hydrophilic ocular drugs because the cornea is constituted by lipophilic (epithelium and endothelium) and hydrophilic (stroma) layers. Besides its poor permeability, the small surface responsible for corneal absorption also obstacles drug delivery (110).

Blinking, drug flow through the nasolacrimal duct, binding to proteins in tear fluid, pathologic condition altering the ocular blood-aqueous barrier represent other factors limiting bioavailability of ocular drugs (104, 109).

Several studies and efforts have been made to enhance this parameter and improve ophthalmic formulations. For example, to increase drug residence time on the cornea, mucoadhesives or viscosity enhancer such as carbomer, polyvinyl alcohol, other cellulose derivatives, can be added to the preparation.

An interesting approach to increase corneal absorption is the development of molecular prodrugs (109). These compounds, commonly esters, when characterized by an increased lipophilicity can cross corneal epithelium more easily than the parent drugs. Therefore, the bioavailability is higher and a reduction of the administered dose may also be possible. However, different factors should be evaluated to apply this strategy: the presence of functional groups that could be derivatized, prodrug solubility, stability in the final product, conversion *in vivo* to the parent compounds (111, 112).

Based on these considerations, my aim was to formulate new eye drops solutions for glaucoma treatment containing as active pharmaceutical ingredient the molecular hybrids **1a**-**1d**, **2a**-**2d**, **3a**-**3d**.

Unfortunately none of the synthetized compounds was soluble in water or any buffer system compatible with ocular formulations (citrate, phosphate, borate and tris-HCl buffer). Considering the results from *in vitro* assays, in this phase I paid attention to the potential development of brinzolamide-HBTA **1c** and brinzolamide-HPI **1d** based eye drops.

Preliminary studies aimed at identifying the best formulation for antiglaucoma hybrids eye drops solutions are underway at Genetic S.p.a. Through an examination of currently available literature, it was found that one of the common strategies to increase the solubility in aqueous solution of a hydrophobic drug is based on the use of cyclodextrins (104, 109, 110). Cyclodextrins (CDs) are cyclic oligosaccharides able to form complex with

water-insoluble drugs, improving their solubility, permeability and bioavailability. CDs are constituted by (α-1,4)-glucopyranose units, presenting a lipophilic central cavity that binds the drug, and a hydrophilic outer surface essential to solubilize the complex in water (113). During the formation of the drug/CD complex no covalent bonds are involved and there is a dynamic equilibrium between the molecular complex and the free drug in aqueous solution (Fig. 1) (114). CDs act as carriers because they solubilize and deliver drugs to the membrane surface, where the free drug is absorbed by the lipophilic layer of the cornea while the hydrophilic cyclodextrin remains in the mucin layer (113).

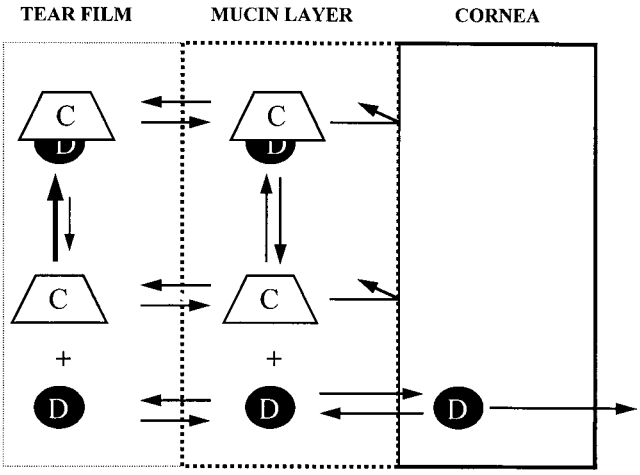

Figure 1. Drug delivery and absorption from the tear film towards the cornea by cyclodextrin eye drops (113).

CDs have been applied in several ocular preparations to solubilize water-insoluble drugs such as cyclosporine A (114), dexamethasone (115), ciprofloxacin (106), brinzolamide (116). Some cyclodextrins-based eye drops have been also registered in Europe such as chloramphenicol (Clorocil®; Edol), diclofenac (Voltaren Ophthalmic®; Novartis) and indomethacin (Indocid®; Merck Sharp & Dohme-Chibret).

Studies suggest that to reach the optimal ocular availability, the concentration of CDs should be approximately 15% or less, because at higher concentration, the drug could be retained as complex in the aqueous tear film, reducing bioavailability (104, 110, 113). In addition, some inactive ingredients could compete with the drug to bind the hydrophobic cavity or, on the contrary, they

could have a drug solubilizing effect, therefore the right amount of CDs to add in the formulation needs to be established after availability studies (113).
In conclusion, thanks to the collaboration with Genetic S.p.a., our target was to develop new molecular hybrids-based eye drops. Studies currently ongoing are focused on the optimization of the formulations, evaluation of solubility of the compounds **1c** and **1d,** and analysis of the features of inclusion complexes between hybrids and cyclodextrins, added in the preparations to improve drugs solubility.
When the ocular dosage forms are ready, further studies *in vitro* will be performed to analyze stability and permeability of the products as well as the release of the active compounds from cyclodextrin complex.

3. Contact Lenses as Innovative Therapeutic Tools

3.1. Introduction

As discussed in the previous chapter, although eye drops are the most common ophthalmic preparations to treat ocular diseases, the poor drug bioavailability is the major limitation related to these dosage forms. Only 5-10% of the instilled drug is absorbed through the cornea and reaches the biological target in the eye (110). Therefore, to achieve the therapeutic effect is necessary to administer high dose of drug and/or the instillation must be performed several times a day, increasing the risk of unwanted side effects. These disadvantages are associated with another factor contributing to the potential failure of eye drops-based therapy, which is the low patients adherence (117). Noncompliance is mainly a consequence of patients inability to correctly instill drops in the eye due to a lack of manual dexterity especially in elderly patients or people with mental or physical deficit (118). This is considered an issue by glaucoma patients because they are subjected to a chronic therapy and most of the time the disease is asymptomatic and slow progressing. As a result, the poor understanding of therapy aim or the absence of an immediate relief contribute to reduce the successful control of the disease (119).

However, even in glaucoma patients with a good adherence to therapy, the risk of IOP fluctuations, associated with an inadequate pharmacokinetics of eye drops, decrease the efficacy of the treatment (120).

In this scenario, several efforts have been made to increase drug bioavailability, reduce the frequency of administration, and improve patient's compliance. Besides the possibility to improve the eye drops formulations with excipients that increase residence time of drug on ocular surface or enhance tissue permeability, advanced drug delivery systems such as nanoparticles, liposomes or ocular implants have been developed (120). A recent approach designed to ensure a sustained drug delivery, improving effectiveness of therapy and patients adherence, is based on the application of contact lenses as a means to release drugs (121).

3.2. Methodologies for the Development of Therapeutic Contact Lenses

Contact lenses (CL) are ocular devices used by approximately 150 million people worldwide (122). They are applied mainly to correct vision impairments but also as cosmetic accessories. CL are divided in two groups based on the materials: soft contact lenses made by hydrogel or silicone-hydrogel polymers and rigid gas permeable contact lenses made by durable plastic. Soft contact lenses are constituted primarily by polymers of 2-hydroxyethyl methacrylate (p-HEMA) and thanks to the softness of the materials and their ability to comply with the shape of the eye, they are more used than rigid lenses (122).

Different studies have proven that CL can be a potential drug delivery system: once the drug eluting contact lenses are applied on ocular surface, the therapeutic agent is released in the tear film and diffuses across the cornea (Fig. 2). The so-called "sink effect" is responsible for the constant and prolonged flow of the drug from the contact lenses because the therapeutic agent is continuously absorbed in ocular tissues, reducing the concentration in the post-lens tear film (123). Therapeutic lenses allow to increase up to 30 min the retention time of drugs on cornea surface, the bioavailability reaches 50% and a reduction of drug fluctuations as well as of administered dose may occur (121, 123).

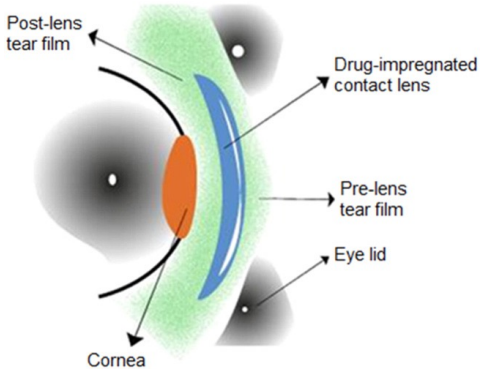

Figure 2. Application of a drug-eluting contact lens on ocular surface and drug release in tear film (123).

Considering that the eye drops are associated with poor patients' adherence, the application of contact lenses on the eye and following discomfort and ocular dryness are causes of concerns. However, taking into account the high number of people daily wearing CL, the potential benefits expected from this system could encourage their use (121).

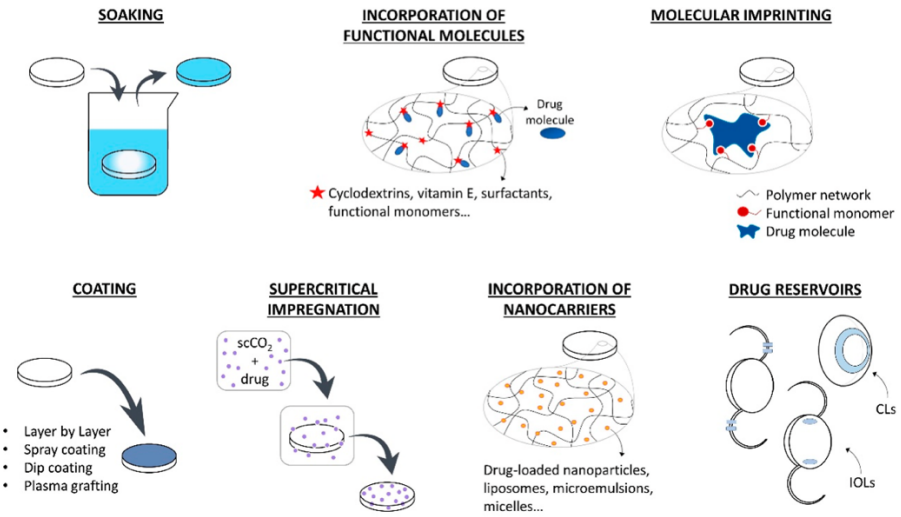

Figure 3. Different strategies to develop drug eluting contact lenses: soaking in a drug solution; incorporation of functional molecules with higher affinity to the drug, molecular imprinting, coating of the lens with the drug, supercritical impregnation, incorporation of nanocarriers, development of drug reservoirs.

To design a therapeutic contact lens, is essential to evaluate drug physico-chemical properties that could compromise optical features of the device, such as oxygen permeability, water content, transparency, flexibility, on which depend comfort and visual quality during lens wearing. In addition, from a

commercial point of view, the drug-eluting contact lens system should be stable in storage condition and compatible with lens care solutions (124).
Different strategies have been described for obtaining therapeutic lenses, including simple method such as “soaking” and more elaborated approaches like “molecular imprinting” (121, 123, 124) (Fig. 3).

3.2.1. Soaking

The simplest method to load a drug is soaking a commercial lens in a drug solution. Although this approach is simple and economic, different parameters influence this process, such as lens material, drug physico-chemical properties, loading time, concentration of the solution. In addition, through this strategy, the drug is quickly released with high initial release rate and a short delivery time (121, 123, 124).
The soaking method has been used for several hydrophilic drugs, commonly applied as eye drops for glaucoma treatment (125, 126). Peng *et al*. (127) tested *in vitro* and *in vivo* the efficacy of CL soaked in timolol maleate-PBS solution (2.67 mg/mL and 8 mg/mL) for seven days. The authors proved that the amount of drug absorbed through the cornea, applying CL, was higher compared to eye drops, while IOP lowering effect was the same, but using a smaller amount of drug in the therapeutic lenses.
Horn *et al.* (128, 129) developed a rapid method for loading a hydrophobic drug, such as latanoprost, in silicone hydrogel CL. The lens was soaked in a n-propanol solution of the drug and in 4 minute it quickly absorbed latanoprost by convection of the solvent. N-propanol, but non the hydrophobic drug, was then removed from the lens by rinsing with water. Latanoprost release was evaluated in artificial tear solution (ATF) and H_2O, showing a slow releasing rate.

3.2.2. Incorporation of Functional Molecules

A strategy to improve the interaction between soft contact lenses and drugs, to increase drug loading, is the incorporation of molecules characterized by a better affinity with the therapeutic agents. Functional molecules, such as cyclodextrins, vitamin E, surfactants, can be co-polymerized with HEMA or

can be added in the drug solution to improve solubility before soaking the lens (121, 123, 124).
Studies have shown that the incorporation of vitamin E creates a diffusion barrier in silicone-hydrogel lens, allowing a prolonged release of hydrophilic drugs (130, 131).

3.2.3. Molecular Imprinting

Molecular imprinting technique is based on the creation of imprinted cavities in the lens using a drug template. During the polymerization step, drug/functional monomer complexes are bound to the polymers, but subsequently the therapeutic molecule is released by washing, leaving a cavity in the lens characterized by high affinity to the drug. The compound is reloaded by soaking the lens in the drug solution. This approach allows to load a higher amount of drug, but is necessary to evaluate the right ratio between drug and functional monomer to avoid that the compound is stuck in the lens (132).
Molecular imprinting was applied to develop reusable timolol eluting contact lenses (133).

3.2.4. Incorporation of Nanocarriers

Drug functionalized nanocarriers, such as nanoparticles, liposomes, microemulsions, micelles, can be incorporated in the lens during the polymerization. Most of the nanoparticles are made by biodegradable polymers, releasing the drug after degradation. For non-degradable nanocarriers, drug release can be induced by light, changes in pH or temperature (121).

3.2.5. Supercritical Impregnation

Supercritical fluids are substances at temperature and pressure higher than the critical point, with intermediate properties between a liquid and a gas. Supercritical fluids, such as CO_2, are good solvents for both hydrophobic and hydrophilic compounds. Drug loading can be performed by soaking the lens in the fluid solution under controlled conditions. After the loading step, CO_2 is spontaneously released without the need of further purification while the drug is retained inside the polymer. Main limitations associated with this technique

are the higher complexity of the procedure compared to other approaches, and the quick release of the drug, usually occurring in few hours (134).
Costa *et al.* through supercritical CO_2 impregnation process, adding H_2O and ethanol as cosolvents to improve drug solubility, developed acetazolamide and timolol-loaded silicone-hydrogel CL. Both compounds were released completely in four hours after an initial burst release period (135).

3.2.6. Coating

Drug-polymer film can be added in the matrix of lens. It is important that drug coating does not affect CL optical properties, as for example transparency. Ciolino and coworkers (136) formulated a latanoprost-eluting therapeutic lens, composed by a latanoprost-poly(lactic-co-glycolic) acid (PLGA) polymer film. The authors performed also *in vitro* and *in vivo* studies in rabbit eyes, demonstrating that CL could release latanoprost for at least one month, in concentration comparable to those achieved with topical daily latanoprost eye drops.

3.2.7. Drug Reservoir

Drug reservoir can be incorporated in contact lenses, allowing a long lasting release of the therapeutic agent. Also in this case, is essential that transparency of the device is not compromised, therefore the reservoirs can be located in the periphery of the lens (121).

3.3. Aim of the Research

Contact lenses can be a promising drug delivery system to manage ocular diseases like glaucoma. Several examples of therapeutic contacts lenses, developed following different strategies, have been described for glaucoma treatment. The future goal of researchers is to properly replace eye drops-based therapy with contact lenses, allowing a less frequent drug administration (124). During my traineeship in Genetic S.p.a with the collaboration of R&D scientists' group, I worked on the development of molecular hybrids eluting contact lenses for the treatment of glaucoma. The focus of my research was to

study hybrids uptake and release by commercial lenses. The first approach was to load drugs in silicone-hydrogel CL by soaking, due to the relatively ease of method execution compared to other techniques.

As for the development of molecular hybrids-based eye drops, the main issue of the study was the insolubility of compounds in aqueous solutions. Therefore, following the strategy described by Horne *et al.* (129) to load a hydrophobic drug like latanoprost in silicone hydrogel lens, I evaluated the solubility of molecular hybrids in n-propanol. Amongst the compound **1a-1d**, **2a-2d**, **3a-3d**, only betaxolol hybrids were soluble in n-propanol (1 mg/mL) and the first attempt to develop an antiglaucoma hybrid-eluting CL was realized with betaxolol-HBTA, compound **2c**. Before starting drug loading and release experiments, a HPLC method for the quantitative determination of compound **2c** in the samples was described and validated.

3.3.1. Materials and Methods

3.3.1.1. Materials

Lens Dailies Total1® (diopter – 3.25, diameter 14.1 mm) from Novartis (Switzerland) were purchased from commercial sources. They are silicone hydrogel contact lenses (67% delefilcon A, 33% water) characterized by the presence of a water gradient: the lens is formed by a silicone hydrogel core surrounded by a high-water content layer.

All the chemicals and solvents (except betaxolol-HBTA) were purchased from Merck (Germany). Deionized water (DI) was used for the experiments.

3.3.1.2. Betaxolol-HBTA loading from n-propanol solutions

Loading solutions of betaxolol-HBTA in n-propanol at different concentrations (0.250 mg/mL, 2.5 mg/mL and 5.0 mg/mL) were prepared. The contact lens was removed from its blister pack, rinsed with deionized water, and gently dabbed with a Kimwipe®. The lenses are stored in a buffer solution, therefore, to reduce any interference before the loading experiment, they were placed in deionized water for 5 hours. Every hour the lens was washed, dabbed and transferred in fresh water. At the end, the lens was blotted dry on a Kimwipe® and soaked in 5.0 mL of the drug solution for 4 minutes under gentle stirring.

In n-propanol the lens instantly began to swell. After 4 minutes, the device was carefully taken it out from the loading solution with rubber-tipped plastic tweezers and washed for three times in 15 mL of DI, while the solution was stirring. After three rinses of 15 seconds each, the contact lens was placed in 8 mL of DI without being stirred. During the washing time, the lens returned to its original size.

3.3.1.3. Determination of Betaxolol-HBTA loaded in the lens

The quantification of betaxolol-HBTA in the loading solution before and after the lens soaking was performed by HPLC (Agilent 1260 Infinity II system, USA). The analytical column was a 3 μm Luna C_{18} (150 mm x 3.0 mm, Phenomenex USA). The mobile phases were acetonitrile as phase A and acetonitrile/phosphate buffer 40:60 as phase B. The phosphate buffer was prepared dissolving 1.73 g of K_2HPO_4 in 1.0 L of deionized water. Then the pH was adjusted to 7.0 with phosphoric acid. Elution was carried out at a flow rate of 0.6 mL/min at room temperature. Gradient = 0–12 min: ramp phase A 0-60%, 12-28 min: ramp phase A 60-80%. Run time was 28 minutes, followed by 5 minutes of post-run. The UV-visible detector was set to 254 nm and 100 μL of the sample were injected (137).

For the determination of betaxolol-HBTA a "standard solution" was prepared: 2.5 mg of betaxolol-HBTA were solubilized in 10 mL of n-propanol. 1 mL of the solution was further diluted to 20 mL with 10 mL of acetonitrile and DI (nominal concentration 0.0125 mg/mL).

To quantify the amount of betaxolol-HBTA in the loading solution a "test solution" was prepared: 1 mL of the loading solution was diluted to 20 mL with 10 mL of acetonitrile and DI. Test solutions were prepared and analyzed by HPLC before and after the lens immersion: the amount of betaxolol-HBTA loaded in the lens was calculated as difference between the assays of test solutions collected before and after the soaking experiments.

3.3.1.4. Betaxolol-HBTA release in STF

Following the loading step, the lens was placed in 3.0 mL of simulated tear fluid (STF) at 35°C. STF is a solution simulating the composition and pH of tear fluid (138, 139). It was prepared dissolving 0.670 g of NaCl, 0.200 g of $NaHCO_3$,

0.008 g of $CaCl_2 \cdot 2\ H_2O$ in 100 mL of deionized water. pH was adjusted to 7.4 with HCl 0.1 N.

To control the temperature during the release experiments, lenses were stored in a heating oven (Thermo Fisher Scientific, USA) set to 35°C.

The lens was rinsed with water, dabbed, and transferred to fresh 3.0 mL of STF at 35°C at the following intervals to ensure semi-sink conditions during drug elution: 24 h, 48 h, 4 days, 6 days, 8 days, 10 days after the beginning of the release experiments. At the end of the elution time, CL was placed, under stirring for 4 minutes, in 3 mL of n-propanol to evaluate the residual amount of betaxolol-HBTA in the lens.

To quantify by HPLC the release of compound **2c**, test solution was prepared as follow: after removing the lens at the intervals reported above, STF was concentrated under reduced pressure using a rotary evaporator (Buchi R-100 Rotary Evaporator System; Switzerland). The residue was diluted with 2 mL of acetonitrile and subsequently 1 mL was further diluted to 2 mL with deionized water. Test solution was also prepared from n-propanol, according to the same procedure, after the last betaxolol-HBTA extraction from the lens in the organic solvent.

The cumulative amount of compound **2c** released from the lens was calculated as sum of the quantities (μg) of betaxolol-HBTA detected in every sample collected during the 10 days of elution experiments.

For each tested concentration of the loading solutions (0.250 mg/mL, 2.5 mg/mL and 5.0 mg/mL), two different experiments were performed and data were reported as mean values.

3.4. Results and Discussion

3.4.1. Betaxolol-HBTA loading

Betaxolol as eye drops for glaucoma treatment is currently available as suspension 0.25% and solution 0.5%. The common dose for glaucoma patients is one drop twice a day for both formulations. As suggested by Horne (129), the required drug dose to ensure a therapeutic effect using contact lenses as drug delivery system, should be between 1 and 10% of the daily dose administered as eye drops. Therefore, in this experiment we started from a less concentrated

solution (0.250 mg/mL) to move next to solutions with the same concentration of commercial eye drops (2.5 mg/mL and 5.0 mg/mL).

The amount of betaxolol-HBTA (μg) loaded in the lenses is reported in Figure 4. Data showed that the quantity of compound absorbed in the lens was proportional to the concentration of the loading solution.

During this phase, swelling of the lens in n-propanol was observed.

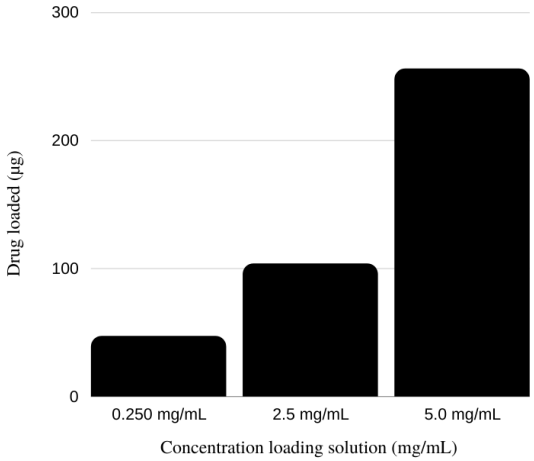

Figure 4. Uptake of betaxolol-HBTA into commercial contact lenses from three different loading solutions in n-propanol (0.250 mg/mL, 2.5 mg/mL and 5.0 mg/mL). Lenses were gently stirred for 4 minutes in the drug solution. Data are reported as mean value of two replicates for each solution.

3.4.2. Betaxolol-HBTA releasing

The study of the releasing stage is essential to evaluate the potential application of contact lenses as therapeutic tools. Data showing betaxolol-HBTA release from Dailies Total1® lenses are reported in Figure 5. As described above for the uptake experiment, also the amount of released compound was proportional to the concentration of the loading solution. However, the quantity of bexatolol-HBTA released from the lenses was quite low (higher cumulative quantity eluted 79.88 μg). Several factors can affect drug releasing process: composition of eluting solution, drug solubility, storage condition, applied methodology. It is interesting that for all the performed experiments, the higher amount of betaxolol-HBTA was released after six days from the beginning of elution study. In addition, it was also quantified betaxolol-HBTA eventually released in deionized water during deswelling of the lenses, but no trace of compound was detected by HPLC.

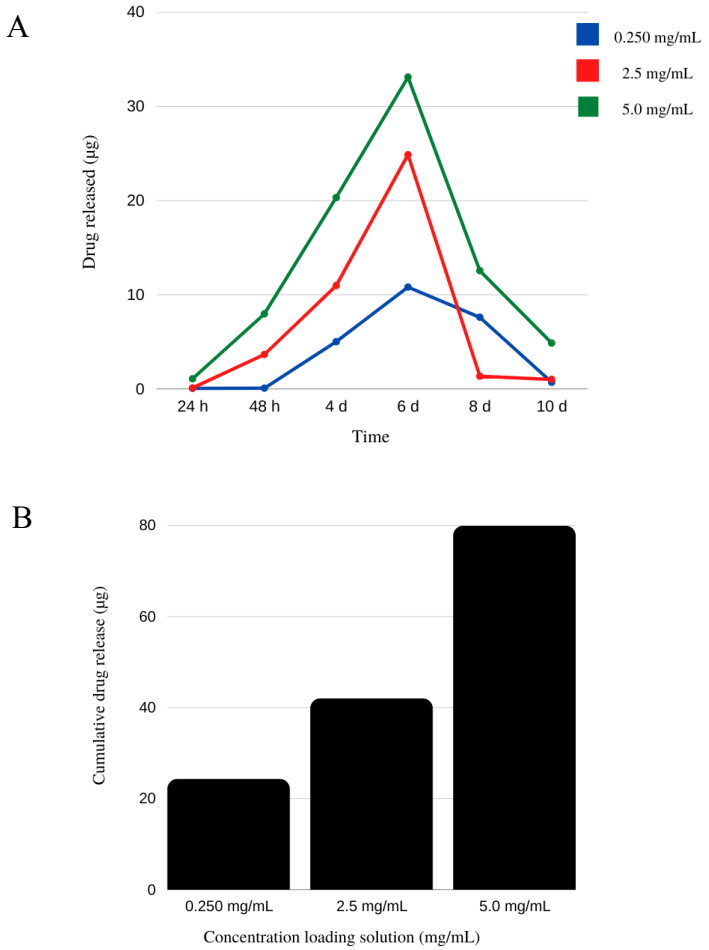

Figure 5. A. Release of betaxolol-HBTA in simulated tear fluid at 35°C from commercial contact lenses soaked in three different loading solutions (blue line 0.250 mg/mL, red line 2.5 mg/mL, green line 5.0 mg/mL). At following intervals 24h, 48h, 4 days, 6 days, 8 days and 10 days, the lenses were washed with water, dabbed, and transferred into fresh STF to maintain "sink conditions". B. Cumulative release of betaxolol-HBTA in STF at 35°C after 10 days. Data are reported as mean value of two replicates for each solution.

At the end of the uptake/release experiments, to evaluate the residual amount of betaxolol-HBTA in the lenses, an extraction in n-propanol was performed (Fig. 6). Data demonstrated that a large part of the loaded compound remained in the device. Therefore, these results confirm that drug solubility and formulation of the releasing solution (in our study represented by simulated tear fluid) are the main factors that control the experiment.

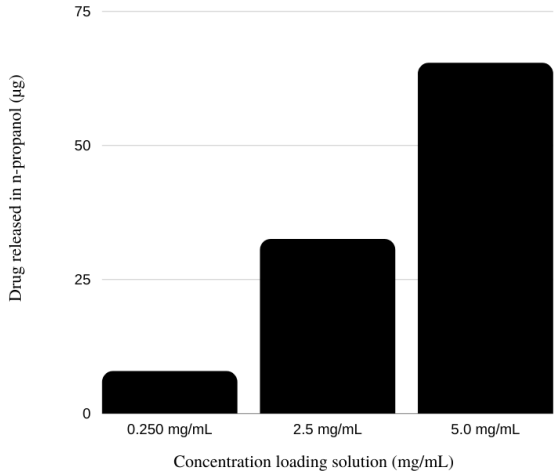

Figure 6. Extraction of betaxolol-HBTA in n-propanol from Dailies Total1® lenses after loading/release experiments. Data are reported as mean value of two replicates for each solution.

3.5. Conclusion

In the last decades, the potential application of contact lenses as drug delivery system has drawn the attention of researchers. CL could offer several advantages in the treatment of ocular diseases such as an increase of drug bioavailability due to a longer residence time on the cornea, reduction of the administered dose and less frequency of administration. Moreover, also patients' compliance and adherence to therapy could be improved using therapeutic contact lenses (121-124).

Several studies reporting promising drug eluting contact lenses for the treatment of glaucoma have been described in the literature. Different strategies, besides the soaking method, have been developed to better control drug release rate and to extend the elution from the lenses over days or weeks, such as molecular imprinting, incorporation of nanoparticles or multiple layers. However, to date no therapeutic contact lens has been commercialized mainly because of the following issues: possible risks of infections related to contact lens wear, feeling of discomfort and dryness, difficulties in inserting and removing the lenses and regulatory problems. Furthermore *in vivo* and clinical studies are still required to define the therapeutic efficacy and long-term safety of this new drug delivery system (140).

Following the approach described by Horne *et al.* (129) for loading a hydrophobic drug into commercial silicone hydrogel contact lenses, in collaboration with Genetic S.p.a., I performed a pilot study to develop an antiglaucoma hybrid eluting contact lens. To load the drug, Dailies Total1® commercial lenses were soaked in n-propanol solution of betaxolol-HBTA (**2c**) at three different concentrations (0.250 mg/mL, 2.5 mg/mL, 5.0 mg/mL). Due to the swelling of the lens in n-propanol, the device absorbed the solvent and the drug. After a deswelling stage in water, the release of the compound from the lenses in STF was evaluated for ten days. The quantitative analysis of betaxolol-HBTA in the solutions were performed by HPLC.

The amount of hybrid loaded in the lens as well as the quantity of compound released, were proportional to the concentration of the loading solution. Solubility of the drug and formulation of simulated tear fluid could play an important role in drug release kinetic. Indeed, through the last extraction of betaxolol-HBTA in n-propanol, a significant amount of compound was released from the lenses after 10 days of elution in STF.

Further analysis must be performed to improve drug uptake and the following elution. However, the applied methodology requires to be reviewed in order to describe with better precision the loading and release kinetics and to identify and characterize the factors involved in such processes.

Appendix

Research project carried out in collaboration with Prof. Ian Baxendale at the Department of Chemistry of University of Durham

Synthesis of new 2-amino-3-benzoylthiophenes as antileishmanial agents

1. Leishmaniasis

1.1. Introduction

Leishmaniasis is a parasitic disease caused by flagellated protozoans belonging to the genus *Leishmania*. This disease is endemic in 98 countries, especially in tropical and subtropical regions and is classified as a neglected tropical disease (NTD). The data mention up to 1.7 million new people infected every year (141). Three different clinical forms of leishmaniasis are described: cutaneous leishmaniasis (CL), mucosal leishmaniasis (ML) and visceral leishmaniasis (VL), characterized by increasing severity. The transmission of the disease in human occurs through the bite of female infected phlebotomine sandflies (141, 142).

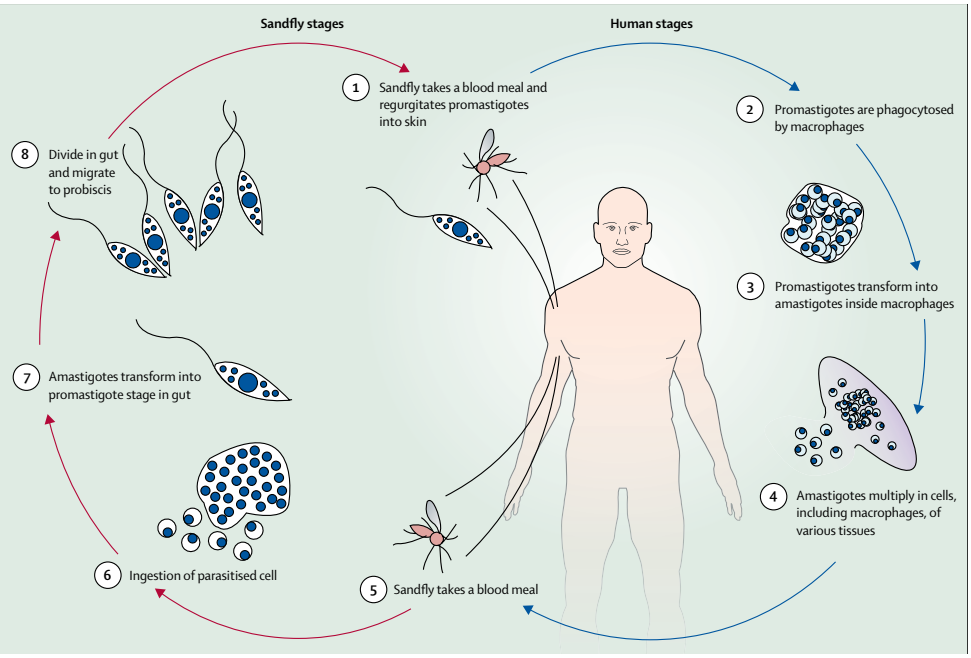

Figure 1. *Leishmania* parasite cycle life (142).

1.2. Transmission cycle

More than 20 species of *Leishmania* are known to be able to infect humans. The infection begins when sandfly injects infective promastigotes into human skin during blood meal (Fig.1; ①). Once in the host (human stages), promastigotes

are phagocytosed by macrophages ② where they transform in amastigotes ③, representing the tissue stage of the parasite. Amastigotes start to replicate, and they infect other mononuclear phagocytic cells ④. The infection of the sandfly (sandflies stages) occurs when they ingest infected cells from human blood ⑤-⑥. In the gut of sandfly, amastigotes become again promastigotes ⑦. They multiply in the gut, to migrate in the end of the cycle to the proboscis of the sandfly ⑧ (143). The spread of the parasites may occur also between infected animals and humans. Domestic dogs and rodents can be "animal reservoirs" of *Leishmania* and mainly *L. infantum* and *L. braziliensis* are known to infect dogs (144). In addition, human transmission can happen also via infect blood transfusion or organ transplantation (145).

1.3. Geographical Distribution

Leishmaniasis affects people predominantly in developing countries, where poverty, malnutrition and poor housing conditions represent strong risk factors for the development of the disease (146). 350 million people are considered at risk of infection (147).

Visceral leishmaniasis is the most severe and life-threatening form of infection and according to the current estimates, 90% of new VL cases have been reported in Bangladesh, Ethiopia, Brazil, India, Sudan, and South Sudan. Indian subcontinent and Eastern part of Africa constitute the main epicenter of VL epidemic (Fig. 2).

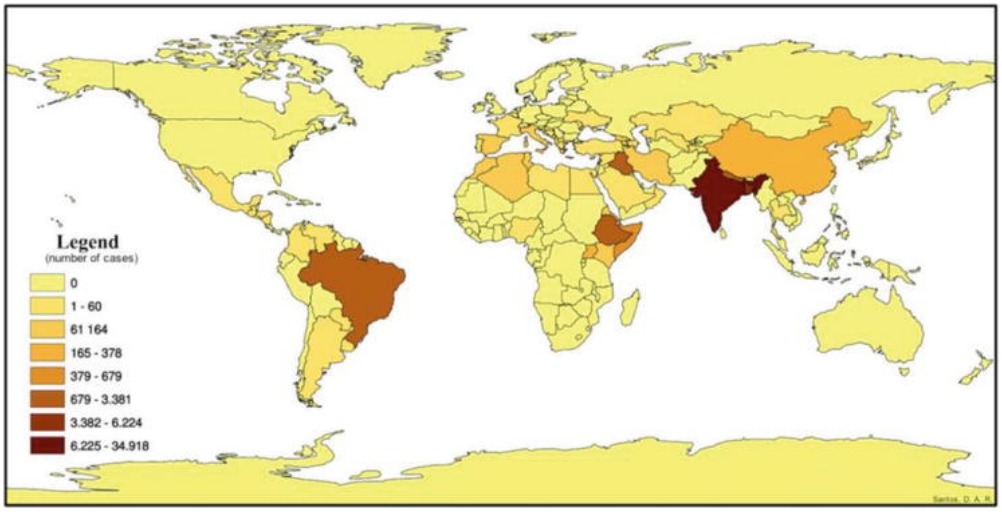

Figure 2. Geographical distribution of VL in the last 10 years (145).

Besides poverty, environmental factors suitable for sandflies growth and population movement towards unoccupied regions that has brought human and animal reservoir closer, may be some of the reasons associated with the prevalence of visceral leishmaniasis in these regions (147-149). The major species responsible for VL are *L. donovani* whose transmission is common in Indian subcontinent, Ethiopia, Sudan, and *L. infantum*, that is prevalent in China, Eastern Mediterranean region and Brazil (142).

Cutaneous leishmaniasis, the most common and mild manifestation of this parasitic disease, has spread mainly in Afghanistan, Pakistan, Syria, Saudi Arabia, Algeria, Iran, Brazil, and Peru (Fig. 3). *Leishmania* parasites causing CL are divided in Old World Species (*L. major*, *L. tropica*, *L. aethiopica*) diffused in Mediterranean region, Middle East, Indian subcontinent, Eastern region of Africa; and New World Species (*L. amazonensies*, *L. mexicana*, *L. braziliensis*, *L. guyanensis*) prevalent in Central and South America (142).

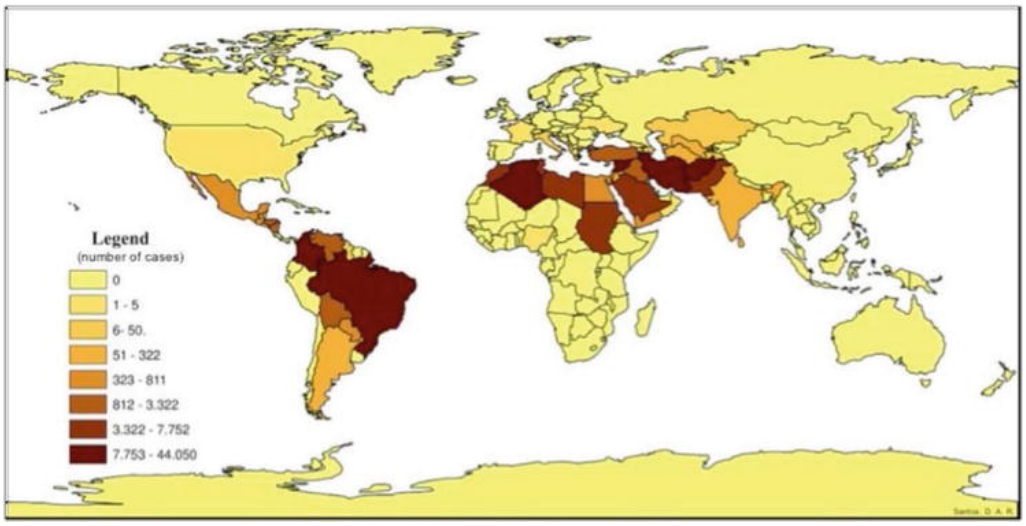

Figure 3. Geographical distribution of CL in the last 10 years (145).

However, because of more frequent international travels, immigration and environmental changes, an increasing number of leishmaniasis cases have been reported in non-endemic areas (147).

1.4. Clinical Features

1.4.1. Visceral Leishmaniasis

Patients with VL, also known as *kala-azar* in India, show persistent fever, weight loss and characteristic organomegaly. Splenomegaly is common while hepatomegaly is rare. Also hypergammaglobulinemia, anemia, thrombocytopenia and neutropenia may occur (150). In patients from Indian subcontinent, darkening of the skin is frequently described, therefore VL has been called *kala-azar*, meaning black fever in Hindi. If untreated, the disease can cause death due to severe anemia or comorbidity like superinfections (150). VL mainly affects children and young adults (142). The infection is associated with suppression of cell mediate immune response and elevated production of the anti-inflammatory cytokine interleukin-10 (IL-10), which can inhibit the activity of antiparasitic proinflammatory cytokines as interferon gamma (IFNγ) and tumor necrosis factor (TNFα), enhancing the parasite persistence (151).
The mortality rate of VL rises up to 26.9% in visceral leishmaniasis-HIV coinfected people (152). HIV caused a re-emergence of VL in Europe in the late 1990s, while nowadays the higher prevalence of the co-infections is in Ethiopia (150). VL is the most frequent opportunistic infection in HIV patients. It has been shown that *Leishmania* parasites accelerate HIV replication and the clinical features of the co-infection get worse. In addition, visceral leishmaniasis may evolve in cutaneous leishmaniasis (142, 150). Treatment of VL in patients with HIV coinfection is challenging and is associated with a high risk of failure (148).

1.4.2. Post-kala-azar Dermal Leishmaniasis

Post-kala-azar dermal leishmaniasis (PKDL) is a dermal complication occurring after the treatment of visceral leishmaniasis caused by *L. donovani*. Following pharmacological treatment, the parasite still persists in the skin leading to dermal lesions. PKDL occurs with macular, erythematous maculopapular or nodular rashes on faces and trunk, but they may extend to the whole body. PKDL is a common condition in Sudan, where it starts to appear 6 months after the VL treatment, while is rare in India where this complication can occur within 2-3 years (142, 148, 150).

1.4.3. Cutaneous Leishmaniasis

Cutaneous Leishmaniasis (CL) is less severe than VL and is usually self-healing. However, social and psychological consequences of cutaneous lesions in young women, children but also men are serious and worrying (153).

CL occurs at first as a localized erythema at site of sandfly bite, subsequently the erythema becomes a papule, then a nodule that ulcerates slowly over a period of few months. Severity, appearance, and time to cure of the lesions depend on the *Leishmania* parasites. Usually CL caused by *L. tropica* and *L. major* heals in a year, leaving permanent scars; infections associated with New World *Leishmania* Species (*i.e. L. mexicana*) are less sever and take few months to heal (142, 154).

Rare clinical manifestations of CL are represented by diffuse cutaneous leishmaniasis, disseminated cutaneous leishmaniasis and leishmania recidivans (142).

The role of $CD4^+$ Th1 cells is essential because these cells produce IFNγ, interleukin 12 and TNFα that activate macrophages. Th2 cells, instead, by producing anti-inflammatory cytokines (IL-4 and 10), prevent diffuse tissue destruction but, on the other hand, promote parasites replications (154, 155). Therefore, clinical manifestation and healing of the human disease may depend also on the activation and involvement of different T-cells.

1.4.4. Mucosal Leishmaniasis

Mucosal leishmaniasis can occur at the same time of CL as mucocutaneous leishmaniasis, or months and years later the cutaneous infection (156). This form of disease must be promptly cured or could be potentially life-threatening (142). *L. braziliensis* has been ranked as the major species responsible for ML. It affects frequently upper respiratory tract, nose, and oral cavity. Usually, the infection starts with inflammation symptoms (nasal inflammation and congestion), later evolves into ulceration and perforation of septum and palate. In severe clinical manifestation, lower respiratory tract and ocular zone may be involved (156, 157).

ML is frequent in immunocompromised people, especially HIV positive patients or under corticosteroids or immunosuppressive therapies (156).

1.5. Therapeutic treatment

The choice of the therapy for leishmaniasis treatment depends on the form of the disease, parasite species as well as comorbidity, and it should follow national or regional guidelines (158). However, currently available antileishmanial drugs are characterized by high toxicity and several side effects. Moreover, the high cost of medications has made treatments inaccessible to many patients.

1.5.1. Pentavalent Antimonials (Sb^V)

Pentavalent antimonials are the first choice drugs for all type of leishmaniasis and they are available as meglumine antimonate (MA) **1** or sodium stibogluconate (SSG) **2** (Fig. 4). For the treatment of VL, antimonials (20 mg/kg body weight) are administered via intramuscular (IM) or intravenous (IV) for 28-30 days (159); instead for CL are administered systemically or intralesionally (IL) (0.2-1.0 mL) and the therapy is shorter (160). The mechanism of action of these drugs is still not well understood. Side effects of antimonials are mainly cardiac (cardiac arrhythmias, prolonged QTc interval, ventricular fibrillation) but also increase of liver and pancreatic enzyme levels may occur. Therefore careful monitoring of patients is required (158-160).
In some countries like in Indian subcontinent, antimonials are no longer used due to parasites resistance (159).

1.5.2. Amphotericin B (AmB)

Amphotericin B **3** (Fig. 4) is a polyene antibiotic and is used as amphotericin deoxycholate in the treatment of leishmaniasis. AmB is administered IV at a dose of 0.75-1.0 mg/Kg/day for 15-20 days as therapy for VL, but it is extended up to 30 days for the treatment of infections caused by *L. infantum*. AmB is recommended also for PKDL therapy, but the period of treatment is 4 months (161). This drug acts by causing cellular membrane damage, after its binding to ergosterol. Despite the effective antileishmanial activity, several side events have been reported such as infusion reactions, fever, nephrotoxicity (158). To reduce its toxicity, lipid formulations of amphotericin B have been developed,

substituting deoxycholate with other lipids, such as liposomal amphotericin B (AmBisome; L-AmB), amphotericin B lipid complex (Abelcet) and amphotericin B colloidal dispersion (Amphocil). Among them, liposomal amphotericin B has been approved by US FDA for leishmaniasis treatment (159). Thank to this formulation, the drug is selectively delivered into organs like liver and spleen allowing a higher concentration in reticuloendothelial cells, the site of disease associated with VL. Liposomal drug delivery enhances drug effectiveness and reduces toxicity. L-AmB dose for visceral leishmaniasis varies by region: a total dose of 20 mg/Kg, given in 5 doses of 3-4 mg/Kg over 10 days is the optimal recommended regimen (160).

1.5.3. Miltefosine (MIL)

Alkylphosphocholine miltefosine **4** (Fig. 4) is an antineoplastic drug, whose antileishmanial activity towards *L. donovani* was described in 1987 (162). It is the only oral drug for the treatment of VL, used in India and Eastern Africa. Furthermore, MIL has shown to be effective also in immunocompromised patients. Therapeutic regimen depends on the weight of patients: a single dose of 50 mg for 28 days for those with weight < 25 Kg; individuals weighing more than 25 Kg require a twice daily dose of 50 mg (161).
Miltefosine is commonly associated with gastrointestinal side effects (nausea, vomiting) and rarely hepatotoxicity and nephrotoxicity may occur. This drug is known to be teratogenic, therefore is contraindicated during pregnancy (158).

1.5.4. Paromomycin

Paromomycin **5** (Fig. 4) is an aminoglycosidic antibiotic and inhibits protein synthesis of parasites by binding 16S ribosomal subunit (159). It is administered IM (15 mg/Kg) for 21 days for the treatment of VL, or in combination with liposomal Amphotericin B (161). Paromomycin is also applied topically as an ointment for CL therapy. Three different preparations are available: paramomycin 15% and methylbenzethonium chloride 12%, paromomycin 15% and urea 10%; paromomycin 15% and gentamicin 0.5% (160). Topical therapy has proved to be effective in both New World and Old World CL, while is not recommended for ML (161).

Common adverse events include mild pain at the injection site, reversible ototoxicity and hepatotoxicity; skin rashes and pruritus may appear in patients treated with the ointment (158, 161). However, due to the low cost, this agent is one of the cheapest option for leishmaniasis treatment but paromomycin monotherapy rises up the risk of parasites resistance (163).

1.5.5. Pentamidine

Pentamidine **6** (Fig. 4) is an aromatic diamidine, whose mechanism of action is based on the inhibition of replication and transcription of the parasite genome. This drug is used for the treatment of all the forms of leishmaniasis. It can be administered via IM or IV, but the intravenous route allows to increase the half-time value compared to the intramuscular administration (54 minutes vs 15 minutes) (158, 160).

The treatment based on pentamidine causes myalgias, pain at site of injection but also more severe side effects such as diabetes mellitus, pancreatitis or hypoglycemia, with following limitations for its use (159). Pentamidine (4 mg/Kg/day on alternate days for 1 week, IV) has been widely used in Brazil for the treatment of *L. braziliensis* infection but it has been shown that this antileishmanial agent is effective also for Old World CL caused by *L. tropica* and *L. major* (159, 161).

1.5.6. Azoles

Azoles (fluconazole **7**, ketoconazole **8** and itraconazole **9**; Fig. 4) are common oral antifungal agents. These drugs by inhibiting sterol synthesis pathway, block also the biosynthesis of *Leishmania* parasites cell membrane (158, 160).

Ketoconazole (600 mg daily for 28-30 days) and fluconazole (200 mg a day for 6 weeks) have been used against *L. mexicana* (New World) and *L. major* (Old World), proving to accelerate time of healing (161). Itraconazole has been tested in Old and New World, but has a low effectiveness (160).

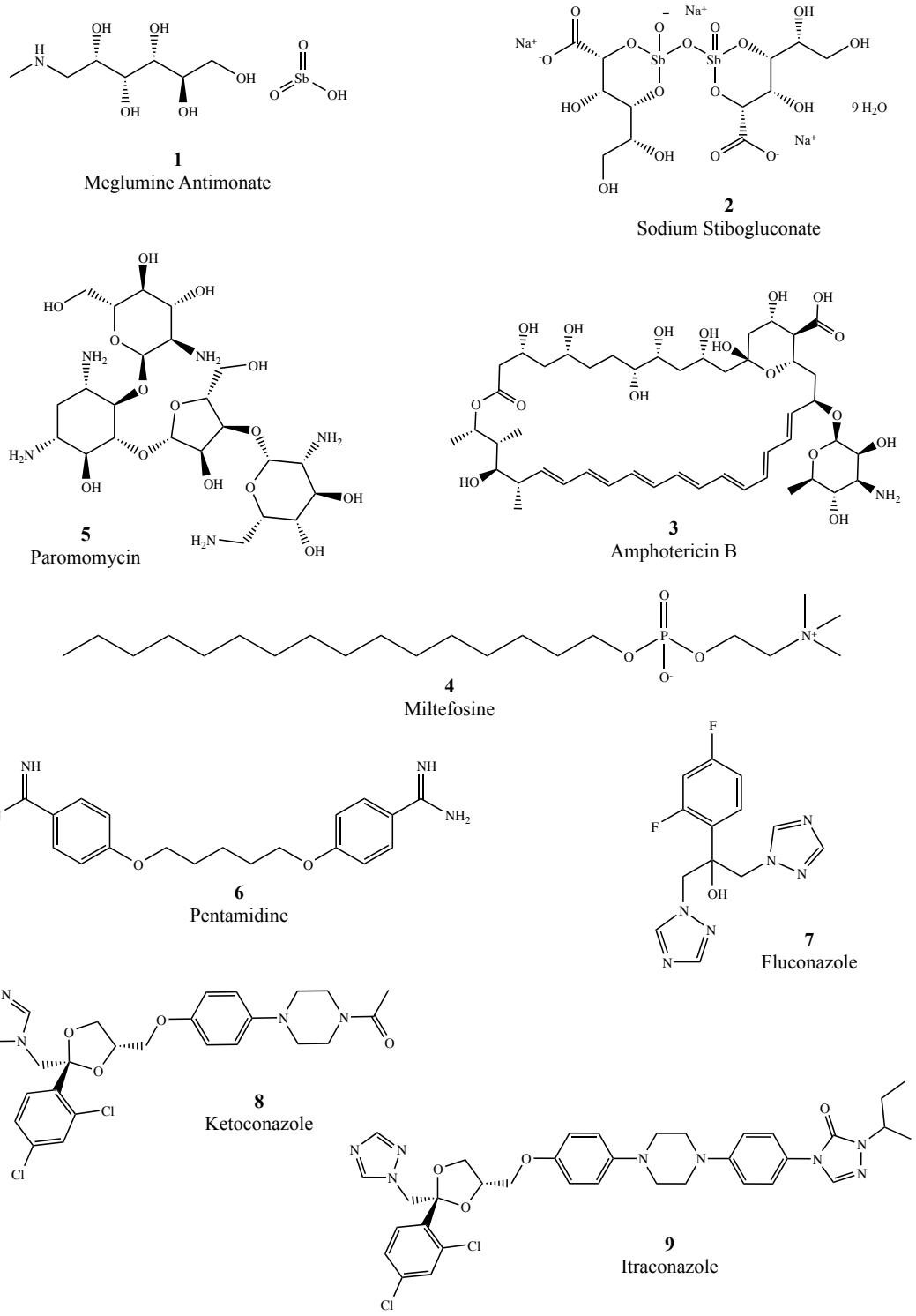

Figure 4. Chemical structures of currently available antileishmanial drugs.

1.5.7. Local therapy

Studies have proven that parasites replication stops at temperature > 39°C *in vitro*, therefore thermotherapy has been developed to treat CL in an effective and safe manner. By heating lesions through radio-frequency waves to 50°C for

few seconds, thermotherapy has shown to be a potential treatment for Old and New World CL lesions (159).

Cryotherapy, instead, is based on the application of liquid nitrogen at -195°C on the cutaneous lesion once or twice a week. It causes cell destruction with following localized ischemic necrosis. This therapy has proven to reduce the treatment time in OWCL infections (164).

CO_2 laser acts through thermolysis of infected tissues with poor side effects. After a single session of treatment, CL patients report a shorter healing time compared to therapy based on intralesional meglumine antimonate administration (165).

1.5.8. Development of Vaccines

The evidence that individuals who had leishmaniasis have developed immunity to future infections caused by the same parasites or other *Leishmania* species, provides the basis for a potential vaccine development. Several efforts and different strategies have been followed in order to obtain an effective and safe human vaccine, however, to date no leishmania vaccine is accessible in therapy (154).

Despite the failure of human studies, animal vaccines are available for dog immunization against *L. infantum* parasite. CaniLeish® and Leishmune®, licensed for veterinary use, protect dogs from leishmaniasis, preventing moreover zoonotic transmission from animal reservoirs to humans (166).

The only approach that has demonstrated to work in humans is the inoculation of the live virulent cutaneous pathogen (*L. major*) and this procedure is called Leishmanization. By inducing an infection, this procedure activates the immune response and protects from future disease (154). Studies have shown that the resulting lesion at the inoculation site is self-healing and this occurs in a short period of time (167). However Leishmanization is no longer used and is not recommended by WHO because of the risk of unacceptable lesions in immunocompromised individuals (154, 167).

Therefore, further strategies have been proposed, such as the inoculation of attenuate parasites, that are able to induce infection persistence but avoiding pathology and symptoms. Different attempts have been made to genetically

attenuate both visceral and cutaneous *Leishmania* parasites (168). Other techniques rely on the possibility to develop vaccines based on the total parasite proteins or composed by an individual or different *Leishmania* antigens, put together as a recombinant product (167).

2. Aim of the Research

The need for innovative treatments for leishmaniasis and other neglected diseases remains critical due to the high cost of available medications, low safety profile, required parental administration and chronic therapeutic regimen, and not least, parasites drug resistance.

Medicinal chemists worldwide have synthetized and evaluated antileishmanial activities of several libraries of new molecules in order to discover novel pharmacological tools (169).

2-Aminothiophenes have been widely used in the drug discovery process and several compounds characterized by this scaffold are undergoing clinical trials. In addition, multiple natural compounds are thiophene-based. 2-Aminothiophenes are known for their antimicrobial, antiviral and antitubercular properties and in the last years, new studies have shown also their potential antileishmanial activity (170).

K.A.F. Rodrigues *et al*. (171) synthetized a new set of ten thiophene derivatives with interesting properties against *L. amazonensis.* The authors proved that all the compounds inhibit parasites growth with an IC_{50} value lower than meglumine antimonate. In addition, selectivity for promastigotes was higher than mammalian cells.

Selected compounds were also tested in a model of *in vitro* infection using murine peritoneal macrophages, showing an antiparasitic effect through increased production of protective cytokines (TNFα and IL-12) as well as gas-transmitter NO.

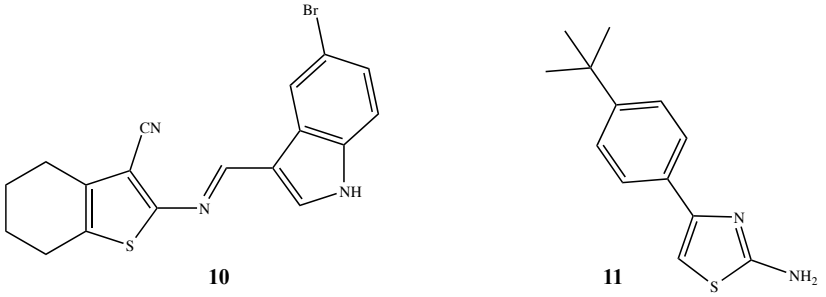

10 **11**

Figure 5. Chemical structure of thiophene (**10**) and thiazole (**11**) derivatives with antileishmanial properties.

The best derivative from *in vitro* study, SB-83 (**10**; Fig. 5), was further evaluated *in vivo* in Swiss mice infected with *L. amazonensis* and the compound demonstrated to be active and safe (172).

An interesting study was performed by C.A. Rodrigues and coworkers. They synthetized and evaluated potential activity of eight new 4-phenyl-1,3-thiazol-2-amines against *L. amazonensis* promastigotes. Furthermore, through a target fishing study the authors showed that the most promising target was human S-methyl-5-thioadenosine phosphorylase and subsequently, a BLAST search was performed to find the corresponding *Leishmania* sp isoform (identity value about 35%). Docking study of the best derivative (**11**; Fig. 5) at S-methyl-5-thioadenosine phosphorylase, found that the synthetized molecule keeps hydrogen bonds and pi-stacking interactions with the target as the original ligand 5'-deoxy-5'-methylthioadenosine (Fig. 6) (173).

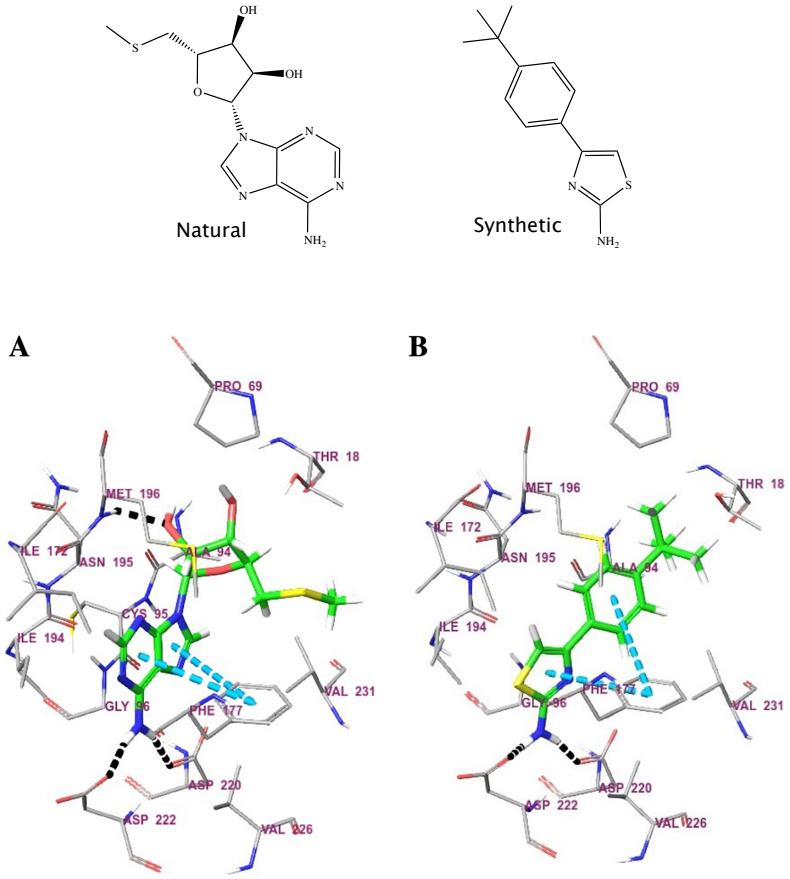

Figure 6. Docking studies performed by Rodrigues *et al.* between S-methyl-5-thioadenosine phosphorylase and its natural ligand (5'-deoxy-5'-methylthioadenosine) (**A**) and the synthetic

agent (**B**). Blue dashes lines represent pi-stacking interactions, black dashes lines represent hydrogen bonds (173).

Based on these data and considering the interesting results reported in the literature about 2-aminothiophenes activity against *Leishmania* parasites, during my stay in the research laboratories of Prof. Ian Baxendale at the Department of Chemistry of Durham University (UK), I worked on the synthesis and characterization of new 2-amino-3-benzoylthiophene derivatives in order to obtain either potential tools for the treatment of the parasitic disease or a new building block to further synthesize new antileishmanial drugs.

The project is at an early stage and synthetic procedures are still ongoing, but once all the compounds are synthetized and characterized, they will be tested *in vitro* against *Leishmania* parasites. Furthermore, structure-activity relationship studies will be performed.

Referring to the results presented by C.A. Rodrigues *et al.*, and considering the structural analogy between the compounds synthetized by the authors and the new thiophene derivatives, molecular docking analysis will be carried out to examine the potential binding of our compounds and the enzyme S-methyl-5-thioadenosine phosphorylase.

With the aim to better explore the binding mode on this target and to enhance the biological activity, our next step is to extend the chemical structure of 2-amino-3-aroylthiophenes with a flexible and hydrophilic chain. Through a reaction of the amine group in position 2 and δ-gluconolactone, by the opening of the monosaccharide ring, we designed the synthesis of new N-arylgluconamides according to the procedure reported in the literature (174).

3. Results and Discussion

The chemical structures of the designed compounds (**3a-3x**) are reported in Table 1. The general synthetic procedure is summarized in Scheme 1 and is based on the conversion of the methyl benzoate substituted at the position 2, 3 or 4 into the corresponding β-ketonitrile (175, 176). Subsequently, through a modified Gewald reaction in the presence of 1,4-dithian-2,5-diol and triethylamine (177), starting from the obtained intermediate in the first step, the thiophene was synthetized.

Table 1. Chemical structures of new 2-amino-3-benzoylthiophenes.

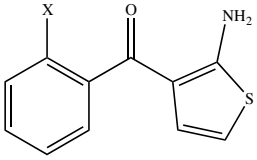		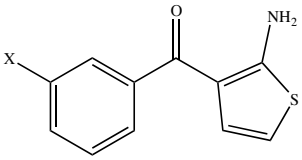		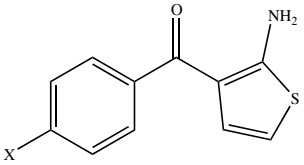	
2-Amino-3-(2-X-benzoyl)thiophene		**2-Amino-3-(3-X-benzoyl)thiophene**		**2-Amino-3-(4-X-benzoyl)thiophene**	
Compound	**X**	**Compound**	**X**	**Compound**	**X**
3a	OMe	**3b**	OMe	**3c**	OMe
3d	Cl	**3e**	Cl	**3f**	Cl
3g	Br	**3h**	Br	**3i**	Br
3j	I	**3k**	I	**3l**	I
3m	Me	**3n**	Me	**3o**	Me
3p	F	**3q**	F	**3r**	F
3s	NO_2	**3t**	NO_2	**3u**	NO_2
3v	CF_3	**3w**	CF_3	**3x**	CF_3

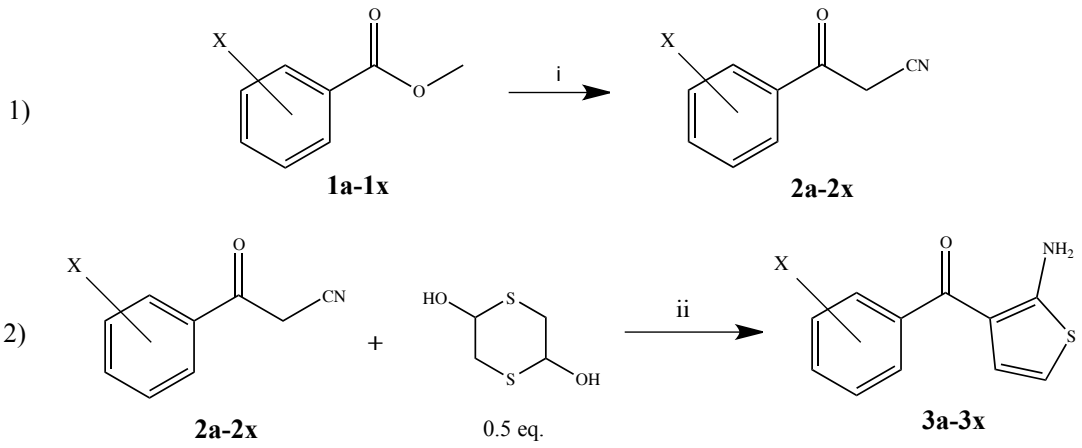

Scheme 1. General synthetic procedure for the synthesis of compounds **3a-3x**.
Reagents and conditions: i) Procedure A: NaH (2 eq.); MeCN (4.7 eq.), dry toluene, 80°C, 18h.
Procedure B: n-BuLi (2.5 M solution in hexane, 2.5 eq.), MeCN (3 eq.), THF, -78°C, 4h.
ii) NEt_3 (1 eq), CF_3CH_2OH, 60°C, overnight.

To date synthesis of compounds **3b, 3e, 3g-3h, 3j-3k, 3n-3o, 3p-3r** were carried out. The synthetic procedures of the remaining derivatives are still ongoing. The final compounds and intermediates were isolated and then characterized by ^{1}H and ^{13}C Nuclear Magnetic Resonance (NMR). Chemical structure as well as purity of the products were confirmed also by LC-MS. Data currently available are reported in the next chapter.

4. Experimental Section

4.1. Materials and Methods

All reagents were purchased from commercial sources. Solvents were obtained from Fisher Scientific (UK) and H_2O was deionized before use. Analytical grade toluene was dried using Innovative Technology Inc. solvent purification system and stored under nitrogen.

^{1}H-NMR and COSY spectra were recorded on Bruker Avanced-400 MHz and Varian VNMRS-600 MHz instruments (UK) and are reported relative to residual solvent DMSO-d_6 (δ 2.50 ppm). ^{13}C-NMR and DEPT spectra were recorded on the same instruments and are reported relative to DMSO-d_6 (δ 39.52 ppm). Chemical shifts are reported in ppm. The following abbreviations are used to describe peak patterns when appropriate: s (singlet), d (doublet), t (triplet), m (multiplet), dd (doublet of doublet), td (triplet of doublets), dt (doublet of triplets), ddd (doublet of doublet of doublets), qd (quartet of doublets) and bs (broad singlet).

Liquid chromatography-mass spectrometry (LCMS) was performed on an Agilent HP 1100 series chromatograph (Mercury Luna 3µ C_{18}(2) column) (USA) attached to a Waters ZQ2000 mass spectrometer (USA) with ESCi ionization source in ESI mode. Elution was carried out at a flow rate of 0.6 mL/min using a reverse phase gradient of MeCN–water containing 0.1% formic acid. Gradient = 0–1 min: hold MeCN 5%, 1–4 min: ramp MeCN 5–95%, 4–5 min: hold MeCN 95%, 5–7 min: ramp MeCN 95–5%, 7–8 min: hold MeCN 5%. Retention times are reported as Rt.

All reactions were followed by thin-layer chromatography, carried out on Merck (Germany) silica gel 60 F_{254} plates with a fluorescent indicator, and the plates were visualized with UV light (254 nm). Preparative chromatographic purifications were performed using a silica gel column (Kieselgel 60). Solutions were dried over anhydrous Na_2SO_4, concentrated under reduced pressure using a Buchi rotary evaporator and high vacuum was achieved using an Edwards RV5 pump and Schlenk line (Switzerland).

4.2. Procedures for the Synthesis of β-ketonitrile Intermediates

4.2.1. Synthesis of compound 3-(3-methoxyphenyl)-3-oxopropanenitrile (2b)

To a solution of methyl 3-methoxybenzoate **1b** (1.00 g; 6.0 mmol) in dry toluene (6 mL), under the protection of nitrogen, NaH (60% dispersion in mineral oil; 0.480 g; 12 mmol) was added. The reaction mixture was heated to 80°C and successively MeCN (1.5 mL; 28.2 mmol) was added. The suspension was heated at reflux for 18 hours. Then it was cooled to room temperature and the system was quenched with H_2O (50 mL). The aqueous phase was acidified to pH 2-6 with HCl 1M and extracted with EtOAc (2 x 25 mL). The combined organic phases were washed with brine, dried over anhydrous Na_2SO_4 and concentrated. The residue was purified by column chromatography on silica gel (hexane:ethyl acetate 6:4 v/v) to obtain the corresponding β-ketonitrile **2b**.

^{1}H NMR (400 MHz, DMSO-d_6) δ: 7.56 - 7.43 (m, 3H), 7.29 (ddd, J = 7.9, 2.7, 1.2 Hz, 1H), 4.77 (s, 2H), 3.84 (s, 3H); ^{13}C NMR (101 MHz, DMSO-d_6) δ: 189.99, 159.93, 136.44, 130.57, 121.34, 120.65, 116.34, 113.49, 55.93, 30.59. LC-MS (MeCN) Rt = 2.10 min, *m/z* $[M+H]^+$ calculated for $C_{10}H_9NO_2$ 175.18, found = 176.2.

4.2.2. Synthesis of compound 3-(3-chlorophenyl)-3-oxopropanenitrile (2e)

Following the synthetic procedure reported above for **2b**, compound **2e** was synthetized starting from methyl 3-chlorobenzoate **1e** (1.00 g; 5.9 mmol), NaH 60% (0.472 g; 11.8 mmol) and MeCN (1.4 mL; 27.7 mmol).

^{1}H NMR (400 MHz, DMSO-d_6) δ: 7.97 (t, J = 2.0 Hz, 1H), 7.94 - 7.87 (m, 1H), 7.77 (dd, J = 7.9, 2.0 Hz, 1H), 7.60 (t, J = 7.9 Hz, 1H), 4.79 (s, 2H); ^{13}C NMR (101 MHz, DMSO-d_6) δ: 189.25, 136.89, 134.33, 134.27, 131.31, 128.59, 127.44, 116.12, 30.71. LC-MS (MeCN) Rt = 2.21 min, *m/z* $[M+H]^+$ calculated for C_9H_6ClNO 179.60, found = 180.5.

4.2.3. Synthesis of compound 3-(2-bromophenyl)-3-oxopropanenitrile (2g)

Following the synthetic procedure reported above for **2b**, compound **2g** was synthetized starting from methyl 2-bromobenzoate **1g** (1.00 g; 4.6 mmol), NaH 60% (0.368 g; 9.2 mmol) and MeCN (1.1 mL; 21.6 mmol).

^{1}H NMR (400 MHz, DMSO-d_6) δ: 7.81 - 7.70 (m, 2H), 7.50 - 7.42 (m, 2H), 4.68 (s, 2H); ^{13}C NMR (101 MHz, DMSO-d_6) δ: 191.58, 170.67, 132.87, 131.73, 130.38, 127.78, 120.71, 117.09, 32.51. LC-MS (MeCN) Rt = 2.09 min, *m/z* $[M+H]^+$ calculated for C_9H_6BrNO 224.05, found = 225.2.

4.2.4. Synthesis of compound 3-(3-bromophenyl)-3-oxopropanenitrile (2h)

Following the synthetic procedure reported above for **2b**, compound **2h** was synthetized starting from methyl 3-bromobenzoate **1h** (1.00 g; 4.6 mmol), NaH 60% (0.368 g; 9.2 mmol) and MeCN (1.1 mL; 21.6 mmol).

^{1}H NMR (400 MHz, DMSO-d_6) δ: 8.10 (t, J = 2.0 Hz, 1H), 7.98 - 7.88 (m, 2H), 7.54 (t, J = 7.9 Hz, 1H), 4.79 (s, 2H); ^{13}C NMR (101 MHz, DMSO-d_6) δ: 189.19, 137.22, 137.10, 131.55, 131.46, 127.79, 122.65, 116.12, 30.67. LC-MS (MeCN) Rt = 2.21 min, *m/z* $[M+H]^+$ calculated for C_9H_6BrNO 224.05, found = 225.4.

4.2.5. Synthesis of compound 3-(2-iodophenyl)-3-oxopropanenitrile (2j)

Following the synthetic procedure reported above for **2b**, compound **2j** was synthetized starting from methyl 2-iodobenzoate **1j** (1.00 g; 3.8 mmol), NaH 60% (0.306 g; 7.6 mmol) and MeCN (0.94 mL; 17.9 mmol).

^{1}H NMR (400 MHz, DMSO-d_6) δ: 7.94 (ddd, J = 9.3, 7.9, 1.1 Hz, 1H), 7.52 - 7.36 (m, 2H), 7.22 (qd, J = 7.6, 1.8 Hz, 1H), 4.69 (s, 2H); ^{13}C NMR (101 MHz, DMSO) δ: 192.43, 140.86, 139.22, 131.46, 129.54, 128.37, 118.42, 96.20, 31.99. LC-MS (MeCN) Rt = 2.22 min, *m/z* $[M+H]^+$ calculated for C_9H_6INO 271.05, found = 272.2.

4.2.6. Synthesis of compound 3-(3-iodophenyl)-3-oxopropanenitrile (2k)

Following the synthetic procedure reported above for **2b**, compound **2k** was synthetized starting from methyl 3-iodobenzoate **1k** (1.00 g; 3.8 mmol), NaH 60% (0.306 g; 7.6 mmol) and MeCN (0.94 mL; 17.9 mmol).

^{1}H NMR (400 MHz, DMSO-d_6) δ: 8.25 (t, J = 1.8 Hz, 1H), 8.05 (dt, J = 7.9, 1.4 Hz, 1H), 7.94 (dt, J = 7.9, 1.4 Hz, 1H), 7.36 (t, J = 7.9 Hz, 1H), 4.76 (s, 2H); ^{13}C NMR (101 MHz, DMSO-d_6) δ: 189.14, 143.01, 137.17, 136.92, 131.39, 128.10, 116.14, 95.68, 30.60. LC-MS (MeCN) Rt = 2.05 min, *m/z* $[M+H]^+$ calculated for C_9H_6INO 271.05, found = 272.1.

4.2.7. Synthesis of compound 3-oxo-3-(m-tolyl)propanenitrile (2n)

Following the synthetic procedure reported above for **2b**, compound **2n** was synthetized starting from methyl 3-methylbenzoate **1n** (1.00 g; 6.7 mmol), NaH 60% (0.536 g; 13.4 mmol) and MeCN (1.6 mL; 31.5 mmol).

^{1}H NMR (400 MHz, DMSO-d_6) δ: 7.82 - 7.71 (m, 2H), 7.57 - 7.43 (m, 2H), 4.74 (s, 2H), 2.39 (s, 3H); ^{13}C NMR (101 MHz, DMSO-d_6) δ: 190.15, 138.83, 135.32, 135.10, 129.24, 129.19, 126.16, 116.40, 30.46, 21.26. LC-MS (MeCN) Rt = 2.13 min, *m/z* $[M+H]^+$ calculated for $C_{10}H_9NO$ 159.18, found = 160.1.

4.2.8. Synthesis of compound 3-oxo-3-(p-tolyl)propanenitrile (2o)

Following the synthetic procedure reported above for **2b**, compound **2o** was synthetized starting from methyl 4-methylbenzoate **1o** (1.00 g; 6.7 mmol), NaH 60% (0.536 g; 13.4 mmol) and MeCN (1.6 mL; 31.5 mmol).

^{1}H NMR (400 MHz, DMSO-d_6) δ: 7.85 (d, J = 7.9 Hz, 2H), 7.34 (d, J = 7.9 Hz, 2H), 4.73 (s, 2H), 2.39 (s, 3H); ^{13}C NMR (101 MHz, DMSO-d_6) δ: 189.59, 145.39, 132.63, 129.89, 128.99, 116.44, 30.31, 21.69. LC-MS (MeCN) Rt = 2.18 min, *m/z* $[M+H]^+$ calculated for $C_{10}H_9NO$ 159.18, found = 160.2.

4.2.9. Synthesis of compound 3-(2-fluorophenyl)-3-oxopropanenitrile (2p)

To a solution of n-BuLi (2.5 M solution in hexane, 6.5 mL; 16.25 mmol) in THF (10 mL), acetonitrile was added dropwise (1.02 mL; 19.5 mmol) at -78 °C and the reaction mixture was stirred for 1 h. Then a solution of methyl 2-fluorobenzoate **1p** (1.00 g; 6.5 mmol) in THF (10 mL) was added slowly, and the mixture was stirred for other 3 h at -78 °C. The reaction was quenched with H_2O (30 mL) and THF was removed in vacuo. The resulting mixture was diluted with EtOAc (20 mL) and the organic layer was separated. The aqueous phase was acidified with HCl 1M to pH 2 and subsequently extracted twice with EtOAc. The combined organic solutions were washed with brine, dried over Na_2SO_4 and concentrated under reduced pressure. The residue was purified by column chromatography on silica gel (hexane:ethyl acetate 7:3 v/v) to obtain compound **2p**.

^{1}H NMR (400 MHz, DMSO-d_6) δ: 7.90 (td, J = 7.7, 1.8 Hz, 1H), 7.77 - 7.71 (m, 1H), 7.42 - 7.36 (m, 2H), 4.62 (d, 2H); ^{13}C NMR (101 MHz, DMSO-d_6) δ: 187.45, 166.46 (d, J = 202.3 Hz), 160.51 (d, J = 253.0 Hz), 136.81 (d, J = 9.4

Hz), 131.00, 125.43 (d, J = 3.4 Hz), 123.46 (d, J = 11.5 Hz), 117.40 (d, J = 22.9 Hz), 33.86; ^{19}F NMR (376 MHz, DMSO-d_6) δ: -108.99. LC-MS (MeCN) Rt = 2.02 min, *m/z* $[M+H]^+$ calculated for C_9H_6FNO 163.15, found = 164.4.

4.2.10. Synthesis of compound 3-(3-fluorophenyl)-3-oxopropanenitrile (2q)

Following the synthetic procedure reported above for **2b**, compound **2q** was synthetized starting from methyl 3-fluorobenzoate **1q** (1.00 g; 6.5 mmol), NaH 60% (0.518 g; 13 mmol) and MeCN (1.6 mL; 30.8 mmol).

^{1}H NMR (400 MHz, DMSO-d_6) δ: 7.85 - 7.69 (m, 2H), 7.65 - 7.47 (m, 2H), 4.77 (s, 2H); ^{13}C NMR (101 MHz, DMSO-d_6) δ: 189.24, 162.59 (d, J = 246.0 Hz), 137.22 (d, J = 6.9 Hz), 131.59 (d, J = 8.6 Hz), 125.09 (d, J = 2.8 Hz), 121.61 (d, J = 21.1 Hz), 115.45 (d, J = 23.4 Hz), 116.13, 30.74; ^{19}F NMR (376 MHz, DMSO-d_6) δ -112.00. LC-MS (MeCN) Rt = 2.12 min, *m/z* $[M+H]^+$ calculated for C_9H_6FNO 163.15, found = 164.2.

4.2.11. Synthesis of compound 3-(4-fluorophenyl)-3-oxopropanenitrile (2r)

Following the synthetic procedure reported above for **2b**, compound **2r** was synthetized starting from methyl 4-fluorobenzoate **1r** (1.00 g; 6.5 mmol), NaH 60% (0.518 g; 13 mmol) and MeCN (1.6 mL; 30.8 mmol).

^{1}H NMR (400 MHz, DMSO-d_6) δ: 8.11 - 7.97 (m, 2H), 7.40 (t, J = 8.8 Hz, 2H), 4.77 (s, 2H); ^{13}C NMR (101 MHz, DMSO-d_6) δ: 188.81, 166.02 (d, J = 253.5 Hz), 131.99 (d, J = 9.8 Hz), 131.86 (d, J = 2.7 Hz), 116.44 (d, J = 22.2 Hz), 116.27, 30.51; ^{19}F NMR (376 MHz, DMSO-d_6) δ: -104.24. LC-MS (MeCN) Rt = 2.09 min, *m/z* $[M+H]^+$ calculated for C_9H_6FNO 163.15, found = 164.1.

4.3. Procedures for the Synthesis of 2-amino-3-aroylthiophenes

4.3.1. Synthesis of compound (2-aminothiophen-3-yl)(3-methoxyphenyl)methanone (3b)

The compound **2b** (1.00 g; 5.7 mmol) was solubilized in trifluoroethanol (10 mL) and 1,4-dithian-2,5-diol (0.434 g; 2.8 mmol) was added. Successively, triethylamine (0.878 mL; 6.3 mmol) was added and the reaction mixture was stirred at reflux overnight. The solvent was evaporated under vacuo. The residue was diluted with EtOAc (30 mL) and extracted with H_2O (2 x 10 mL) and brine. The combined organic layers were dried on anhydrous Na_2SO_4 and concentrated

under reduced pressure. Purification by column chromatography (hexane:ethyl acetate 7:3 v/v) gave compound **3b**.

^{1}H NMR (400 MHz, DMSO-d_6) δ: 8.36 (bs, 2H), 7.46 - 7.34 (m, 1H), 7.15 (dt, J = 7.6, 1.2 Hz, 1H), 7.12 - 7.03 (m, 2H), 6.75 (d, J = 5.9 Hz, 1H), 6.26 (d, J = 5.9 Hz, 1H), 3.80 (s, 3H); ^{13}C NMR (101 MHz, DMSO-d_6) δ: 189.28, 167.88, 159.44, 142.76, 129.83, 127.03, 120.40, 116.69, 113.30, 113.23, 106.68, 55.66. LC-MS (MeCN) Rt = 2.22 min, *m/z* $[M+H]^+$ calculated for $C_{12}H_{11}NO_2S$ 233.29, found = 234.6.

4.3.2. Synthesis of compound (2-aminothiophen-3-yl)(3-chlorophenyl)methanone (3e)

Compound **3e** was obtained according to the procedure reported above for compound **3b** from intermediate **2e** (1.00 g; 5.6 mmol) and 1,4-dithian-2,5-diol (0.426 g; 2.8 mmol) in the presence of NEt_3 (0.864 mL; 6.2 mmol).

^{1}H NMR (400 MHz, DMSO-d_6) δ: 8.42 (bs, 2H), 7.63 - 7.48 (m, 4H), 6.70 (d, J = 5.9 Hz, 1H), 6.29 (d, J = 5.9 Hz, 1H); ^{13}C NMR (151 MHz, DMSO-d_6) δ: 187.61, 168.32, 143.24, 133.54, 130.68, 130.67, 127.73, 126.74, 126.63, 113.03, 107.06. LC-MS (MeCN) Rt = 2.53 min, *m/z* $[M+H]^+$ calculated for $C_{11}H_8ClNOS$ 237.71, found = 239.0.

4.3.3. Synthesis of compound (2-aminothiophen-3-yl)(2-bromophenyl)methanone (3g)

Compound **3g** was obtained according to the procedure reported above for compound **3b** from intermediate **2g** (1.00 g; 4.5 mmol) and 1,4-dithian-2,5-diol (0.342 g; 2.25 mmol) in the presence of NEt_3 (0.689 mL; 4.95 mmol).

^{1}H NMR (400 MHz, DMSO-d_6) δ: 8.39 (bs, 2H), 7.68 (dd, J = 7.9, 1.1 Hz, 1H), 7.46 (td, J = 7.4, 1.2 Hz, 1H), 7.40 - 7.33 (m, 2H), 6.19 (s, 2H); ^{13}C NMR (101 MHz, DMSO-d_6) δ: 187.95, 167.25, 142.42, 132.66, 130.65, 128.16, 127.70, 126.16, 118.18, 113.35, 106.71. LC-MS (MeCN) Rt = 3.35 min, *m/z* $[M+H]^+$ calculated for $C_{11}H_8BrNOS$ 282.16, found = 283.2.

4.3.4. Synthesis of compound (2-aminothiophen-3-yl)(3-bromophenyl)methanone (3h)

Compound **3h** was obtained according to the procedure reported above for compound **3b** from intermediate **2h** (1.00 g; 4.5 mmol) and 1,4-dithian-2,5-diol (0.342 g; 2.3 mmol) in the presence of NEt_3 (0.689 mL; 4.95 mmol).

^{1}H NMR (400 MHz, DMSO-d_6) δ: 8.42 (bs, 2H), 7.72 (t, J = 7.8 Hz, 1H), 7.71 (d, J = 7.8 Hz, 1H), 7.58 (d, J = 7.8 Hz, 1H), 7.45 (t, J = 7.8 Hz, 1H), 6.70 (d, J = 5.9 Hz, 1H), 6.29 (d, J = 5.9 Hz, 1H); ^{13}C NMR (101 MHz, DMSO-d_6) δ: 187.53, 168.36, 143.46, 133.61, 130.99, 130.62, 127.14, 126.65, 122.07, 113.02, 107.12. LC-MS (MeCN) Rt = 2.61 min, *m/z* $[M+H]^+$ calculated for $C_{11}H_8BrNOS$ 282.16, found = 283.3.

4.3.5. Synthesis of compound (2-aminothiophen-3-yl)(2-iodophenyl)methanone (3j)

Compound **3j** was obtained according to the procedure reported above for compound **3b** from intermediate **2j** (1.00 g; 3.7 mmol) and 1,4-dithian-2,5-diol (0.281 g; 1.8 mmol) in the presence of NEt_3 (0.571 mL; 4.1 mmol).

^{1}H NMR (400 MHz, DMSO-d_6) δ: 8.38 (bs, 2H), 7.90 (dd, J = 7.9, 1.1 Hz, 1H), 7.47 (td, J = 7.5, 1.1 Hz, 1H), 7.27 (dd, J = 7.6, 1.6 Hz, 1H), 7.18 (td, J = 7.7, 1.7 Hz, 1H), 6.18 (d, J = 5.9 Hz, 1H), 6.17 (d, J = 5.9 Hz, 1H) ^{13}C NMR (101 MHz, DMSO-d_6) δ: 189.95, 167.28, 146.34, 138.92, 130.48,128.12, 127.32, 126.34, 112.85, 106.59, 92.75. LC-MS (MeCN) Rt = 3.51 min, *m/z* $[M+H]^+$ calculated for $C_{11}H_8INOS$ 329.16, found = 330.4

4.3.6. Synthesis of compound (2-aminothiophen-3-yl)(3-iodophenyl)methanone (3k)

Compound **3k** was obtained according to the procedure reported above for compound **3b** from intermediate **2k** (1.00 g; 3.7 mmol) and 1,4-dithian-2,5-diol (0.281 g; 1.8 mmol) in the presence of NEt_3 (0.571 mL; 4.1 mmol).

^{1}H NMR (400 MHz, DMSO-d_6) δ: 8.40 (bs, 2H), 7.93 - 7.80 (m, 2H), 7.58 (dt, J = 7.7, 1.3 Hz, 1H), 7.32 - 7.24 (m, 1H), 6.68 (d, J = 5.9 Hz, 1H), 6.28 (d, J = 5.9 Hz, 1H); ^{13}C NMR (101 MHz, DMSO-d_6) δ: 187.15, 167.81, 142.89, 138.96, 135.97, 130.44, 126.99, 126.22, 112.57, 106.62, 94.68. LC-MS

(MeCN) Rt = 2.86 min, *m/z* $[M+H]^+$ calculated for $C_{11}H_8INOS$ 329.16, found = 330.4.

4.3.7. Synthesis of compound (2-aminothiophen-3-yl)(m-tolyl)methanone (3n)

Compound **3n** was obtained according to the procedure reported above for compound **3b** from intermediate **2n** (1.00 g; 6.3 mmol) and 1,4-dithian-2,5-diol (0.487 g; 3.2 mmol) in the presence of NEt_3 (0.961 mL; 6.9 mmol).

^1H NMR (400 MHz, DMSO-d_6) δ: 8.34 (bs, 2H), 7.44 - 7.21 (m, 4H), 6.73 (d, *J* = 5.9 Hz, 1H), 6.25 (d, *J* = 5.9 Hz, 1H), 2.36 (s, 3H); ^{13}C NMR (101 MHz, DMSO-d_6) δ: 189.81, 167.72, 141.42, 137.99, 131.52, 128.60, 128.53, 127.15, 125.32, 113.42, 106.57, 21.42. LC-MS (MeCN) Rt = 2.58 min, *m/z* $[M+H]^+$ calculated for $C_{12}H_{11}NOS$ 217.29, found = 218.6.

4.3.8. Synthesis of compound (2-aminothiophen-3-yl)(p-tolyl)methanone (3o)

Compound **3o** was obtained according to the procedure reported above for compound **3b** from intermediate **2o** (1.00 g; 6.3 mmol) and 1,4-dithian-2,5-diol (0.487 g; 3.2 mmol) in the presence of NEt_3 (0.961 mL; 6.9 mmol).

^1H NMR (400 MHz, DMSO-d_6) δ: 8.30 (bs, 2H), 7.50 (d, *J* = 7.9 Hz, 2H), 7.29 (d, *J* = 7.9 Hz, 2H), 6.76 (d, *J* = 5.9 Hz, 1H), 6.27 (d, *J* = 5.9 Hz, 1H), 2.37 (s, 3H); ^{13}C NMR (101 MHz, DMSO-d_6) δ: 189.47, 167.60, 140.86, 138.63, 129.20, 128.35, 127.11, 113.39, 106.54, 21.48. LC-MS (MeCN) Rt = 2.43 min, *m/z* $[M+H]^+$ calculated for $C_{12}H_{11}NOS$ 217.29, found = 218.7.

4.3.9. Synthesis of compound (2-aminothiophen-3-yl)(2-fluorophenyl)methanone (3p)

Compound **3p** was obtained according to the procedure reported above for compound **3b** from intermediate **2p** (1.00 g; 6.1 mmol) and 1,4-dithian-2,5-diol (0.464 g; 3.0 mmol) in the presence of NEt_3 (0.934 mL; 6.7 mmol).

^1H NMR (400 MHz, DMSO-d6) δ: 8.42 (bs, 2H), 7.70 - 7.62 (m, 1H), 7.55 - 7.49 (m, 1H), 7.43 (m, 1H), 7.32 - 7.23 (m, 1H), 6.43 (dd, *J* = 5.9, 2.4 Hz, 1H), 6.22 (d, *J* = 5.9 Hz, 1H); ^{13}C NMR (101 MHz, DMSO-d_6) δ: 185.00, 167.23, 158.29 (d, *J* = 6.0 Hz), 156.87 (d, *J* = 246.2 Hz), 131.65 (d, *J* = 8.1 Hz), 129.16 (d, *J* = 3.7 Hz), 126.13 (d, *J* = 2.5 Hz), 124.56 (d, *J* = 3.1 Hz), 115. 86 (d, *J* =

21.6 Hz), 114.07, 106.66; ^{19}F NMR (376 MHz, DMSO-d_6) δ: -111.55. LC-MS (MeCN) Rt = 3.12 min, *m/z* $[M+H]^+$ calculated for $C_{11}H_8FNOS$ 221.25, found = 222.4.

4.3.10. Synthesis of compound (2-aminothiophen-3-yl)(3-fluorophenyl)methanone (3q)

Compound **3q** was obtained according to the procedure reported above for compound **3b** from intermediate **2q** (1.00 g; 6.1 mmol) and 1,4-dithian-2,5-diol (0.464 g; 3.0 mmol) in the presence of NEt_3 (0.934 mL; 6.7 mmol).

^{1}H NMR (400 MHz, DMSO-d_6) δ: 8.41 (bs, 2H), 7.58 - 7.49 (m, 1H), 7.44 - 7.31 (m, 3H), 6.72 (d, *J* = 5.9 Hz, 1H), 6.28 (d, *J* = 5.9 Hz, 1H); ^{13}C NMR (101 MHz, DMSO-d_6) δ: 187.34 (d, *J* = 2.0 Hz), 163.04, 160.61, 143.14 (d, *J* = 6.4 Hz), 130.44 (d, *J* = 8.1 Hz), 126.30, 123.82 (d, J = 2.9 Hz), 117.30 (d, *J* = 21.7 Hz), 114.38 (d, *J* = 21.7 Hz), 112.62, 106.56; ^{19}F NMR (376 MHz, DMSO-d_6) δ: -109.92. LC-MS (MeCN) Rt = 2.43 min, *m/z* $[M+H]^+$ calculated for $C_{11}H_8FNOS$ 221.25, found = 222.6.

4.3.11. Synthesis of compound (2-aminothiophen-3-yl)(4-fluorophenyl)methanone (3r)

Compound **3r** was obtained according to the procedure reported above for compound **3b** from intermediate **2r** (1.00 g; 6.1 mmol) and 1,4-dithian-2,5-diol (0.464 g; 3.0 mmol) in the presence of NEt_3 (0.934 mL; 6.7 mmol).

^{1}H NMR (400 MHz, DMSO-d_6) δ: 8.36 (bs, 2H), 7.66 (ddd, *J* = 8.6, 5.5, 2.0 Hz, 2H), 7.31 (dt, *J* = 8.6, 2.0 Hz, 2H), 6.74 (d, *J* = 5.9 Hz, 1H), 6.28 (d, *J* = 5.9 Hz, 1H); ^{13}C NMR (101 MHz, DMSO-d_6) δ: 188.18, 167.97, 163.57 (d, *J* = 253 Hz), 137.82 (d, *J* = 2.9 Hz), 130.81 (d, *J* = 8.8 Hz), 126.9, 115.64 (d, *J* = 21.5 Hz), 113.17, 106.81; ^{19}F NMR (376 MHz, DMSO-d_6) δ -112.57. LC-MS (MeCN) Rt = 2.27 min, *m/z* $[M+H]^+$ calculated for $C_{11}H_8FNOS$ 221.25, found = 222.7.

5. Conclusion

Leishmaniasis is a zoonotic, vector-borne disease, widespread mostly among people from the poorest countries in the world. The infection is transmitted through the bite of an infected female sandfly. More than 20 species of *Leishmania* parasites are responsible for the disease in humans and animals. The main clinical manifestations include visceral leishmaniasis (VL), cutaneous leishmaniasis (CL) and mucosal leishmaniasis (MC) (141, 142).

Several risk factors have been associated with this disease such as environmental and socioeconomic factors, malnutrition, poor hygienic condition. Due to globalization, climate change, increased tourism to endemic areas, leishmaniasis prevalence is growing also in non-endemic countries. Therefore, in the future, leishmaniasis could be not only a poverty related disease, but a global public health problem. This scenario highlights the need for further studies and new therapeutic instruments (146, 147).

Currently available therapies for leishmaniasis treatment are far from ideal because of their high toxicity, elevated cost, lack of efficacy due to parasites drug resistance.

Looking forward for a safe and effective human vaccine that could be useful to protect susceptible subjects in developing countries, the scientific research is focused on the design and synthesis of small molecules as new potential antileishmanial drugs. Recent studies have proven that different heterocyclic compounds have interesting activities against *Leishmania* parasites *in vitro* and/or *in vivo* (178).

Based on the data from literature, a new set of 2-amino-3-benzoylthiophene derivatives (compounds **3a**-**3x**) was designed by the research group of Prof. Ian Baxendale at the Department of Chemistry of University of Durham.

During my experience as PhD visiting student in the laboratories of Prof. Baxendale, I collaborated in the synthesis and characterization of this new molecular library.

Actually, the synthetic procedures and structural characterizations are ongoing. Once the full library of compounds is completed, thiophene derivatives will be tested *in vitro* against *Leishmania* parasites to evaluate their potential antileishmanial activity, aiming to find new therapeutic agents.

References

Part I:

1. Weinreb RN, Aung T, Medeiros FA. The pathophysiology and treatment of glaucoma: a review. Jama. **2014**;311(18):1901-11.

2. Allocco AR, Ponce JA, Riera MJ, Magurno MG. Critical pathway for primary open angle glaucoma diagnosis. International journal of ophthalmology. **2017**;10(6):968.

3. Tham Y-C, Li X, Wong TY, Quigley HA, Aung T, Cheng C-Y. Global prevalence of glaucoma and projections of glaucoma burden through 2040: a systematic review and meta-analysis. Ophthalmology. **2014**;121(11):2081-90.

4. Cioffi CL. Drug Delivery Challenges and Novel Therapeutic Approaches for Retinal Diseases: Springer; **2020**.

5. Goel M, Picciani RG, Lee RK, Bhattacharya SK. Aqueous humor dynamics: a review. The open ophthalmology journal. **2010**;4:52.

6. Kang JM, Tanna AP. Glaucoma. Med Clin North Am. **2021**;105(3):493-510.

7. Tamm ER. The trabecular meshwork outflow pathways: structural and functional aspects. Experimental eye research. **2009**;88(4):648-55.

8. Braunger BM, Fuchshofer R, Tamm ER. The aqueous humor outflow pathways in glaucoma: A unifying concept of disease mechanisms and causative treatment. European Journal of Pharmaceutics and Biopharmaceutics. **2015**;95:173-81.

9. Toris CB, Gagrani M, Ghate D. Current methods and new approaches to assess aqueous humor dynamics. Expert Review of Ophthalmology. **2021**;16(3):139-60.

10. Wang YX, Xu L, Wei WB, Jonas JB. Intraocular pressure and its normal range adjusted for ocular and systemic parameters. The Beijing Eye Study 2011. PLoS One. **2018**;13(5):e0196926.

11. Jonas JB, Aung T, Bourne RR, Bron AM, Ritch R, Panda-Jonas S. Glaucoma. Lancet. **2017**;390(10108):2183-93.

12. Suzuki Y, Iwase A, Araie M, Yamamoto T, Abe H, Shirato S, et al. Risk factors for open-angle glaucoma in a Japanese population: the Tajimi Study. Ophthalmology. **2006**;113(9):1613-7.

13. Foster PJ, Buhrmann R, Quigley HA, Johnson GJ. The definition and classification of glaucoma in prevalence surveys. British journal of ophthalmology. **2002**;86(2):238-42.
14. Weinreb RN, Leung CK, Crowston JG, Medeiros FA, Friedman DS, Wiggs JL, et al. Primary open-angle glaucoma. Nature Reviews Disease Primers. **2016**;2(1):1-19.
15. Jonas JB, Berenshtein E, Holbach L. Anatomic relationship between lamina cribrosa, intraocular space, and cerebrospinal fluid space. Investigative ophthalmology & visual science. **2003**;44(12):5189-95.
16. Das P, Nirmala S, Medhi JP, editors. Detection of glaucoma using neuroretinal Rim information. 2016 International Conference on Accessibility to Digital World (ICADW); **2016**: IEEE.
17. Jonas JB, Fernández MC, Stürmer J. Pattern of glaucomatous neuroretinal rim loss. Ophthalmology. **1993**;100(1):63-8.
18. Hogan MJ, Alvarado JA, Weddell JE. Histology of the Human Eye: An Atlas and Textbook: Saunders; **1971**.
19. Yu D-Y, Cringle SJ, Balaratnasingam C, Morgan WH, Paula KY, Su E-N. Retinal ganglion cells: energetics, compartmentation, axonal transport, cytoskeletons and vulnerability. Progress in retinal and eye research. **2013**;36:217-46.
20. Nickells RW, Howell GR, Soto I, John SW. Under pressure: cellular and molecular responses during glaucoma, a common neurodegeneration with axonopathy. Annual review of neuroscience. **2012**;35:153-79.
21. Nickells RW. The cell and molecular biology of glaucoma: mechanisms of retinal ganglion cell death. Investigative ophthalmology & visual science. **2012**;53(5):2476-81.
22. Chidlow G, Ebneter A, Wood JP, Casson RJ. The optic nerve head is the site of axonal transport disruption, axonal cytoskeleton damage and putative axonal regeneration failure in a rat model of glaucoma. Acta neuropathologica. **2011**;121(6):737-51.
23. Quigley HA, McKinnon SJ, Zack DJ, Pease ME, Kerrigan–Baumrind LA, Kerrigan DF, et al. Retrograde axonal transport of BDNF in retinal ganglion cells is blocked by acute IOP elevation in rats. Investigative ophthalmology & visual science. **2000**;41(11):3460-6.

24. Mansour-Robaey S, Clarke D, Wang Y, Bray G, Aguayo A. Effects of ocular injury and administration of brain-derived neurotrophic factor on survival and regrowth of axotomized retinal ganglion cells. Proceedings of the National Academy of Sciences. **1994**;91(5):1632-6.

25. Weber AJ, Viswanáthan S, Ramanathan C, Harman CD. Combined application of BDNF to the eye and brain enhances ganglion cell survival and function in the cat after optic nerve injury. Investigative ophthalmology & visual science. **2010**;51(1):327-34.

26. Zimmerman TJ, Kooner KS. Clinical Pathways in Glaucoma: Thieme; **2001**.

27. Weinreb RN, Khaw PT. Primary open-angle glaucoma. The lancet. **2004**;363(9422):1711-20.

28. Ferreira SM, Lerner SF, Brunzini R, Evelson PA, Llesuy SF. Oxidative stress markers in aqueous humor of glaucoma patients. American journal of ophthalmology. **2004**;137(1):62-9.

29. Chrysostomou V, Rezania F, Trounce IA, Crowston JG. Oxidative stress and mitochondrial dysfunction in glaucoma. Current opinion in pharmacology. **2013**;13(1):12-5.

30. Sharif NA, May JA. Potential for serotonergic agents to treat elevated intraocular pressure and glaucoma: focus on 5-HT2 receptor agonists. Expert Review of Ophthalmology. **2011**;6(1):105-20.

31. Osborne N, Wood J, Melena J, Chao H, Nash M, Bron A, et al. 5-Hydroxytryptamine 1A agonists: potential use in glaucoma. Evidence from animal studies. Eye. **2000**;14(3):454-63.

32. May JA, McLaughlin MA, Sharif NA, Hellberg MR, Dean TR. Evaluation of the ocular hypotensive response of serotonin 5-HT1A and 5-HT2 receptor ligands in conscious ocular hypertensive cynomolgus monkeys. Journal of Pharmacology and Experimental Therapeutics. **2003**;306(1):301-9.

33. Zhang N, Wang J, Li Y, Jiang B. Prevalence of primary open angle glaucoma in the last 20 years: a meta-analysis and systematic review. Scientific Reports. **2021**;11(1):1-12.

34. Ang G, Eke T. Lifetime visual prognosis for patients with primary open-angle glaucoma. Eye. **2007**;21(5):604-8.

35. Kong X, Chen Y, Chen X, Sun X. Influence of family history as a risk factor on primary angle closure and primary open angle glaucoma in a Chinese population. Ophthalmic epidemiology. **2011**;18(5):226-32.
36. Kwon YH, Fingert JH, Kuehn MH, Alward WL. Primary open-angle glaucoma. New England Journal of Medicine. **2009**;360(11):1113-24.
37. Fingert J. Primary open-angle glaucoma genes. Eye. **2011**;25(5):587-95.
38. Sun X, Dai Y, Chen Y, Yu D-Y, Cringle SJ, Chen J, et al. Primary angle closure glaucoma: what we know and what we don't know. Progress in retinal and eye research. **2017**;57:26-45.
39. Stamper RL, Lieberman MF, Drake MV, Becker B. Becker-Shaffer's Diagnosis and Therapy of the Glaucomas: Mosby/Elsevier; **2009**.
40. Choong YF, Irfan S, Menage MJ. Acute angle closure glaucoma: an evaluation of a protocol for acute treatment. Eye. **1999**;13(5):613-6.
41. George R, Panda S, Vijaya L. Blindness in glaucoma: primary open-angle glaucoma versus primary angle-closure glaucoma—a meta-analysis. Eye. **2021**:1-7.
42. Vajaranant TS, Nayak S, Wilensky JT, Joslin CE. Gender and glaucoma: what we know and what we need to know. Curr Opin Ophthalmol. **2010**;21(2):91-9.
43. Mitchell P, Hourihan F, Sandbach J, Wang JJ. The relationship between glaucoma and myopia: the Blue Mountains Eye Study. Ophthalmology. **1999**;106(10):2010-5.
44. Coleman AL, Stone KL, Kodjebacheva G, Yu F, Pedula KL, Ensrud KE, et al. Glaucoma risk and the consumption of fruits and vegetables among older women in the study of osteoporotic fractures. Am J Ophthalmol. **2008**;145(6):1081-9.
45. Alexander CL, Miller SJ, Abel SR. Prostaglandin analog treatment of glaucoma and ocular hypertension. Ann Pharmacother. **2002**;36(3):504-11.
46. Yadav KS, Rajpurohit R, Sharma S. Glaucoma: Current treatment and impact of advanced drug delivery systems. Life Sci. **2019**;221:362-76.
47. Costagliola C, dell'Omo R, Romano MR, Rinaldi M, Zeppa L, Parmeggiani F. Pharmacotherapy of intraocular pressure: part I. Parasympathomimetic, sympathomimetic and sympatholytics. Expert Opin Pharmacother. **2009**;10(16):2663-77.

48. Dikopf MS, Vajaranant TS, Edward DP. Topical treatment of glaucoma: established and emerging pharmacology. Expert Opin Pharmacother. **2017**;18(9):885-98.
49. Brooks AM, Gillies WE. Ocular beta-blockers in glaucoma management. Clinical pharmacological aspects. Drugs Aging. **1992**;2(3):208-21.
50. Orzalesi N, Rossetti L, Invernizzi T, Bottoli A, Autelitano A. Effect of timolol, latanoprost, and dorzolamide on circadian IOP in glaucoma or ocular hypertension. Invest Ophthalmol Vis Sci. **2000**;41(9):2566-73.
51. Mincione F, Nocentini A, Supuran CT. Advances in the discovery of novel agents for the treatment of glaucoma. Expert Opin Drug Discov. **2021**;16(10):1209-25.
52. Wu X, Yang X, Liang Q, Xue X, Huang J, Wang J, et al. Drugs for the treatment of glaucoma: Targets, structure-activity relationships and clinical research. Eur J Med Chem. **2021**;226:113842.
53. Wang R. Two's company, three's a crowd: can H_2S be the third endogenous gaseous transmitter? Faseb j. **2002**;16(13):1792-8.
54. Corvino A, Frecentese F, Magli E, Perissutti E, Santagada V, Scognamiglio A, et al. Trends in H_2S-Donors Chemistry and Their Effects in Cardiovascular Diseases. Antioxidants (Basel). **2021**;10(3).
55. Zanardo RC, Brancaleone V, Distrutti E, Fiorucci S, Cirino G, Wallace JL. Hydrogen sulfide is an endogenous modulator of leukocyte-mediated inflammation. Faseb j. **2006**;20(12):2118-20.
56. Feng Y, Prokosch V, Liu H. Current Perspective of Hydrogen Sulfide as a Novel Gaseous Modulator of Oxidative Stress in Glaucoma. Antioxidants (Basel). **2021**;10(5).
57. Khattak S, Zhang QQ, Sarfraz M, Muhammad P, Ngowi EE, Khan NH, et al. The Role of Hydrogen Sulfide in Respiratory Diseases. Biomolecules. **2021**;11(5).
58. Kimura H. Production and physiological effects of hydrogen sulfide. Antioxid Redox Signal. **2014**;20(5):783-93.
59. Lin VS, Chen W, Xian M, Chang CJ. Chemical probes for molecular imaging and detection of hydrogen sulfide and reactive sulfur species in biological systems. Chem Soc Rev. **2015**;44(14):4596-618.

60. Cuevasanta E, Möller MN, Alvarez B. Biological chemistry of hydrogen sulfide and persulfides. Arch Biochem Biophys. **2017**;617:9-25.
61. Hughes MN, Centelles MN, Moore KP. Making and working with hydrogen sulfide: The chemistry and generation of hydrogen sulfide in vitro and its measurement in vivo: a review. Free Radic Biol Med. **2009**;47(10):1346-53.
62. Huang CW, Moore PK. H_2S Synthesizing Enzymes: Biochemistry and Molecular Aspects. Handb Exp Pharmacol. **2015**;230:3-25.
63. Kabil O, Banerjee R. Enzymology of H_2S biogenesis, decay and signaling. Antioxid Redox Signal. **2014**;20(5):770-82.
64. Maclean KN, Kraus JP. Hydrogen Sulfide Production and Metabolism in Mammalian Tissues. In: Wang R, editor. Signal Transduction and the Gasotransmitters: NO, CO, and H2S in Biology and Medicine. Totowa, NJ: Humana Press; **2004**. p. 275-92.
65. Wang R. Physiological implications of hydrogen sulfide: a whiff exploration that blossomed. Physiol Rev. **2012**;92(2):791-896.
66. Elsey DJ, Fowkes RC, Baxter GF. L-cysteine stimulates hydrogen sulfide synthesis in myocardium associated with attenuation of ischemia-reperfusion injury. J Cardiovasc Pharmacol Ther. **2010**;15(1):53-9.
67. Yang J, Minkler P, Grove D, Wang R, Willard B, Dweik R, et al. Non-enzymatic hydrogen sulfide production from cysteine in blood is catalyzed by iron and vitamin B(6). Commun Biol. **2019**;2:194.
68. Levitt MD, Furne J, Springfield J, Suarez F, DeMaster E. Detoxification of hydrogen sulfide and methanethiol in the cecal mucosa. J Clin Invest. **1999**;104(8):1107-14.
69. Magli E, Perissutti E, Santagada V, Caliendo G, Corvino A, Esposito G, et al. H_2S Donors and Their Use in Medicinal Chemistry. Biomolecules. **2021**;11(12).
70. Martelli A, Citi V, Testai L, Brogi S, Calderone V. Organic Isothiocyanates as Hydrogen Sulfide Donors. Antioxid Redox Signal. **2020**;32(2):110-44.
71. Lin Y, Yang X, Lu Y, Liang D, Huang D. Isothiocyanates as H_2S Donors Triggered by Cysteine: Reaction Mechanism and Structure and Activity Relationship. Org Lett. **2019**;21(15):5977-80.

72. Han Y, Shang Q, Yao J, Ji Y. Hydrogen sulfide: a gaseous signaling molecule modulates tissue homeostasis: implications in ophthalmic diseases. Cell Death Dis. **2019**;10(4):293.
73. Kulkarni M, Njie-Mbye YF, Okpobiri I, Zhao M, Opere CA, Ohia SE. Endogenous production of hydrogen sulfide in isolated bovine eye. Neurochem Res. **2011**;36(8):1540-5.
74. George AK, Homme RP, Stanisic D, Tyagi SC, Singh M. Protecting the aging eye with hydrogen sulfide. Can J Physiol Pharmacol. **2021**;99(2):161-70.
75. Huang S, Huang P, Liu X, Lin Z, Wang J, Xu S, et al. Relevant variations and neuroprotecive effect of hydrogen sulfide in a rat glaucoma model. Neuroscience. **2017**;341:27-41.
76. Liu H, Anders F, Thanos S, Mann C, Liu A, Grus FH, et al. Hydrogen Sulfide Protects Retinal Ganglion Cells Against Glaucomatous Injury In Vitro and In Vivo. Invest Ophthalmol Vis Sci. **2017**;58(12):5129-41.
77. Persa C, Osmotherly K, Chao-Wei Chen K, Moon S, Lou MF. The distribution of cystathionine beta-synthase (CBS) in the eye: implication of the presence of a trans-sulfuration pathway for oxidative stress defense. Exp Eye Res. **2006**;83(4):817-23.
78. Lin Z, Huang S, Yu H, Sun J, Huang P, Zhong Y. Analysis of Plasma Hydrogen Sulfide, Homocysteine, and L-Cysteine in Open-Angle Glaucoma Patients. J Ocul Pharmacol Ther. **2020**;36(8):649-57.
79. Li P, Liu H, Shi X, Prokosch V. Hydrogen Sulfide: Novel Endogenous and Exogenous Modulator of Oxidative Stress in Retinal Degeneration Diseases. Molecules. **2021**;26(9).
80. Scheid S, Goeller M, Baar W, Wollborn J, Buerkle H, Schlunck G, et al. Hydrogen Sulfide Reduces Ischemia and Reperfusion Injury in Neuronal Cells in a Dose- and Time-Dependent Manner. Int J Mol Sci. **2021**;22(18).
81. Tang G, Wu L, Wang R. Interaction of hydrogen sulfide with ion channels. Clin Exp Pharmacol Physiol. **2010**;37(7):753-63.
82. Erisgin Z, Ozer MA, Tosun M, Ozen S, Takir S. The effects of intravitreal H_2S application on apoptosis in the retina and cornea in experimental glaucoma model. Int J Exp Pathol. **2019**;100(5-6):330-6.
83. Kulkarni KH, Monjok EM, Zeyssig R, Kouamou G, Bongmba ON, Opere CA, et al. Effect of hydrogen sulfide on sympathetic neurotransmission and

catecholamine levels in isolated porcine iris-ciliary body. Neurochem Res. **2009**;34(3):400-6.

84. Perrino E, Uliva C, Lanzi C, Soldato PD, Masini E, Sparatore A. New prostaglandin derivative for glaucoma treatment. Bioorg Med Chem Lett. **2009**;19(6):1639-42.

85. Osborne NN, Ji D, Abdul Majid AS, Fawcett RJ, Sparatore A, Del Soldato P. ACS67, a hydrogen sulfide-releasing derivative of latanoprost acid, attenuates retinal ischemia and oxidative stress to RGC-5 cells in culture. Invest Ophthalmol Vis Sci. **2010**;51(1):284-94.

86. Salvi A, Bankhele P, Jamil JM, Kulkarni-Chitnis M, Njie-Mbye YF, Ohia SE, et al. Pharmacological Actions of Hydrogen Sulfide Donors on Sympathetic Neurotransmission in the Bovine Anterior Uvea, In Vitro. Neurochem Res. **2016**;41(5):1020-8.

87. Corvino A, Citi V, Fiorino F, Frecentese F, Magli E, Perissutti E, et al. H_2S donating corticosteroids: Design, synthesis and biological evaluation in a murine model of asthma. J Adv Res. **2022**;35:267-77.

88. Severino B, Corvino A, Fiorino F, Luciano P, Frecentese F, Magli E, et al. 1,2,4-Thiadiazolidin-3,5-diones as novel hydrogen sulfide donors. Eur J Med Chem. **2018**;143:1677-86.

89. Ercolano G, De Cicco P, Frecentese F, Saccone I, Corvino A, Giordano F, et al. Anti-metastatic Properties of Naproxen-HBTA in a Murine Model of Cutaneous Melanoma. Front Pharmacol. **2019**;10:66.

90. Giordano F, Corvino A, Scognamiglio A, Citi V, Gorica E, Fattorusso C, et al. Hybrids between H_2S-donors and betamethasone 17-valerate or triamcinolone acetonide inhibit mast cell degranulation and promote hyperpolarization of bronchial smooth muscle cells. Eur J Med Chem. **2021**;221:113517.

91. Martelli A, Testai L, Citi V, Marino A, Pugliesi I, Barresi E, et al. Arylthioamides as H_2S Donors: l-Cysteine-Activated Releasing Properties and Vascular Effects in Vitro and in Vivo. ACS Med Chem Lett. **2013**;4(10):904-8.

92. Wallace JL, Cirino G, Caliendo G, Sparatore A, Santagada V, Fiorucci S. Derivatives of 4-or 5-aminosalicylic acid. Google Patents; **2011**.

93. Martelli A, Citi V, Calderone V. Vascular Effects of H_2S-Donors: Fluorimetric Detection of H_2S Generation and Ion Channel Activation in Human Aortic Smooth Muscle Cells. Methods Mol Biol. **2019**;2007:79-87.
94. Citi V, Martelli A, Bucci M, Piragine E, Testai L, Vellecco V, et al. Searching for novel hydrogen sulfide donors: The vascular effects of two thiourea derivatives. Pharmacol Res. **2020**;159:105039.
95. Mannermaa E, Vellonen KS, Urtti A. Drug transport in corneal epithelium and blood-retina barrier: emerging role of transporters in ocular pharmacokinetics. Adv Drug Deliv Rev. **2006**;58(11):1136-63.
96. Davies NM. Biopharmaceutical considerations in topical ocular drug delivery. Clin Exp Pharmacol Physiol. **2000**;27(7):558-62.
97. Scozzafava A, Menabuoni L, Mincione F, Briganti F, Mincione G, Supuran CT. Carbonic anhydrase inhibitors. Synthesis of water-soluble, topically effective, intraocular pressure-lowering aromatic/heterocyclic sulfonamides containing cationic or anionic moieties: is the tail more important than the ring? J Med Chem. **1999**;42(14):2641-50.
98. Petrović SD, Stojanović ND, Antonović DG, Mijin DŽ, Nikolić AD. Conformations of unsymmetrical N-t-butyl-N-substituted 2-phenylacetamides. Journal of Molecular Structure. **1997**;410-411:35-8.
99. Isbrandt L, Tung WCT, Rogers MT. An NMR study of hindered internal rotation in some unsymmetrically N,N-disubstituted acetamides. Journal of Magnetic Resonance (1969). **1973**;9(3):461-6.
100. LaPlanche LA, Rogers MT. Configurations in Unsymmetrically N,N-Disubstituted Amides. Journal of the American Chemical Society. **1963**;85(23):3728-30.
101. Zheng Y, Tice CM, Singh SB. Conformational control in structure-based drug design. Bioorganic & medicinal chemistry letters. **2017**;27(13):2825-37.
102. Causes of blindness and vision impairment in 2020 and trends over 30 years, and prevalence of avoidable blindness in relation to VISION 2020: the Right to Sight: an analysis for the Global Burden of Disease Study. Lancet Glob Health. **2021**;9(2):e144-e60.
103. Sampath Kumar HM, Herrmann L, Tsogoeva SB. Structural hybridization as a facile approach to new drug candidates. Bioorg Med Chem Lett. **2020**;30(23):127514.

Part II:

104. Baranowski P, Karolewicz B, Gajda M, Pluta J. Ophthalmic drug dosage forms: characterisation and research methods. The Scientific World Journal. **2014**;2014.

105. Davies NM. Biopharmaceutical considerations in topical ocular drug delivery. Clinical and experimental pharmacology and physiology. **2000**;27(7):558-62.

106. Dubald M, Bourgeois S, Andrieu V, Fessi H. Ophthalmic drug delivery systems for antibiotherapy—a review. Pharmaceutics. **2018**;10(1):10.

107. Pisella P, Pouliquen P, Baudouin C. Prevalence of ocular symptoms and signs with preserved and preservative free glaucoma medication. British Journal of Ophthalmology. **2002**;86(4):418-23.

108. da Silva Aquino KA. Sterilization by gamma irradiation. Gamma radiation. **2012**;9:172-202.

109. Lanier OL, Manfre MG, Bailey C, Liu Z, Sparks Z, Kulkarni S, et al. Review of Approaches for Increasing Ophthalmic Bioavailability for Eye Drop Formulations. AAPS PharmSciTech. **2021**;22(3):107.

110. Achouri D, Alhanout K, Piccerelle P, Andrieu V. Recent advances in ocular drug delivery. Drug Development and Industrial Pharmacy. **2013**;39(11):1599-617.

111. Barot M, Bagui M, R Gokulgandhi M, K Mitra A. Prodrug strategies in ocular drug delivery. Medicinal Chemistry. **2012**;8(4):753-68.

112. Kour J, Kumari N, Sapra B. Ocular prodrugs: Attributes and challenges. Asian Journal of Pharmaceutical Sciences. **2021**;16(2):175-91.

113. Loftsson T, Stefánsson E. Cyclodextrins in eye drop formulations: enhanced topical delivery of corticosteroids to the eye. Acta Ophthalmologica Scandinavica. **2002**;80(2):144-50.

114. Jóhannsdóttir S, Jansook P, Stefánsson E, Loftsson T. Development of a cyclodextrin-based aqueous cyclosporin A eye drop formulations. International journal of pharmaceutics. **2015**;493(1-2):86-95.

115. Kristinsson JK, Fridriksdóttir H, Thorisdottir S, Sigurdardottir AM, Stefansson E, Loftsson T. Dexamethasone-cyclodextrin-polymer co-complexes

in aqueous eye drops. Aqueous humor pharmacokinetics in humans. Investigative ophthalmology & visual science. **1996**;37(6):1199-203.
116. Zhang Y, Ren K, He Z, Li H, Chen T, Lei Y, et al. Development of inclusion complex of brinzolamide with hydroxypropyl-β-cyclodextrin. Carbohydrate polymers. **2013**;98(1):638-43.
117. Winfield A, Jessiman D, Williams A, Esakowitz L. A study of the causes of non-compliance by patients prescribed eyedrops. British Journal of Ophthalmology. **1990**;74(8):477-80.
118. McVeigh KA, Vakros G. The eye drop chart: a pilot study for improving administration of and compliance with topical treatments in glaucoma patients. Clinical ophthalmology (Auckland, NZ). **2015**;9:813.
119. Newman-Casey PA, Robin AL, Blachley T, Farris K, Heisler M, Resnicow K, et al. The most common barriers to glaucoma medication adherence: a cross-sectional survey. Ophthalmology. **2015**;122(7):1308-16.
120. Adams CM, Papillon JP. Recent Developments for the Treatment of Glaucoma. Drug Delivery Challenges and Novel Therapeutic Approaches for Retinal Diseases. **2020**:189-256.
121. Toffoletto N, Saramago B, Serro AP. Therapeutic ophthalmic lenses: A review. Pharmaceutics. **2021**;13(1):36.
122. Moreddu R, Vigolo D, Yetisen AK. Contact lens technology: from fundamentals to applications. Advanced healthcare materials. **2019**;8(15):1900368.
123. Carvalho I, Marques C, Oliveira R, Coelho P, Costa P, Ferreira D. Sustained drug release by contact lenses for glaucoma treatment—A review. Journal of controlled release. **2015**;202:76-82.
124. Peral A, Martinez-Aguila A, Pastrana C, Huete-Toral F, Carpena-Torres C, Carracedo G. Contact Lenses as Drug Delivery System for Glaucoma: A Review. Applied sciences. **2020**;10(15):5151.
125. Hillman JS. Management of acute glaucoma with pilocarpine-soaked hydrophilic lens. Br J Ophthalmol. **1974**;58(7):674-9.
126. Schultz CL, Poling TR, Mint JO. A medical device/drug delivery system for treatment of glaucoma. Clinical and Experimental Optometry. **2009**;92(4):343-8.

127. Peng CC, Ben-Shlomo A, Mackay EO, Plummer CE, Chauhan A. Drug delivery by contact lens in spontaneously glaucomatous dogs. Curr Eye Res. **2012**;37(3):204-11.
128. Horne RR, Rich JT, Bradley MW, Pitt WG. Latanoprost uptake and release from commercial contact lenses. Journal of Biomaterials Science, Polymer Edition. **2020**;31(1):1-19.
129. Horne RR, Judd KE, Pitt WG. Rapid loading and prolonged release of latanoprost from a silicone hydrogel contact lens. Journal of Drug Delivery Science and Technology. **2017**;41:410-8.
130. Peng C-C, Burke MT, Carbia BE, Plummer C, Chauhan A. Extended drug delivery by contact lenses for glaucoma therapy. Journal of controlled release. **2012**;162(1):152-8.
131. Hsu K-H, Carbia BE, Plummer C, Chauhan A. Dual drug delivery from vitamin E loaded contact lenses for glaucoma therapy. European Journal of Pharmaceutics and Biopharmaceutics. **2015**;94:312-21.
132. Chen L, Wang X, Lu W, Wu X, Li J. Molecular imprinting: perspectives and applications. Chemical Society Reviews. **2016**;45(8):2137-211.
133. Anirudhan TS, Nair AS, Parvathy J. Extended wear therapeutic contact lens fabricated from timolol imprinted carboxymethyl chitosan-g-hydroxy ethyl methacrylate-g-poly acrylamide as a onetime medication for glaucoma. European Journal of Pharmaceutics and Biopharmaceutics. **2016**;109:61-71.
134. Yañez F, Martikainen L, Braga ME, Alvarez-Lorenzo C, Concheiro A, Duarte CM, et al. Supercritical fluid-assisted preparation of imprinted contact lenses for drug delivery. Acta biomaterialia. **2011**;7(3):1019-30.
135. Costa VP, Braga MEM, Duarte CMM, Alvarez-Lorenzo C, Concheiro A, Gil MH, et al. Anti-glaucoma drug-loaded contact lenses prepared using supercritical solvent impregnation. The Journal of Supercritical Fluids. **2010**;53(1):165-73.
136. Ciolino JB, Stefanescu CF, Ross AE, Salvador-Culla B, Cortez P, Ford EM, et al. In vivo performance of a drug-eluting contact lens to treat glaucoma for a month. Biomaterials. **2014**;35(1):432-9.
137. Dulger B, Basci NE, Sagdic-Yalvac I, Temizer A. Determination of betaxolol in human aqueous humour by high-performance liquid

chromatography with fluorescence detection. Journal of Chromatography B. **2002**;772(1):179-83.
138. Marques MR, Loebenberg R, Almukainzi M. Simulated biological fluids with possible application in dissolution testing. Dissolution Technol. **2011**;18(3):15-28.
139. Jug M, Hafner A, Lovrić J, Kregar ML, Pepić I, Vanić Ž, et al. An overview of in vitro dissolution/release methods for novel mucosal drug delivery systems. Journal of pharmaceutical and biomedical analysis. **2018**;147:350-66.
140. Lanier OL, Christopher KG, Macoon RM, Yu Y, Sekar P, Chauhan A. Commercialization challenges for drug eluting contact lenses. Expert Opinion on Drug Delivery. **2020**;17(8):1133-49.

Appendix:

141. Steverding D. The history of leishmaniasis. Parasit Vectors. **2017**;10(1):82.
142. Burza S, Croft SL, Boelaert M. Leishmaniasis. The Lancet. **2018**;392(10151):951-70.
143. https://www.cdc.gov/parasites/.
144. Dantas-Torres F. The role of dogs as reservoirs of Leishmania parasites, with emphasis on Leishmania (Leishmania) infantum and Leishmania (Viannia) braziliensis. Vet Parasitol. **2007**;149(3-4):139-46.
145. Inceboz T. Epidemiology and ecology of leishmaniasis. Current topics in neglected tropical diseases: IntechOpen London; **2019**. p. 1-15.
146. Oryan A, Akbari M. Worldwide risk factors in leishmaniasis. Asian Pacific journal of tropical medicine. **2016**;9(10):925-32.
147. Okwor I, Uzonna J. Social and Economic Burden of Human Leishmaniasis. Am J Trop Med Hyg. **2016**;94(3):489-93.
148. Gyapong J, Boatin B. Neglected tropical diseases-sub-Saharan Africa: Springer; **2016**.
149. Abdullah AYM, Dewan A, Shogib MRI, Rahman MM, Hossain MF. Environmental factors associated with the distribution of visceral leishmaniasis in endemic areas of Bangladesh: modeling the ecological niche. Trop Med Health. **2017**;45:13.

150. van Griensven J, Diro E. Visceral Leishmaniasis. Infectious Disease Clinics of North America. **2012**;26(2):309-22.

151. Faleiro RJ, Kumar R, Hafner LM, Engwerda CR. Immune Regulation during Chronic Visceral Leishmaniasis. PLOS Neglected Tropical Diseases. **2014**;8(7):e2914.

152. Coutinho JVSC, Santos FSd, Ribeiro RdSP, Oliveira IBB, Dantas VB, Santos ABFS, et al. Visceral leishmaniasis and leishmaniasis-HIV coinfection: comparative study. Revista da Sociedade Brasileira de Medicina Tropical. **2017**;50:670-4.

153. Bennis I, Thys S, Filali H, De Brouwere V, Sahibi H, Boelaert M. Psychosocial impact of scars due to cutaneous leishmaniasis on high school students in Errachidia province, Morocco. Infectious Diseases of Poverty. **2017**;6(1):46.

154. Reithinger R, Dujardin J-C, Louzir H, Pirmez C, Alexander B, Brooker S. Cutaneous leishmaniasis. The Lancet infectious diseases. **2007**;7(9):581-96.

155. Scott P, Novais FO. Cutaneous leishmaniasis: immune responses in protection and pathogenesis. Nature Reviews Immunology. **2016**;16(9):581-92.

156. Strazzulla A, Cocuzza S, Pinzone MR, Postorino MC, Cosentino S, Serra A, et al. Mucosal Leishmaniasis: An Underestimated Presentation of a Neglected Disease. BioMed Research International. **2013**;2013:805108.

157. Goto H, Lauletta Lindoso JA. Cutaneous and Mucocutaneous Leishmaniasis. Infectious Disease Clinics of North America. **2012**;26(2):293-307.

158. Organization WH. Control of the leishmaniases: report of a meeting of the WHO Expert Commitee on the Control of Leishmaniases, Geneva, 22-26 March 2010: World Health Organization; **2010**.

159. Chakravarty J, Sundar S. Current and emerging medications for the treatment of leishmaniasis. Expert Opinion on Pharmacotherapy. **2019**;20(10):1251-65.

160. Monzote L. Current treatment of leishmaniasis: a review. The Open Antimicrobial Agents Journal. **2009**;1(1).

161. Mcgwire BS, Satoskar A. Leishmaniasis: clinical syndromes and treatment. QJM: An International Journal of Medicine. **2014**;107(1):7-14.

162. Croft S, Neal R, Pendergast W, Chan J. The activity of alkyl phosphorylcholines and related derivatives against Leishmania donovani. Biochemical pharmacology. **1987**;36(16):2633-6.
163. Wiwanitkit V. Interest in paromomycin for the treatment of visceral leishmaniasis (kala-azar). Therapeutics and clinical risk management. **2012**;8:323.
164. López-Carvajal L, Cardona-Arias JA, Zapata-Cardona MI, Sánchez-Giraldo V, Vélez ID. Efficacy of cryotherapy for the treatment of cutaneous leishmaniasis: meta-analyses of clinical trials. BMC infectious diseases. **2016**;16(1):1-11.
165. Asilian A, Sharif A, Faghihi G, Enshaeieh S, Shariati F, Siadat A. Evaluation of CO_2 laser efficacy in the treatment of cutaneous leishmaniasis. International journal of dermatology. **2004**;43(10):736-8.
166. Ikeogu NM, Akaluka GN, Edechi CA, Salako ES, Onyilagha C, Barazandeh AF, et al. Leishmania immunity: advancing immunotherapy and vaccine development. Microorganisms. **2020**;8(8):1201.
167. Iborra S, Solana JC, Requena JM, Soto M. Vaccine candidates against leishmania under current research. Expert review of vaccines. **2018**;17(4):323-34.
168. Gannavaram S, Dey R, Avishek K, Selvapandiyan A, Salotra P, Nakhasi HL. Biomarkers of safety and immune protection for genetically modified live attenuated Leishmania vaccines against visceral leishmaniasis–discovery and implications. Frontiers in immunology. **2014**;5:241.
169. Tiuman TS, Santos AO, Ueda-Nakamura T, Dias Filho BP, Nakamura CV. Recent advances in leishmaniasis treatment. International Journal of Infectious Diseases. **2011**;15(8):e525-e32.
170. Bozorov K, Nie LF, Zhao J, Aisa HA. 2-Aminothiophene scaffolds: Diverse biological and pharmacological attributes in medicinal chemistry. European journal of medicinal chemistry. **2017**;140:465-93.
171. da Franca Rodrigues KA, de Sousa Dias CN, do Nascimento Neris PL, da Câmara Rocha J, Scotti MT, Scotti L, et al. 2-Amino-thiophene derivatives present antileishmanial activity mediated by apoptosis and immunomodulation in vitro. European journal of medicinal chemistry. **2015**;106:1-14.

172. da Franca Rodrigues KA, Silva DKF, de Lima Serafim V, Andrade PN, Alves AF, Tafuri WL, et al. SB-83, a 2-Amino-thiophene derivative orally bioavailable candidate for the leishmaniasis treatment. Biomedicine & Pharmacotherapy. **2018**;108:1670-8.

173. Rodrigues CA, Santos PFd, Costa MOLd, Pavani TFA, Xander P, Geraldo MM, et al. 4-Phenyl-1, 3-thiazole-2-amines as scaffolds for new antileishmanial agents. Journal of Venomous Animals and Toxins including Tropical Diseases. **2018**;24.

174. Arévalo MaJ, Avalos Mn, Babiano R, Cabanillas A, Cintas P, Jiménez JL, et al. Optically active sugar thioamides from δ-gluconolactone. Tetrahedron: Asymmetry. **2000**;11(9):1985-95.

175. Liu C, Yuan J, Zhang Z, Gridnev ID, Zhang W. Asymmetric Hydroacylation Involving Alkene Isomerization for the Construction of C3-Chirogenic Center. Angewandte Chemie. **2021**;133(16):9079-84.

176. Xu K, Liu H, Hou Y, Shen J, Liu D, Zhang W. A Pd-catalyzed asymmetric allylic substitution cascade via an asymmetric desymmetrization for the synthesis of bicyclic dihydrofurans. Chemical Communications. **2019**;55(88):13295-8.

177. Mallia CJ, Englert L, Walter GC, Baxendale IR. Thiazole formation through a modified Gewald reaction. Beilstein journal of organic chemistry. **2015**;11(1):875-83.

178. Gupta O, Pradhan T, Bhatia R, Monga V. Recent Advancements in Anti-leishmanial Research: Synthetic strategies and Structural Activity Relationships. European Journal of Medicinal Chemistry. **2021**:113606.